Reproductive Biology and Distribution of Neuropeptide APGWamide in

the Brain and Reproductive Organs of Pygmy Squid,

Idiosepius pygmaeus **(Steenstrup, 1881)**

Pattanasuda Sirinupong

A Thesis Submitted in Partial Fulfillment of the Requirements for the Degree of

Doctor of Philosophy in Biology

Prince of Songkla University

2012

Thesis Title   Reproductive Biology and Distribution of Neuropeptide APGWamide in the Brain and Reproductive Organs of Pygmy Squid, *Idiosepius pygmaeus* (Steenstrup, 1881)
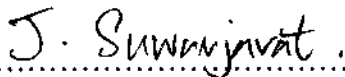
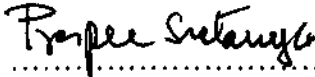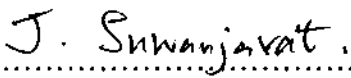**Author**   Mrs. Pattanasuda Sirinupong

Major Program   Biology

Major Advisor:

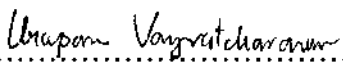..........J. Suwanjarat..........

(Assoc. Prof. Jintamas Suwanjarat)

Co-advisor:

....

(Prof. Dr. Jan van Minnen)

Examining Committee:

..........Prapee Sretarugsa..........Chairperson

(Assoc. Prof. Prapee Sretarugsa)

..........J. Suwanjarat..........

(Assoc. Prof. Jintamas Suwanjarat)

..........Uraporn Vongvatcharanon..........

(Assist. Prof. Dr. Uraporn Vongvatcharanon)

The Graduate School, Prince of Songkla University, has approved this thesis as partial fulfillment of the requirements for the Doctor of Philosophy Degree in Biology

..........A. Phongdara..........

(Prof. Dr. Amornrat Phongdara)

Dean of Graduate School

ชื่อวิทยานิพนธ์	ชีววิทยาการสืบพันธุ์และการกระจายของฮอร์โมน APGWamide ใน สมองและระบบสืบพันธุ์ของหมึกแคระ *Idiosepius pygmaeus* (Steenstrup, 1881)
ผู้เขียน	นางพัฒนสุดา ศิรินุพงศ์
สาขาวิชา	ชีววิทยา
ปีการศึกษา	2554

บทคัดย่อ

หมึกแคระ *Idiosepius pygmaeus* จัดอยู่ในกลุ่มหมึกกระดองที่มีขนาดเล็กที่สุด ในการศึกษาครั้งนี้มุ่งเน้นด้านชีววิทยาการสืบพันธุ์และการกระจายของฮอร์โมน APGWamide ในสมองและอวัยวะสืบพันธุ์ จากการศึกษาหมึกแคระ *I. pygmaeus* ตัวเต็มวัยจำนวน 190 ตัว ซึ่งเก็บจากบริเวณใกล้สะพานสารสิน ในฝั่งทะเลอันดามัน จังหวัดภูเก็ต ตั้งแต่เดือนมกราคมถึง เดือนธันวาคม พ.ศ. 2551 เป็นระยะเวลา 12 เดือน แสดงให้เห็นว่าหมึกแคระเพศเมียมีขนาด ความยาวลำตัว (dorsal mantle length) และน้ำหนักตัว (body weight) มากกว่าหมึกแคระเพศ ผู้อย่างมีนัยสำคัญทางสถิติ (P<0.0001) สำหรับในหมึกแคระเพศผู้พบว่าขนาดของถุงเก็บ สเปิร์ม (spermatophore length) แปรผันตามความยาวลำตัวอย่างมีนัยสำคัญทางสถิติ (P=0.02) โดยตัวที่มีขนาดใหญ่สามารถผลิตถุงเก็บสเปิร์ม (spermatophore length) ได้ใหญ่ กว่าตัวที่มีขนาดเล็ก และเมื่อพิจารณาความยาวของลำตัวหมึกแคระทั้งสองเพศพบว่าจะค่อย ๆ เพิ่มสูงขึ้นจากระยะวัยอ่อน (immature) จนถึงระยะปล่อยไข่ในเพศเมีย / ระยะปล่อยอสุจิในเพศ ผู้ (spawning) ขณะเดียวกันอัตราส่วนจำนวนของเพศผู้จะมีค่าสูงกว่าเพศเมียอย่างมีนัยสำคัญ ทางสถิติ (P<0.05) ด้วยสัดส่วนที่สูงที่สุดคือคือ 7:3 ซึ่งประเมินจากจำนวนตัวอย่างทั้งหมด จากการวิเคราะห์การเปลี่ยนแปลงของเนื้อเยื่อภายในรังไข่และอัณฑะของหมึกแคระตัวเต็มวัย *I. pygmaeus* สามารถแบ่งวงจรสืบพันธุ์ของหมึกแคระออกเป็น 4 ระยะคือ ระยะที่ 1 ระยะวัย อ่อน (immature), ระยะที่ 2 ระยะกำลังพัฒนา (maturing), ระยะที่ 3 ระยะก่อนการวางไข่ในเพศ เมีย (pre-spawning) / ระยะอสุจิเจริญเต็มที่ในเพศผู้ (mature), ระยะที่ 4 ระยะปล่อยไข่ในเพศ เมีย / ระยะปล่อยอสุจิในเพศผู้ (spawning) การศึกษาครั้งนี้ยังพบว่ากระบวนการสร้างเซลล์ สืบพันธุ์ในหมึกแคระทั้งสองเพศเกิดขึ้นอย่างต่อเนื่องตลอดทั้งปี ซึ่งเมื่อพิจารณาค่า GI พบว่ามี ค่าสูงอยู่ในระดับเดียวกัน 3 ช่วงคือเดือนมกราคม สิงหาคมและเดือนตุลาคม แสดงถึงช่วง เริ่มต้นของฤดูการผสมพันธุ์ในหมึกแคระ *I. pygmaeus* การศึกษาครั้งนี้เพื่อบรรยายลักษณะ โครงสร้างโดยละเอียดของกระบวนการสร้างเซลล์สืบพันธุ์ในเพศผู้โดยใช้กล้องจุลทรรศน์ อิเล็กตรอนแบบส่องผ่าน (transmission electron microscope) ตั้งแต่เซลล์สเปอร์มาโตโกเนีย

เซลล์สเปอร์มาโตไซด์ เซลล์สเปอร์มาติด และสเปิร์มมาโตซัว (อสุจิ)   สำหรับเซลล์อสุจิของ
หมึกแคระในระยะเต็มวัยจะพบส่วนที่มีลักษณะเรียงยาวของอโครโซม (acrosome) เชื่อมต่อกับ
ส่วนของนิวเคลียสซึ่งมีลักษณะตรงและยาว โดยทั้งสองส่วนถูกล้อมรอบด้วยเยื่อหุ้มเซลล์ ส่วน
ของไมโทคอนเดรียมีลักษณะการจัดเรียงตัวเป็นแบบแถวยาวขนานไปกับแฟลกเจลลัมเรียกว่า
mitochondrial sleeve   โดยพบเพียงข้างเดียวเท่านั้น ซึ่งเป็นลักษณะเฉพาะต่างจากหมึกชนิด
อื่น ขณะเดียวกันส่วนของแฟลกเจลลัมจะปรากฏโครงสร้างการจัดเรียงตัวของ axoneme แบบ
9+2

　　　　　　สำหรับการศึกษาการกระจายของฮอร์โมน APGWamide ในสมองและอวัยวะ
สืบพันธุ์ของหมึกแคระตัวเต็มวัยเพศผู้และเพศเมียโดยใช้วิธีอิมมิวโนไซโตเคมี
(Immunocytochemistry)   พบเซลล์ประสาทและใยประสาทที่ผลิตฮอร์โมน APGWamide ใน
สมองของหมึกแคระเพศผู้และเพศเมียตรงตำแหน่งสมองส่วน dorsal basal lobe และ vertical
lobe ของ supraesophageal mass, ส่วน palliovisceral lobe ของ posterior subesophageal
mass และ olfactory lobe ของ optic tract   ผลการศึกษายังแสดงให้เห็นว่าในหมึกแคระเพศผู้
เซลล์ประสาทที่ผลิตฮอร์โมน APGWamide มีมากที่สุดอยู่ในสมองส่วน palliovisceral lobe และ
olfactory lobe เช่นเดียวกับในหมึกแคระเพศเมียพบเซลล์ประสาทที่ผลิตฮอร์โมนชนิดนี้สูงที่สุด
ในสมองส่วน palliovisceral lobe และ olfactory lobe สำหรับจำนวนเซลล์ประสาทที่ผลิต
ฮอร์โมน APGWamide ในสมองของหมึกแคระ *I. pygmaeus* เพศผู้นั้นมีค่าสูงกว่าของเพศเมีย
อย่างมีนัยสำคัญทางสถิติ　　　　　นอกจากนี้ในการศึกษายังพบใยประสาทที่ผลิตฮอร์โมน
APGWamide   ตรงบริเวณอวัยวะสืบพันธุ์และเยื่อเมนเทิลในชั้นกล้ามเนื้อของหมึกแคระเพศผู้
ด้วย แต่ไม่พบในเพศเมีย

　　　　　　การศึกษาครั้งนี้ได้พบความสัมพันธ์เชิงบวกระหว่างความยาวลำตัวเพศผู้กับ
ความยาวของถุงเก็บสเปิร์ม (r= 0.417) ซึ่งข้อมูลนี้จะเป็นประโยชน์ต่อการคาดคะเนความ
สมบูรณ์หรือความพร้อมในการสืบพันธุ์ของหมึกแคระเพศผู้จากขนาดลำตัว ส่วนหมึกแคระเพศ
ผู้สามารถปล่อยเซลล์อสุจิได้อย่างต่อเนื่องเช่นเดียวกับเพศเมียที่สามารถวางไข่ได้อย่างต่อเนื่อง
ในช่วงฤดูผสมพันธุ์ในเดือนมกราคม สิงหาคมและเดือนตุลาคม การศึกษาครั้งนี้เป็นครั้งแรกที่มี
การรายงานโครงสร้างโดยละเอียดของกระบวนการสร้างเซลล์สืบพันธุ์ในสกุล Idiosepius และ
การกระจายของฮอร์โมน APGWamide ในสมองของหมึกแคระทั้งสองเพศและในระบบสืบพันธุ์
ของเพศผู้ ผลการศึกษาฮอร์โมนชนิดนี้ยังชี้ให้เห็นถึงบทบาทของฮอร์โมน APGWamide ในการ
ควบคุมการสืบพันธุ์ในหมึกแคระเพศผู้ด้วย

Thesis Title   Reproductive Biology and Distribution of Neuropeptide

APGWamide in the Brain and Reproductive Organs of

Pygmy Squid, *Idiosepius pygmaeus* (Steenstrup, 1881)

Author   Mrs. Pattanasuda Sirinupong

Major Program   Biology

Academic year   2011

ABSTRACT

The study of the tiniest cuttlefish, *Idiosepius pygmaeus* Pygmy squid, was conducted in the aspect of its reproductive biology and the distribution of neuropeptide APGWamide in its brain and reproductive organs. The total 190 samples of adult *I. pygmaeus*, monthly collected from the Andaman Sea near Sarasin Bridge, Phuket province, for a period of 12 months between January 2008 - December 2008, showed that the females of *I. pygmaeus* were on average significantly larger (P< 0.0001) than the males, both by dorsal mantle length and by weight. This study also revealed that their spermatophore length varied significantly in accordance with their dorsal mantle length (P=0.02) and the dorsal mantle length of both sexes gradually increased until spawning stage. The monthly variation in sex ratio was significantly different (P<0.05) with the excess of males up to 7:3 ratio when estimated from the total number of specimens. The histological examination of adult *I. pygmaeus* divided their gonadal development into four stages: immature, maturing, pre-spawning (for females) or mature (for males), and spawning. Gonadal index curves for both sexes showed high values synchronously in January, August and October which implied the initiating periods of the breeding seasons. TEM analysis was applied to male specimens to record their spermatogenesis ultrastructure as well as their spermatogenic cells including spermatogonia, spermatocytes, spermatids and spermatozoa. Mature spermatozoon was identified by the presence of three parts: the head, the midpiece and the flagellum. The head consisted of an elongated acrosomal complex and a long straight nucleus, with plasmalemma surrounding them entirely. In the midpiece, the mitochondria of the sperm appeared only on one side with straightly arranged outline, called "mitochondrial sleeve", along the flagellum. This

characteristic was unique to *I. pygmaeus*. In the flagellum of the mature sperm a normal "9 + 2" axoneme arrangement was found.

The distribution of neuropeptide, APGWamide in the brain and reproductive organs of adult, sexually mature male and female specimens of *I. pygmaeus* using immunocytochemistry was investigated. Experiments showed that APGWamide–immunoreactive neurons and fibers were localized in the dorsal basal and vertical lobes of the supraesophageal mass, the palliovisceral lobe of the posterior subesophageal mass, and the olfactory lobe of the optic tract in male and female brains, with the highest number of APGWamide-immunoreactive neurons in the palliovisceral and olfactory lobes in males. In the female *I. pygmaeus* brain, only the palliovisceral and olfactory lobes contained APGWa-immunoreactive neurons, with siginificantly less in number of APGWamide-immunoreactive neurons than in males. Furthermore, APGWamide-immunoreactive fibers were localized exclusively in male reproductive organs and mantle muscles.

The study indicated a positive correlation between dorsal mantle length and spermatophore length which was used to estimate the perfect reproduction in male *I. pygmaeus*. The assessment of the reproductive cycle of *I. pygmaeus*, the Pygmy squid, confirmed that this species is a continuous spawner with breeding seasons in January, August and October. Both the ultrastructure of spermatogenesis and the distribution of APGWamide in the Pygmy squid were here observed for the first time. The presence of APGWamide immunoreactivity especially in the male brain and reproductive organs strongly indicated the role of APGWamide neurohormone in controlling the reproduction of the male *I. pygmaeus*.

ACKNOWLEDGEMENTS

CONTENTS

CONTENTS (Continued)

CONTENTS (Continued)

LIST OF TABLES

LIST OF FIGURES

LIST OF FIGURES (Continued)

LIST OF ABBREVIATIONS AND SYMBOLS

A	=	Arm
Ac	=	Acrosome
ANOVA	=	Analysis of variance
APGWamide	=	Ala-Pro-Gly-Trp-NH2
ASM	=	Anterior subesophageal mass
ax	=	Axoneme
bm	=	Buccal mass
BW	=	Body weight
CC	=	Ceacum
cGnRH-I	=	Chicken gonadotropin-releasing hormones I
CNS	=	Central nervous system
Cyt	=	Cytoplasm
DAB	=	Diaminobenzidine
dbl	=	Dorsal basal lobe
DML	=	Dorsal mantle length
DSc	=	Diplotene spermatocyte
es	=	Esophagus
et al.	=	Et. Ali (Latin), and others
ey, EY	=	Eye
f	=	Flagellum
F	=	Funnel
Fc	=	Follicle cell
Fe	=	Follicular epithelium
Fm	=	Female
FMRFamide	=	Phe-Met-Arg-Phe-N
Fs	=	Follicular syncytium
G	=	Gills
GD	=	Distal part of genital duct
GI	=	Gonadal index

LIST OF ABBREVIATIONS AND SYMBOLS (Continued)

gld	=	Gladius
GnRH	=	Gonadotropin-releasing hormone
HRP	=	Horseradish peroxidase
ibl	=	Inferior buccal lobe
IgG	=	Immunoglobulin G
IM	=	Incubation medium
L	=	Longitudinal muscle
LS	=	Longitudinal section
LSc	=	Leptotene spermatocytes
m	=	Male
M	=	Mitochondria
Ma	=	Muscular layer of mantle
MC	=	Mantle cavity
ML	=	Muscle layer
ms	=	microtubular sheath
MSM	=	Middle subesophageal mass
MT	=	Middle tunic
n	=	Number
N	=	Nucleus
NA	=	Non-available
ND	=	Not determined
Nf	=	Number of females
NF	=	Darkly stained immunoreactive nerve fibers
nfb	=	Nerve fiber
NG	=	Nidamental glands
Nm	=	Number of males
nr	=	Nerve ring
ns	=	Not significant
NS	=	Needham's sac

LIST OF ABBREVIATIONS AND SYMBOLS (Continued)

Nt	=	Total number of males and females
Nu	=	Nucleolus
Ofl	=	Olfactory lobe
OL	=	Optic lobe
OT	=	Outer tunic
OTR	=	Optic tract region
OV	=	Ovary
P	=	Penis
Pa	=	Proacrosome
PBS	=	Phosphate buffered saline
PEM	=	Periesophageal mass
PG	=	Prostate gland
pl	=	Plasmalemma
Pm	=	Perinuclear microtubule
PNS	=	Peripheral nervous system
ppt	=	Parts per thousand
Psc	=	Primary spermatocyte
PSc	=	Pachytene spermatocyte
PSM	=	Posterior subesophageal mass
pvl	=	Palliovisceral lobe
r	=	Correlation coefficient
RER	=	Rough endoplasmic reticulum
RIA	=	Radioimmunoassay
RT	=	Room temperature
sa	=	Subacrosome
sbl	=	Superior buccal mass
SBM	=	Subesophageal mass
Sc	=	Spermatocytes
SC	=	Significance of correlation

LIST OF ABBREVIATIONS AND SYMBOLS (Continued)

Sd   =   Spermatid

SD   =   Standard deviation

Sg   =   Spermatogonia

SM   =   Sperm mass

SP   =   Spermatophore

SPM   =   Supraesophageal mass

SPS   =   Spermatophoric sac

Ssc   =   Secondary spermatocyte

st   =   Statocyst

St   =   Stage

Sz   =   Spermatozoa

T   =   Transverse muscle

TE   =   Testis

TEM   =   Transmission electron microscope

TKMCT   =   Tukey-Kramer multiple comparisons test

TS   =   Transverse section

VD   =   Vas deferens

vtl   =   Vertical lobe

Zsc   =   Zygotene spermatocyte

CHAPTER 1

INTRODUCTION

The species of the cephalopod group exhibit a remarkable diversity of size and form with their body sizes ranging from a dwarf to a giant. Many cephalopods such as cuttlefishes (*Sepia* sp.), squids (*Loligo* sp.), and octopods (*Octopus* sp.), are of considerable economic importance to human beings. Furthermore, they are vital to ecosystem. The smallest currently known cephalopod: *Idiosepius pygmaeus* is not significant economically at present, but it is crucial ecologically because it has an important role as a secondary and tertiary consumer in the trophic chain. The scarcity in its number and related information led to this research on *I. pygmaeus* in the Andaman Sea, specifically around Sarasin Bridge in Phuket Province.

There have only been two studies on *I. pygmaeus*: on its reproductive seasons (Jackson, 1992) and its feeding behaviour (Semmens et al., 1995). Its reproductive biology has never been investigated although there have been intensive researches in the same area on other species in cephalopod group such as *Sepietta oweniana* (Salman, 1998); *Loligo vulgaris* (Krstulovic Sifner and Vrgoc, 2004); *Sepia officinalis* (Onsoy and Salman, 2005); *Octopus vulgaris* (Hernandez-Garcia et al., 2002; Otero et al., 2007) and *Rossia macrosoma* (Salman and Onsoy, 2010). Since there is a small population of *I. pygmaeus* in Thailand, its reproductive biology needs foremost attention. This thesis concentrated on the structure of its reproductive organs, the structure of gametogenesis, and the neurohormones affecting its reproduction, particularly APGWamide (APGWa).

Concerning the structure of reproductive organs of *I. pygmaeus*, this work examined the dorsal mantle length - body weight and dorsal mantle length - spermatophore length relationships, sex ratios, histology of gonads, changes of dorsal mantle length in various gonadal stages of males and females, gonadal index (GI), and reproductive cycles.

The study on the gametogenesis in *I. pygmaeus* included both males and females. This kind of investigation has never been carried out although there have

been extensive studies on gametogenesis in other genera and species. For example, there have been publications on spermatogenesis in cephalopods using transmission electron microscope (Grieb and Beeman, 1978; Healy, 1990a, b, 1993; Zhu et al., 2005), on the relationship between *V. infernalis* and *Octopus* (Healy, 1990a), and on similarities of ultrastructure between *Octopus* and *Eledone* during spermiogenesis (Selmi, 1996). As for the ultrastructural analysis of oogenesis in cephalopods there has been only a descriptive report by Botteke (1974). While these researchers used only a light microscope or a transmission electron microscope in their studies, this thesis used both microscopes for spermatogenesis and a light microscope for oogenesis of *I. pygmaeus*. Providing detailed illustrations of the species'gametogenesis, this method is hoped to help prevent its extinction and to offer a tool for observing any relationship between *I. pygmaeus* with other *Idiosepius* species and differences between *Idiosepius* species and other cephalopods.

As for neurohormones affecting the reproduction of *I. pygmaeus*, this study focused on APGWamide. Neurohormones are involved in the gametogenesis control in the reproduction of invertebrates. The neurohormones are triggered by a stimulus, usually an external factor such as photoperiod, water temperature, water quality, tides and cycles of the moon, and nutrition (Rottmann et al., 1991). Various reproductive neurohormones have been studied, such as APGWamide in *Sepia officinalis* (Henry and Zatylny, 2002) and *Octopus vulgaris* (Di Cristo et al., 2005); FMRFamide in *O. vulgaris* (Di Cristo et al., 2003) and *I. notoides* (Wollesen et al., 2008); and GnRH in *L. bleekeri* (Amano et al., 2008) and *O. vulgaris* (Di Cristo et al., 2002). The neuropeptide, APGWamide (APGWa) or Ala-Pro-Gly-Trp-NH_2 plays an important role as a neurotransmitter and a neuromodulator in the control of reproductive behavior in several species of molluscs (Oberdorster et al., 2005). Apart from being found in the brain, APGWa containing axons was found in the reproductive organs of the gastropod, *Lymnaea stagnalis* (Croll and Van Minnen 1992; De Lange and Van Minnen 1998) and of the sea scallop, *Placopecten magellanicus* (Smith et al., 1997). The expression of APGWa and its role in male reproductive process were detected in the testis of *Haliotis asinine* (Chansela et al., 2008). In the cephalopod, *Octopus vulgaris*, APGWa containing neurons occured in the central nervous system, whereas the oviducal gland was innervated by APGWa

immunoreactive axons (Di Cristo et al., 2005; Di Cristo and Di Cosmo 2007). In the cuttlefish, *Sepia officinalis*, APGWa inhibits the motility of the mature oviduct (Henry et al., 1997). This thesis revealed that APGWamide also appeared in some lobes of the brain of *I. pygmaeus*, that it linked with different stages of gonadal development, and that the distributions of APGWa in the central nervous system and reproductive organs of *I. pygmaeus* were correlated.

Literature review

1. Biology of Pygmy squid, *Idiosepius pygmaeus*

1.1 Taxonomy *Idiosepius pygmaeus* has been classified (Ruppert et al., 2004) as follows:

Phylum   Mollusca

Class   Cephalopoda

Subclass   Coleoida

Order   Sepiolida

Family   Idiosepiidae

Genus   Idiosepius

Species   *Idiosepius pygmaeus*
(Steenstrup, 1881)

Idiosepius pygmaeus is the smallest species in size, with the maximum size of mature males and females on average being 17 and 22 mm in dorsal mantle length, respectively (Fig. 1). The mantle is characteristically rather elongate and slightly pointed at the posterior end, then the location of the dorsal mantle appears the structure as oval attachment organ called "adhesive organ" for attaching the substrates (Nabhitabhata, 1998). Both small fins are kidney-shaped and attached to the lateral side in the posterior end of the mantle. There is no fusion between the anterior edge of mantle and the head including without the nuchal cartilage. The large head is prominent while the bulbous eyes are covered by corneas (Lu and Dunning, 1998). In *I. pygmaeus*, there are 2 rows of suckers on sessile arms and 2-4 rows on tentacular

club (Hylleberg and Nateewathana, 1991a, b). Both ventral arms of mature male are modified as hectocotylised arms. This species is known as having a short lifespan and inhabiting seagrass beds and algae. Generally, it is found in the region of mangroves area in the Andaman Sea of Phuket Island (Hylleberg and Nateewathana, 1991a, b) and the tropics from Southeast Asia to Australia (Jackson, 1992; Lewis and Choat, 1993). It feeds on wild copepods and mysids (Nabhitabhata, 1994a, b, 1998).
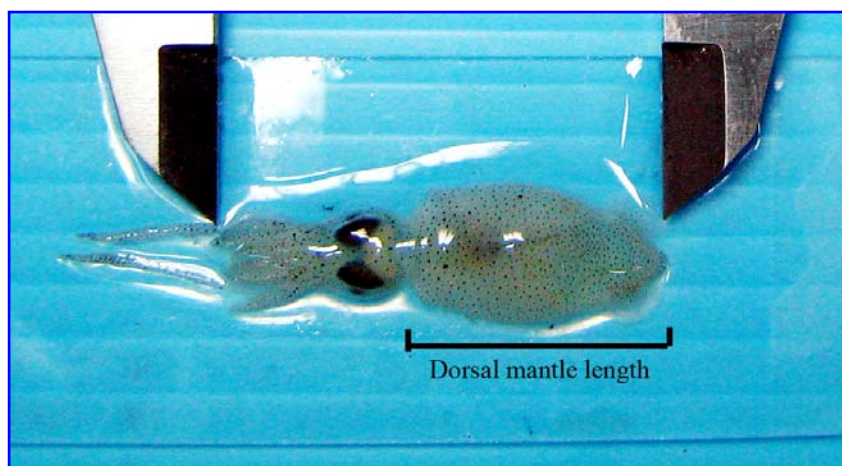
Figure 1.   External morphology of *I. pygmaeus*.

2. Reproductive biology

2.1 Reproductive organ

Idiosepius pygmaeus is dioecious and the *Idiosepius* male has a complicated system of spermatophoric glands. The spermatophoric sac includes many spermatozoa that are packed in form of "spermatophore" within the spermatophoric gland and occupies half of the length of individual spermatophores. In the region of the spermatophoric organs, testis, glands and prostate are tightly packed together on the left hand side, and its penis is rather short (Fig. 2A). Cement body, supporting cylinder, and ejaculatory apparatus constitute the other half while ejaculatory apparatus is coiled, terminated with long filament. A large ovary of *Idiosepius* female is located at the posterior body and connected with both oviduct and oviducal gland. Its oviduct is only functional at the left side and contains mature oval eggs. The

oviduct extending from the oviducal gland opens via the female gonopore into the mantle cavity and is located in anterior to the left branchial heart (Fox, 2001). The released mature eggs from the ovary pass into the oviduct and spawn later (Boyle and Rodhouse, 2005). Next to the nidamental glands is a huge paired organ in the ventral body as an elongated oval with short lips at anterior ends and to aid in development of the egg. Generally, these glands are involved in secretion of egg cases or the jelly of egg masses – they are composed of numerous lamellae (Fig. 2B) (Young et al., 1999). The accessory nidamental glands of *I. pygmaeus* are located next to the nidamental gland and do not project anterior to the nidamental glands (Modified from Hylleberg and Nateewathana, 1991a, b).
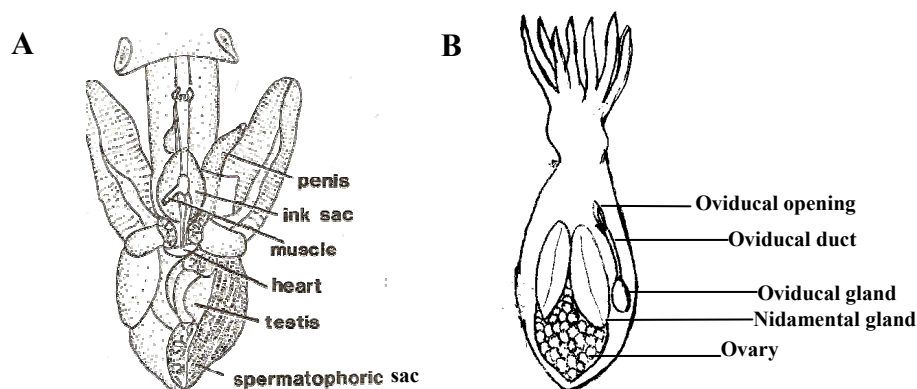
Figure 2.   Diagram of the reproductive organ of *I. pygmaeus*. **A**: male. **B:** female (A: Hylleberg and Nateewathana, 1991a, b; B: from author).

2.2 Breeding, gonad index and reproductive cycle

The *Idiosepius pygmaeus* has a short life-span of about 3 months only (Boletzky, 2003). During mating, *I. pygmaeus* male transfers its spermatophores into the buccal region of the female and the mating occurs in a head–to–head position (Lewis and Choat, 1993). Gonad index has been used to study the reproductive cycle of Invertebrates including *I. pygmaeus* as it can resolve, as a quantitative measure, monthly fluctuations in gonadal development for both sexes. The reproductive cycle of this genus was only studied in *Idiosepius paradoxu*s from Zostera beds on the coast of central Japan using histological analysis. The results showed that the spawning periods in *I. paradoxus* took place for the small sizes in summer from June to October and for the large sizes in spring from November to May; a seasonal size variation was

observed for adults, apparently representing different generations. Also environmental effects such as the photoperiod affected spermatogenesis and spawning (Kasugai et al., 2003). However, the data on reproductive cycle of *I. pygmaeus* from the Andaman Sea, Phuket province has not yet been observed and studied here.

2.3 Oogenesis and spermatogenesis with the gonadal development

The ovary of a mature *Idiosepius* female holds simultaneously many stages of developing oocytes, and maturation occurs continuously with an asynchronous ovulation pattern. This pattern differs from other cuttlefish, such as the *Sepia* species, which has a synchronous ovulation pattern (Laptikhovsky et al., 2007). The developing oocytes in *Idiosepius* species have a pattern similar to other cephalopods as a follicular epithelium surrounds the ova. The follicle cells attach to the surface of newly formed oocytes, proliferate and invaginate into the cytoplasm. Consequently a syncytium is formed by fusion (Arnold and Williams-Arnold, 1977). Histological analysis has been extensively used for examining the stages of oogenesis in various cephalopods species, such as in *Loligo gah*i (Laptikhovsky and Arkhipkin, 2001), *L. opalescens* (Knipe and Beeman, 1978), and *Alloteuthis subulata* (Bottke, 1974), and their oogenesis has been characterized with eight, six, and three stages, respectively. Such staging is subjective and depends on the individual researchers, who have to consider the degree of follicular cell development in association with oogonia and oocytes. The staging is also somewhat arbitrary by its nature, a difficulty more pronounced with females than with males.

For instance, the stages of gonadal development of *Sepia pharaonis* and *S. dollfusi* can be divided into four stages: stage I immature, stage II maturing, stage III pre-spawning and stage IV spawning, respectively (Gabr et al., 1998). These are similar to those of *Octopus vulgaris* (Rodriquez-Rua et al., 2005). In *Rossia* spp. and *Neorossia* spp. as known in the family Sepiolidae, the gonadal development was divided into four stages as stage I immature, stage II maturing, III mature and stage IV spent (Labtikhovsky et al., 2008). Generally, in male cephalopod, the spermatogenesis will explain all types of germ cells, namely spermatogonia, spermatocytes, spermatid, and spermatozoa found in each seminiferous tubule. Its spermatogenesis is used for determining the stages of gonadal development similar to

the oogenesis of female. Previous researches on various species, such as *S. pharaonis* and *S. dollfusi* (Gabr et al., 1998), *O. vulgari*s (Rodriquez-Rua et al., 2005), *Rossia* spp. and *Neorossia* spp (Labtikhovsky et al., 2008) have shown a similar pattern in the testicular stages.

The ultrastructural technique has been used to clarify oogenesis and spermatogenesis by examining ultrastructural changes of ovary and testis in a mature cephalopod. Various data on oogenesis and spermatogenesis in the cephalopod group have been reported by using electron microscope techniques to provide clear reproduction information in accordance with individual species evolution. Ultrastructural characterization during oogenesis and spermatogenesis has been reported for a number of cephalopods including *Alloteuthis subulata (*Bottke, 1974), *Vampyroteuthis infernalis* (Healy, 1990a), *Spirula spirula* (Healy, 1990b), *Opisthoteuthis Persephone* (Healy, 1993), *O. tankahkeei* (Zhu et al., 2005), *S. officinalis* (Martinez-Soler et al., 2007).

One part of this work, therefore, was to study the gametogenesis of *I. pygmaeus* with concentration on the ultrastructure during spermatogenesis.

2.4 Neuropeptides involved in the cephalopod reproduction

In recent years, neuropeptides have been extensively studied in the phylum mollusca, including, for example, gastropods and the cephalopod groups of bivalves. However, few studies of neuropeptides in cephalopods exist currently. The most important neuropeptides known to play a role in the reproductive process include GnRH, FMRFamide, and APGWamide. GnRH is the Gonadotropin-releasing hormone. It was first isolated from brain of *O. vulgaris* and the structural pattern of this peptide is similar to that of the vertebrate (Iwakoshi et al., 2002). The expression and distribution of GnRH in the central nervous system (CNS) was observed in situ hybridization and immunohistochemical analysis in *O. vulgaris*. A specific antiserum against GnRH revealed its presence in the subpedunculate lobe, posterior olfactory lobe and optic gland. In addition, the peripheral organs, namely heart, oviduct, and oviducal gland have many immunoreactive fibers (Iwakoshi-Ukena et al., 2004). Di Cosmo and Di Cristo (1998) studied both of the neuropeptides GnRH and FMRFamide in the optic gland region of *O. vulgaris* using immunohistochemical

analysis. The results are in agreement to those of Iwakoshi et al. In a cephalopod, the optic gland is an important endrocrine organ that controls the gonadal maturation (Wells and Wells, 1959). In 2002, both neuropeptides (cGnRH-I and FMRFamide) were found in cell bodies and fibers of the fusiform ganglion and reproductive ducts, the oviducal gland and seminal vesicle of *O. vulgaris,* using immunohistochemical analysis (Di Cristo et al., 2002). The published results support the hypothesis that in *O. vulgaris* both cGnRH-I and FMRFamide are linked to control of the reproductive ducts (Di Cristo et al., 2002).

Similar to other investigations of GnRH, it was also found in the brain and ovary of *Sepia officinalis* (Di Cristo et al., 2009). In *Loligo bleekeri* the GnRH-like immunoreactive cell bodies were found in the central and outer part of the ventral magnocellular lobe, olfactory lobe, palliovisceral lobe, and the optic gland including the fibers of the brain region (Amano et al., 2008). In 1987, the tetrapeptide, FMRFamide was first found in the neurosecretory system of vena cava in *O. vulgaris*. Later, there was a report of CNS of *S. officinalis* by Le Gall et al. in 1988. In 1994, the study on FMRFamide in *L. pealei* by using RIA and radioligand receptor assays indicated the presence of this neuropeptide in optic lobes (Chin et al., 1994). Later on the neuropeptide FMRFamide has been studied, also using immunohistochemical analysis. The presence of FMRFamide in CNS, such as optic, olfactory and subpedunculate lobes including the peripheral nervous system (PNS) of *O. vulgaris* was studied and revealed by Di Cosmo and Di Cristo, 1998 and Di Cristo et al., 2002, 2003. Immunohistochemical techniques have been extensively used with other cephalopods such as *S. officinalis* (Le Gall et al., 1988) and *I. notoides* (Wollesen et al., 2008). *I. notoides* was the first *Idiosepius* species in which the neuropeptides were detected by immunohistochemical analysis. The experiment showed the distribution of FMRFamide in the CNS as well as the immunoreactivities in dorsal basal, central palliovisceral, olfactory, and optic lobes but it was not found in the middle subesophageal mass (Wollesen et al., 2008). Additionally, APGWamide also plays an important role in the cephalopod reproduction, similar to the other neuropeptides discussed above.

3. The structure and function of *Idiosepius* brain

The *Idiosepius* brain has 4 main parts: the ventrally located subesophageal mass (SBM), the dorsally located supraesophageal mass (SPM) and a pair of optic lobes. The subesophageal mass can be subdivided into anterior (ASM), middle (MSM), and posterior (PSM) subesophageal masses (Fig. 3). The ASM consists of two lobes, the prebrachial lobe and the brachial lobe. They function as intermediates for arm movement. The middle subesophageal mass consists of four lobes: anterior chromatophore lobe (controlling the skin in arms and head), anterior pedal lobe (controlling the arm movement), posterior pedal lobe (controlling the swimming center), and ventral magnocellular lobe (controlling the jet propulsion). The posterior subesophageal mass consists of six lobes: dorsal magnocellular lobe (controlling the jet propulsion), posterior magnocellular lobe (controlling the escape reaction), palliovisceral lobe (controlling the muscles), visceral lobe (center of viscera), fin lobe (controlling the fin action), and posterior chromatophore lobe (controlling the color change). The supraesophageal mass (SPM) consists of 20 lobes: subpedunculate lobe (controlling the ocular pressure), precommissure lobe (unknown function), anterior basal lobe is composed of anterior anterior basal lobe, lateral anterior basal lobe and posterior anterior basal lobe controlling the steering, posterior basal lobes are composed of median basal lobe, dorsal basal lobe (controlling the steering and jet proplusion), lateral basal lobe (controlling control the color change) and interbasal lobe (controlling the tentacle movement), while the vertical lobe complex is composed of inferior frontal lobe (learning and memory for tactile information), superior frontal lobe (learning and memory for visual information), subvertical lobe (unknown function), and vertical lobe (learning and memory for visual and tactile information). The regions of optic tract (OTR) are laterally connected to SPM by the optic lobes. The optic lobes are composed of olfactory lobe (control center of olfactory information), peduncle lobe (control center of visuomotor information) and dorso-lateral lobe (control center of olfactory information). The pair of optic lobes functions as a visual center. Normally, paired and unpaired brain lobes are included together in the brain region. (Yamamoto et al., 2003; Shigeno and Yamamoto, 2002).
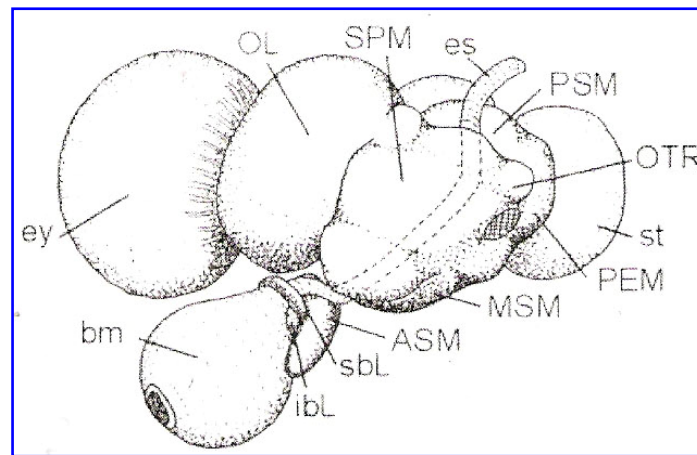
Figure 3.   Diagram of brain in *I. pygmaeus* (Shigeno and Yamamoto, 2002). (**Abbreviations**: ASM= anterior subesophageal mass, bm= buccal mass, es= esophagus, ey= eye, ibl= inferior buccal lobe, MSM= middle subesophageal mass, OL= optic lobe, OTR= optic tract region, PEM= periesophageal mass, PSM= posterior subesophageal mass, sbl= superior buccal mass, SPM= suprasubesophageal mass, st= statocyst).

4. APGWamide in Invertebrate

The neuropeptide, APGWamide has been studied extensively in the invertebrate animal groups for its controlling role in male reproduction. Specifically, there have been studies of this neuropeptide in molluscs group including gastropods, bivalves, and cephalopods and, very recently, also in crustaceans. The majority of this neuropeptide has been detected in the central nervous system and the peripheral organs (Kuroki et al., 1990; Chen and Walker, 1992; Croll and Van Minnen, 1992; Griffond et al., 1992; Smith et al., 1992; Favrel and Mathieu, 1996; De Boer et al., 1997; Fan et al., 1997; Henry et al., 1997; Macrohan and Croll, 1997; Smith et al., 1997; De Lange and Van Minnen, 1998; Di Cristo et al., 2005; Chansela et al., 2008, 2010; Palasoon et al., 2011).   In the first reference, for example, the neurons containing the neuropeptide, APGWamide were found in the ganglia of prosobranch, *Fusinus ferrugineus*, affecting the contraction of some muscles (Kuroki et al., 1990). The presence of this neuropeptide has also been detected in several ganglions within the brain of snails, *Lymnaea stagnalis*, both in the right anterior and ventral lobes of

cerebral ganglia and in the region between cerebral and buccal ganglia. In the region of cerebral ganglia there are nerves connected to the eyes and the tentacles, while in the buccal ganglion the nerves connect to the radula and the mouth affecting feeding function. The neuropeptide has also been found in other ganglia such as in the visceral, right pedal and parietal ganglia which have nerves connected to the visceral mass, foot muscles, and gill and olfactory organs, respectively. Besides, various studies have reported the expression of APGWamide in the nerve fibers within male reproductive organ such as penis, prostate gland and vas deferens (Croll and Van Minnen, 1992; Smith et al., 1992; De Boer et al., 1997). In contrast, in the snail *Helix aspersa*, neurons containing APGWamide were not detected in pedal ganglia (Griffond et al., 1992). In sea scallop, *Placopecten magellanicus*, the presence of this neuropeptide was mostly detected in pedal, cerebral and parietovisceral ganglia of the central nervous system and in the gonad (Smith et al., 1997). In the sea slug, *Aplysia californica*, which is a hermaphrodite animal, the presence of APGWamide was also found in the central nervous system and the region of male reproductive organs – similar to other non-hermaphrodite gastropods (Fan et al., 1997; De Lange and Van Minnen, 1998). In addition, presence of the neuropeptide APGWamide has only been observed in the testis of abalone, *Haliothis asinine*, suggesting this neuropeptide affects male reproductive control (Chansela et al., 2008, 2010). Similar to observations in gastropods, the presence of APGWamide has been reported in the central nervous system of bivalve, *Mytilus edulis* (Favrel and Mathieu, 1996). For the crustaceans such as the giant freshwater prawn, *Macrobrachium*, APGWamide is present within the sinus gland (SG) of its eyestalk; the neuropeptide modulates the release of neurohormones in this gland (Palasoon et al., 2011). Moreover, this neuropeptide was also found in the central nervous system and the reproductive organ of cephalopod groups such as the cuttlefish, *Sepia officinali*s (Henry et al., 1997) and *Octopus vulgaris* (Di Cristo et al., 2005).

5. APGWamide and other neuropeptides in Cephalopoda

APGWamide in the cephalopod groups has not been sufficiently studied. APGWamide (Ala-Pro-Gly-Trp-NH$_2$) is an amidated tetrapeptide. It is related to the control of the cephalopod reproduction. The first relevant publication dates back to 1997, showing the presence of this neuropeptide in the optic lobe of mature *Sepia officinalis*. The observations suggested that it can cause inhibition of the oviductal motility (Henry et al., 1997). Next, in 2005, a study on the local presence of APGWamide in *O. vulgaris* reported use of immunohistochemical analysis for detection (Di cristo et al., 2005). The immunoreactivity to APGWamide in neurons and fibers was confined to just the posterior olfactory lobule (control center of olfactory information) and inferior frontal lobe (learning and memory for tactile information). Both lobes are involved in the control of reproductive behavior. Moreover, this peptide also appears in the reproductive duct of *Octopus* female, particularly in the oviducal gland (Di cristo et al., 2007). Although there are reports on the existence and localization of APGWamide in the cephalopod groups, this neuropeptide has not yet been studied in *I. pygmaeus* and other *Idiosepius* species. Only FMRFamide has been studied in *I. notoides* (Wollesen et al., 2008). Therefore, a gap in body of knowledge can be addressed in this investigation.

Objectives

1. To understand the reproductive biology of *I. pygmaeus* based on samples collected in Andaman Sea, Phuket province, by providing information on the relationships between dorsal mantle length and body weight, dorsal mantle length and spermatophore length, sex ratios, the changes of dorsal mantle length in various gonadal stages of male and female, reproductive cycle, and seasonal changes in gonadal index (GI).

2. To learn about the gametogenesis of *I. pygmaeus* in details, especially the ultrastructure of spermatogenesis.

3. To investigate the neuropeptide, APGWamide in the brain and reproductive organs, and its relation to the gonadal stages of *I. pygmaeus*, by use of immunocytochemical analysis technique for observations.

Benefits

1. To provide new data characteristics of the reproductive biology of *I. pygmaeus* in the Andaman Sea, Phuket province.

2. To offer information about ultrastructure of sperm and spermatogenesis in *I. pygmaeus* for future scientific studies and application.

3. To understand the distribution of APGWamide in *I. pygmaeus.*

4. To distribute the results via international journals.

CHAPTER 2
MATERIALS AND METHODS

1. Study site and specimen collection

The Pygmy squid, *Idiosepius pygmaeus* were monthly collected by random sampling for 12 months from floating baskets in Andaman Sea water near Sarasin Bridge (08° $11^{'}$ $956^{''}$ N, 098° $17^{'}$ $927^{''}$ E) in Mai Kwaw subdistrict, Talang District, Phuket province, Thailand using a dip net (Fig. 4). The location of the study site has three seasons: dry season from mid February to mid May, wet season from mid May to mid October and cool season from mid October to mid February (source: Thai Meteorological Department; http://www.tmd.go.th/index.php). The environmental parameters such as temperature, transparency, alkaline, hardness, ammonia, nitrite, nitrate, phosphate, pH and salinity in the study site were recorded for a one-year period of study (source: Tipaporn Traithong Phangnga Coastal Fisheries Research and Development center). The specimens of *I. pygmaeus* were transfered to laboratory at Department of Biology, Faculty of Science, Prince of Songkla University, Hat Yai, Songkhla province.

2. Stages of gonadal development and reproductive cycle

Pygmy squids were anesthetized in 7% $MgCl_2$. Their dorsal mantle length was measured by using a digital vernier. Then, wet weight was recorded to the nearest 0.001 g and sex identified. In male *I. pygmaeus*, the spermatophores were randomly selected to measure the length with ocular and stage micrometers. Because the external morphology of both sexes of *I. pygmaeus* was not clear enough to identified stages of gonadal development, a histological examination was carried out. As shown in Fig. 5A, detailed anatomical structure of the reproductive system of female *I. pygmaeus*, the ventral part of reproductive organ revealed a large ovary and nidamental glands.
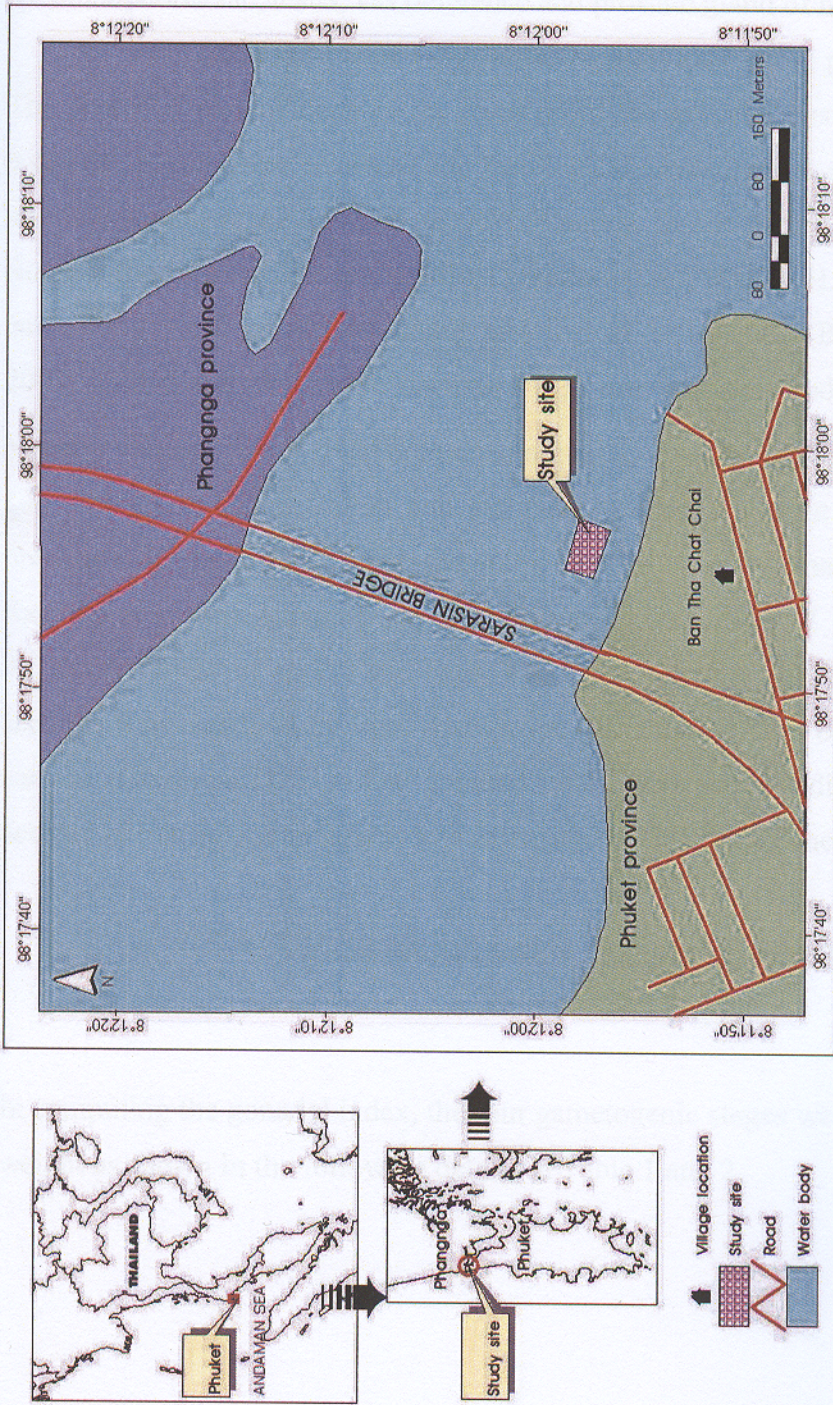
Figure 4. Map of study site and surrounding area. (printed by GEO-Informatics Research Center for Natural Resource and Environment, Prince of Songkla University).

Fig. 5B revealed two gills, gladius and ceacum, while Fig. 5C revealed the spermatophoric sac, testis, vas deference and prostate gland of male *I. pygmaeus*.

Each sample of *I. pygmaeus* was divided into 2 pieces: head and body. The posterior part of body is the location of the gonadal tissue where ovarian and testicular tissue were removed for histological investigation and the head was for immunocytochemical analysis of APGWamide in the brain. Tissue was fixed in Bouin's fluid for 8-12 hours, and then transferred to 70% EtOH. Clearing and paraffin embedding were performed using histological techniques (Bancroft and Gamble, 2002). Ovary and testis were sectioned at 6 μm thickness and stained with Harris's hematoxylin and Eosin (H&E). Stained sections of ovary and testis were examined at 100 and 400X magnification and assigned to a development stage of 4 stages: I: immature, II: maturing, III: pre-spawning (female) /mature (male) and IV: spawning. Examination of the gonadal stages in both male and female *I. pygmaeus* focused on the development of sperm and eggs. The light micrographic images of histological sections were captured by light microscope (Olympus BX51) equipped with a digital camera (Olympus DP71). The gonadal index (GI) as an indicator of reproductive activity of marine invertebrates was calculated as follows (Meneghetti, 2004):

$$GI = \frac{SUM\ (numerical\ weight \times number\ of\ each\ gonadal\ stage)}{Total\ number\ of\ squids}$$

In computing the gonadal index, the four gametogenic stages were assigned numerical weight as shown in the following details in Table 1 and 2.

Table 1. Determination of numerical weight in each stage of male *I. pygmaeus*.

Stage	Numerical weight	Determination
I: Immature	1	Early germ cells start to develop as showing many spermatogonia and rather few spermatocytes.
II: Maturing	2	In the seminiferous tubules, only the spermatogonia, spermatocytes and a few of early spermatid are found.
III: Mature	3	Fully developed spermatozoa are found inside the lumen of seminiferous tubules and other germ cells as spermatogonia, spermatocytes, spermatid still also appear.
IV: Spawning	1	No residual or few spermatozoa within the seminiferous tubules; then the newly developed spermatogonia and spermatocytes start appearing inside the wall of seminiferous tubules.

Table 2. Determination of numerical weight in each stage of female *I. pygmaeus*.

Stage	Numerical weight	Determination
I: Immature	1	The young oocytes or early oocytes (stages 1-4) start appearing inside the ovaries.
II: Maturing	2	The oocytes inside the ovaries continuously developed in stages 5-6.
III: Pre-spawning	3	Development of oocytes inside the ovaries is complete with appearance of all stages of oocytes (1-10).
IV: Spawning	1	Inside the ovaries, only oocyte of stages 8-10 still appear and the onset of new development of early oocytes begins.
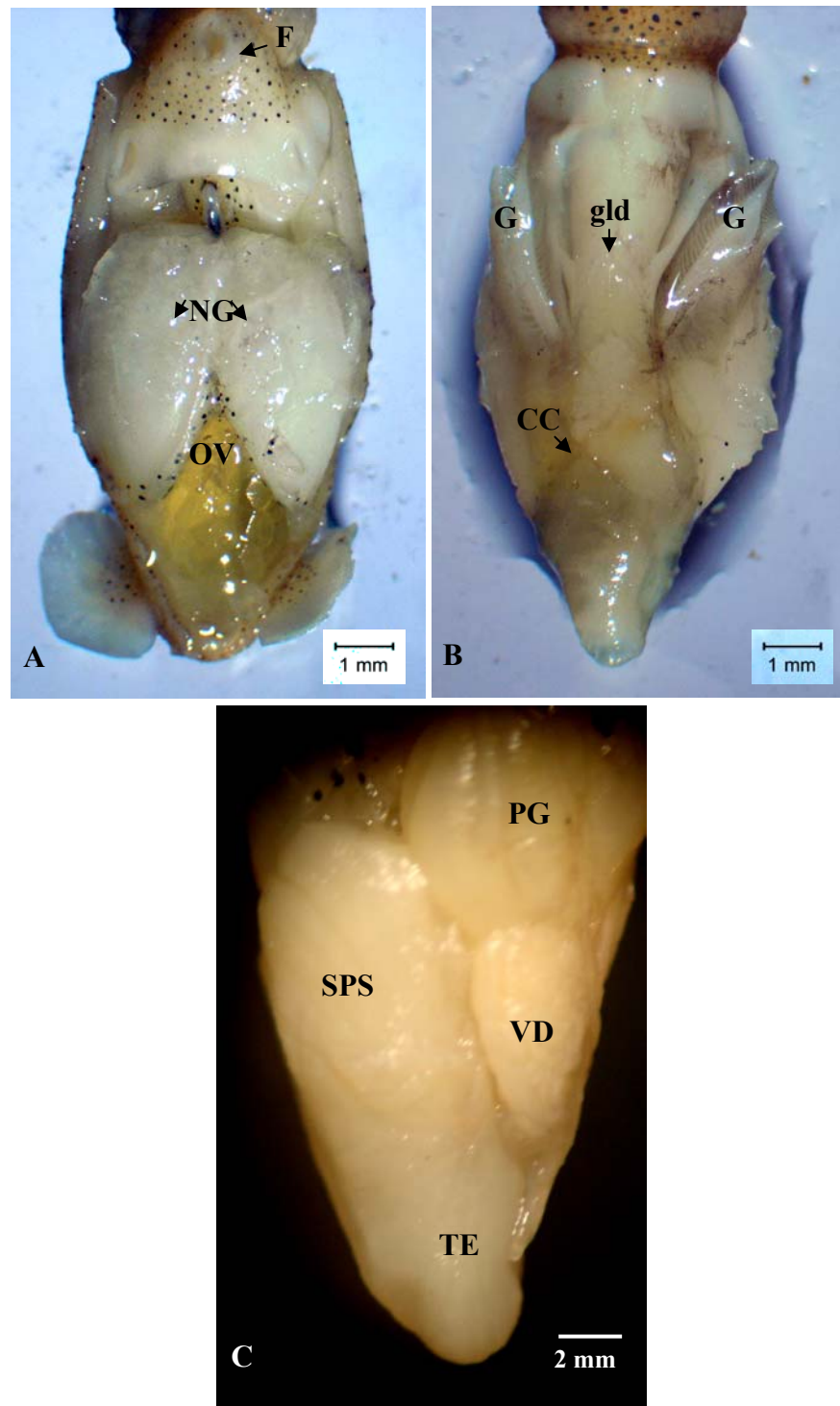
Figure 5. The morphology of reproductive organs of *I. pygmaeus*. **A:** female (ventral). **B:** female (dorsal). **C:** male (ventral). CC= caecum, F= funnel, G= gills, gld= gladius, NG= nidamental glands, OV= ovary, PG= prostate gland, SPS= spermatophoric sac, TE= testis, VD= vas deference.

The percentage occurrence of each gonadal stage of both male and female *I. pygmaeus* in different months was computed by pooling the data for one year and represented graphically. Length distribution in male and female *I. pygmaeus* relate to gonadal stages was shown graphically in our results.

3. Ultrastructural investigations

For transmission electron microscopy, testicular tissue was pre-fixed in 2.5% glutaraldehyde and 2% paraformaldehyde in 0.1 M phosphate buffer, pH 7.4 for 4 h at 4 ^{0}C, then post-fixed in osmium tetroxide, dehydrated through a graded series of acetone and subsequently embedded in the epoxy resin (Epon 812). Thick sections were stained with toluidine blue for light microscopy. Ultrathin sections were stained with uranyl acetate and lead citrate before examined with a transmission electron microscopy (TEM) (Philips Tecnai F20).

4. Immunocytochemical detection

4.1 Immunocytochemistry

Before detecting APGWamide by immunocytochemistry in *I. pygmaeus* brain, some brain sections of *I. pygmaeus* were stained with Harris's hematoxylin and Eosin (H&E) for examining the positions in each brain lobe. The sections of brains and reproductive organs of male and female *I. pygmaeus* received from classification of the gonadal stages which were based on the description of gonadal maturation of *Sepia pharaonis* and *S. dollfusi* (Gabr et al., 1998). As stage III and IV *I. pygmaeus* have fully matured and functional reproductive organs, so this study focused on these stages. Since, this study was unable to collect stage IV male animals, it investigated the occurrence of APGWa-immunoreactivity in stage III animals instead.

Sections of brains and reproductive organs of all stages of males and females were deparaffinized, rehydrated, and washed in phosphate buffered saline (PBS, pH 7.4).Next, they were incubated in rabbit polyclonal anti-APGWamide (1:500; Croll and Van Minnen, 1992) (source: anti APGWamide was generously

provided by Professor Jan van Minnen) in PBS containing 5% normal goat serum for 16-18 hours at 4 ^{0}C, washed 2x in PBS for 10 min, and subsequently incubated with horseradish peroxidase-conjugated swine- anti- rabbit IgG (Pierce, Milan, Italy), diluted 1:100 in PBS/goat serum for 1 h at room temperature. After washing 2x in PBS for 10 min, HRP was visualized by means of 0.05% 3, 3 − diaminobenzidine (DAB) and the sections were subsequently mounted in Entellan. As a control for the immunocytochemical staining, sections were treated with normal rabbit serum (diluted 1:100) instead of the anti-APGWa serum. No immunoreactivity was observed following this treatment (data not shown).

4.2 Quantification of APGWa immunoreactive neurons

The number of anti-APGWamide-positive neurons in the various brain regions of males and females, i.e. the supraesophageal mass (dorsal basal lobe), supraesophageal mass (vertical lobe), posterior subesophageal masses (palliovisceral lobe) and optic tract region (olfactory lobe), were determined in all five stage *I. pygmaeus*. Images were photographed using a BX51 microscope (Olympus) equipped with a DP71 digital camera (Olympus).

5. Statistical analyses

Sex ratio was analysed by a Chi-square test at *P*-value < 0.05 as statistically significant. The relationship between the neuropeptide, APGWamide numbers and gonadal stages was tested by Kruskal-Wallis nonparametric at *P*- value < 0.05. The numbers of anti-APGWamide-positive neurons in the various brain regions were tested for statistically significant differences by means of a one - way analysis of variance followed by Tukey-Kramer multiple comparisons test (TKMCT). The correlations between dorsal mantle length and body weight and dorsal mantle length and spermatophore mean length in a year round were analysed by Pearson's correlation coefficient at *P*- value < 0.05.

CHAPTER 3
RESULTS

1. Biological parameters

1. 1 Length - weight relationships of *I. pygmaeus*

Length-weight relationships in both sexes of *I. pygmaeus* were calculated using linear regression. All the specimens were used in the analysis of length-weight relationship. The DML of *I. pygmaeus* ranged from 10.29 to 18.17 mm in female and 9.17 to 15.17 mm in male. The body weight of female and male was 0.106 to 0.532 g and 0.097 to 0.274 g BW, respectively. The dorsal mantle length in both sexes of *I. pygmaeus* showed significant increase in relation to body weight as revealed by length-weight relationships of male and female. The expression for equations of both sexes was as followed: Males: $BW = 0.002DML^{1.689}$ (n = 129; Pearson's correlation (R) = 0.575; P< 0.0001) (Fig. 6), Female: $BW = 0.0012DML^{2.0405}$ (n = 61; Pearson's correlation (R) =0.764; P< 0.0001) (Fig. 7).
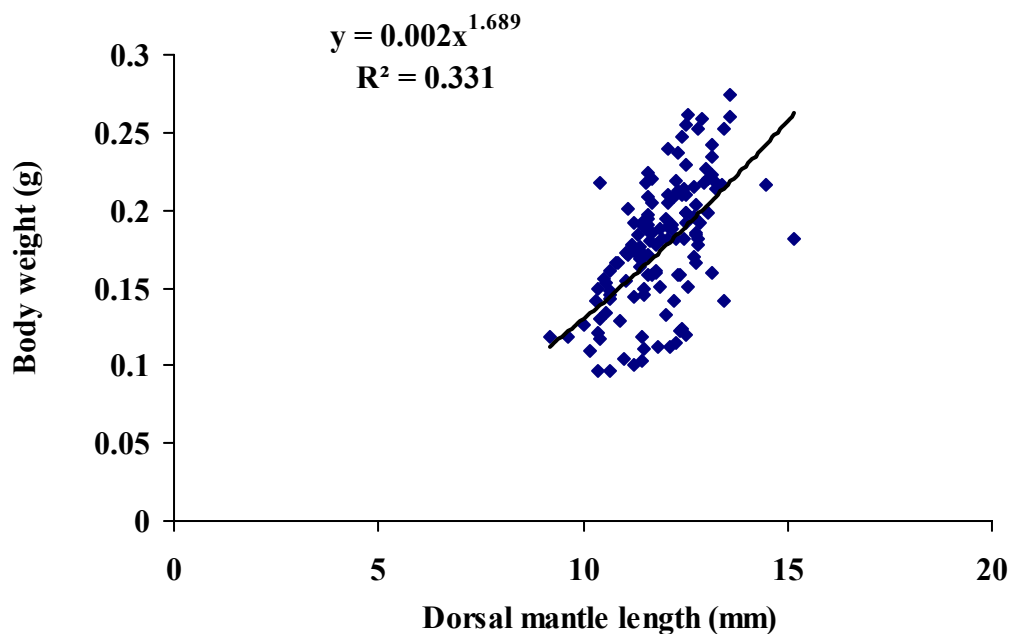
Figure 6. Length-weight relationship in male *I. pygmaeus* (n = 129).

$$y = 0.0012x^{2.0405}$$
$$R^2 = 0.5833$$

Body weight (g)

Dorsal mantle length (mm)
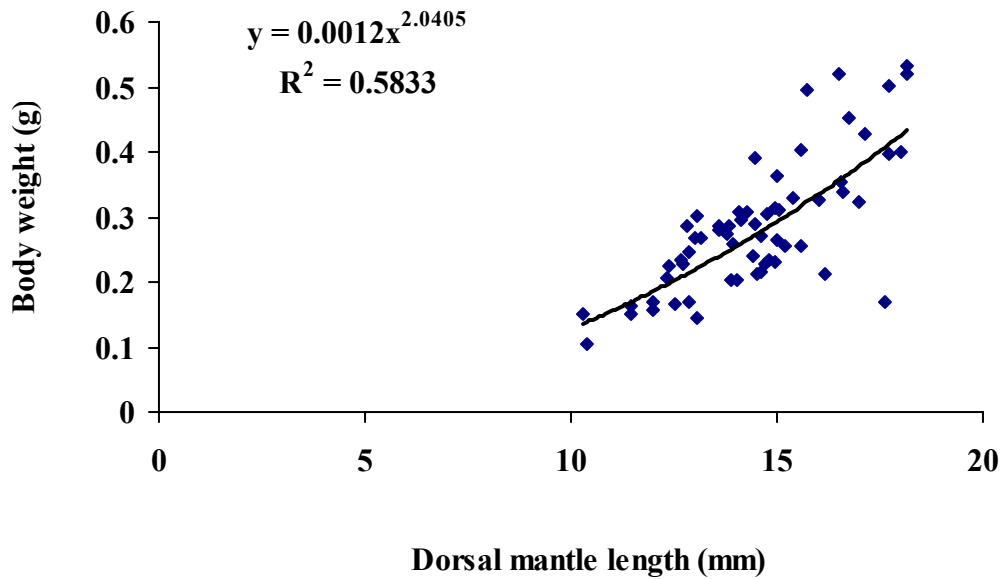
Figure 7.   Length- weight relationship in female *I. pygmaeus* (n = 61).

1.2 Relationship between dorsal mantle length and spermatophore length

Spermatophore lengths of male *I. pygmaeus* were between 1.44 and 2.07 mm (mean 1.58 mm), by considering the dorsal mantle length in each specimen. The relationship between dorsal mantle length and spermatophore length was statistically significantly with equation SP = 0.0726DML + 0.7233 (n = 30; Pearson's correlation (R) = 0.417; P = 0.02), indicating that the dorsal mantle length related to the spermatophore length (Fig. 8).

$$y = 0.0726x + 0.7233$$
$$R^2 = 0.1755$$

Spermatophore length (mm)

Dorsal mantle length (mm)
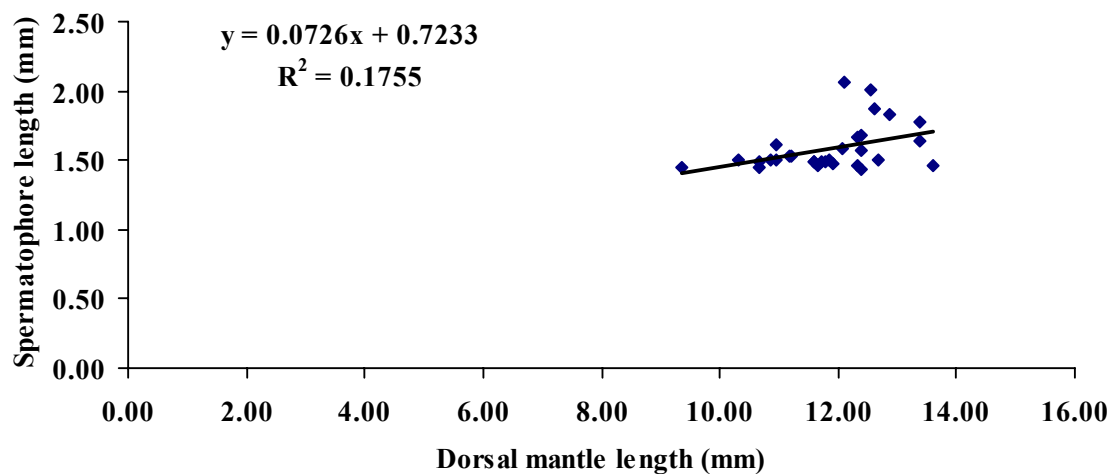
Figure 8.   Relationship between dorsal mantle length and spermatophore length of *I. pygmaeus* (n = 30).

1.3 Sex Ratio

Of the 190 *I. pygmaeus* examined, 129 were males and 61 were females. The overall sex ratio of males to females was 7:3 which it was estimated from the total number of specimens. Statistically, these data showed that the number of males was significantly higher than the number of females (χ^2 = 24.34; P< 0.05) (Table 3).

A preponderance of males over the females was observed throughout the year except July, September and October as shown in Table 3; Figure 9. The sex ratio showed monthly variations with peaks in January (♂:♀: 9:1, n = 43), April (♂:♀: 8:2, n = 26) and December (♂:♀: 9:1, n =10) during the sampling period. As the whole analysed specimens, the sex ratio showed that in February, March, July, August, September, October and November, male/female ratio were close to 1:1, especially in September, while the significant difference occurred in January, April and December (P<0.05).

Table 3.   Monthly variation in the sex ratio of *I. pygmaeus* collected from Andaman Sea, Phuket province during January 2008 and December 2008.

Month	Nm	Nf	Nt	%m	%f	m/f	χ^2
Jan	38	5	43	88.37	11.63	9:1	25.33*
Feb	7	4	11	63.64	36.36	6:4	0.82
Mar	25	16	41	60.98	39.02	6:4	1.98
Apr	21	5	26	80.77	19.23	8:2	9.85*
May	NA	NA	NA	NA	NA	NA	NA
Jun	NA	NA	NA	NA	NA	NA	NA
Jul	3	4	7	42.86	57.14	4:6	0.14
Aug	6	3	9	66.67	33.33	7:3	1.00
Sep	5	5	10	50	50	1:1	0.00
Oct	9	15	24	37.5	62.5	4:6	1.50
Nov	6	3	9	66.67	33.33	7:3	1.00
Dec	9	1	10	90	10	9:1	6.4*
Total	129	61	190	67.9	32.11	7:3	24.34*

* = significant difference (χ^2 test, P< 0.05), f= female, NA= Non-available, Nm= number of males, Nf= number of females, Nt= total number of males and females, m= male.
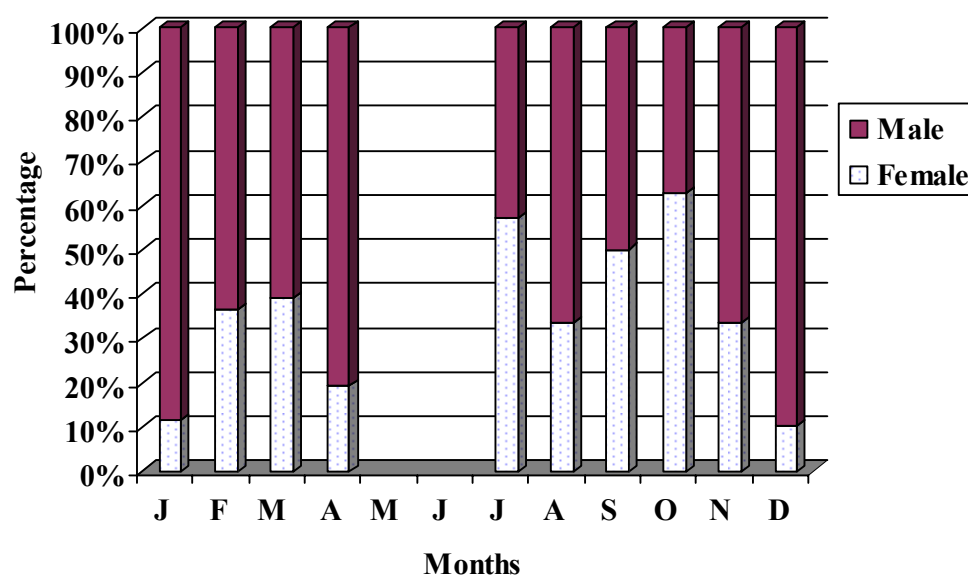
Figure 9. Monthly sex ratio of *I. pygmaeus* during January 2008 and December 2008 (Data not available in May and June).

1.4 The changes of dorsal mantle length in various gonadal stages of male and female *I. pygmaeus*

The comparison of the mean DML in each month of both sexes showed that in male *I. pygmaeus*, the mean DML in maturing stage was highest in November (12.53 mm) and lowest in July (10.93 mm), while in mature stage, the highest and lowest of mean DML were in July (12.87 mm) and October (11 mm), respectively. In October, only one male in spawning stage was captured and its DML was 10.41 mm. In female *I. pygmaeus*, the first gonadal stage showed the minimum DML was 11.73 mm in February and the maximum was 14.33 mm in November. In maturing stage, the mean DML of females was higher than that of males between 12.87 mm (April) and 16.5 mm (July) and in pre-spawning stage, the highest and lowest of mean DML was in October (17.03 mm) and in March (14.51 mm). As for spawning stage, the mean DML was highest in March (16.63 mm). No specimen in the immature stage was available as shown in Fig. 10.
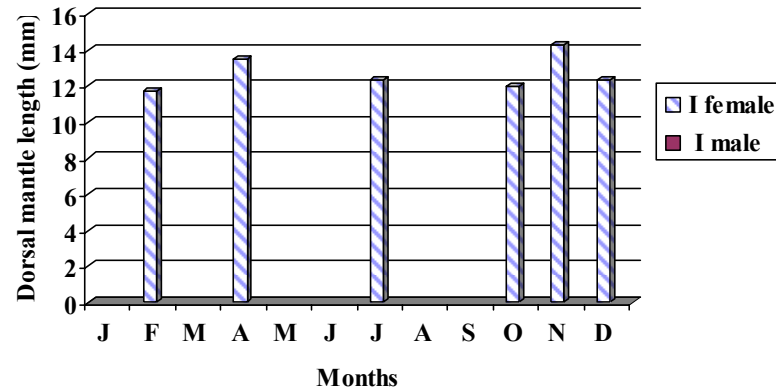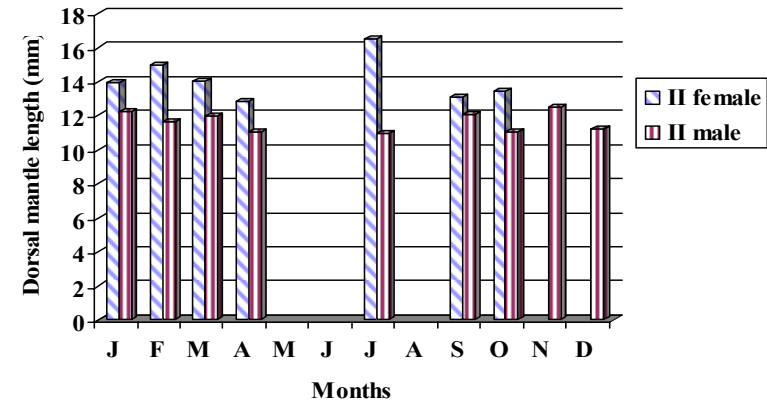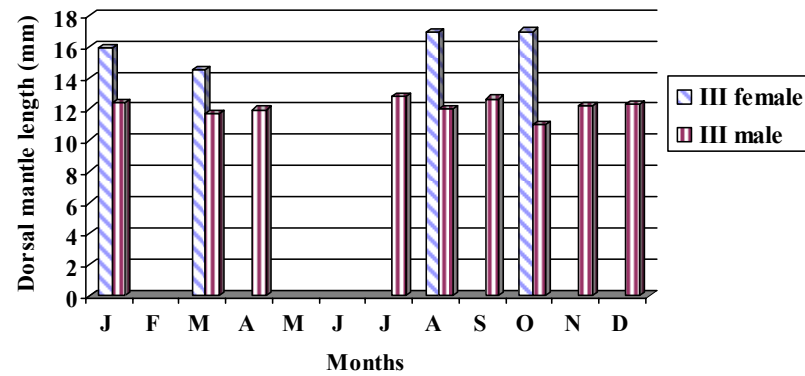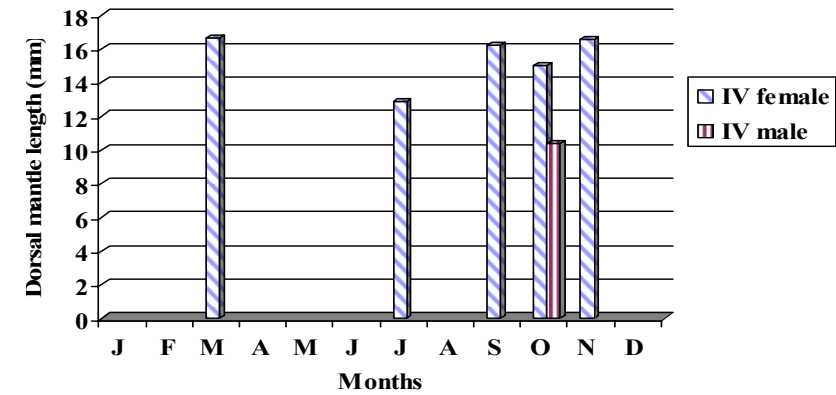
Figure 10. Monthly changes of dorsal mantle lengths of male and female *I. pygmaeus* during January 2008 and December 2008. **A:** Stage I, immature. **B:** Stage II, maturing. **C:** Stage III, mature (male) and pre-spawning (female). **D:** Stage IV, spawning. There was no the specimens in immature stage of male *I. pygmaeus*.

2. Reproductive cycle of *I. pygmaeus*

Based on the histological analysis, the ovarian and testicular developmental stages of *I. pygmaeus* were classified into 4 stages: immature, maturing, pre-spawning (female) /mature (male) and spawning stages as described in Table 4. The histological changes of ovary and testis during the reproductive cycle are illustrated in Figs. 11 - 16.

Table 4. Stages and histological characteristic of ovary and testis during gonadal development in *I. pygmaeus* (Modified from Gabr et al., 1998).

Gonadal stage	Histological characteristic	
	Ovary*	Testis
I. Immature	Stages 1-4 oocyte occurred	Many spermatogonia assemble along the internal wall of seminiferous tubule. Spermatocytes are rather few.
II. Maturing	Stages 1-6 oocyte occurred	Spermatogonia still present. Number of spermatocytes in the center of seminiferous tubule are higher than Stage I, while the early spermatid and spermatozoa begin appearing.
III. Pre-spawning (female) /mature(male)	Stages 1-10 oocyte occurred	Large seminiferous tubule with all types of germ cells: spermatogonia, spermatocytes, spermatid, and spermatozoa. Many spermatozoas show predominance and abundance in the center of the seminiferous tubule.
IV. Spawning	Stage 8-10 oocyte and partially stages 1-3 oocyte occurred	A number of Spermatozoas are almost unseen with the emptiness of lumen, but spermatogonia and spermatocytes still appear.

* Histological characteristics of oocyte stage 1-10 in *Idiosepius* female

Stage 1: The oocytes are partially surrounded by a layer of squamous follicle cells (Fig. 16A).

Stage 2: The oocytes are entirely surrounded by increased layers of squamous follicle cells (Fig. 16B).

Stage 3: The oocytes are entirely surrounded by the layers of cuboidal follicle cells, which fold and penetrate only a little into the oocytes (Fig. 16C).

Stage 4: The oocytes are entirely surrounded by the layers of cuboidal follicle cells, folded and penetrate approximately 50% into the oocytes (Fig. 16D).

Stage 5: The oocytes are entirely surrounded by the layers of cuboidal follicle cells, folded and penetrate approximately 90% into the oocytes (Fig. 16E).

Stage 6: The follicle cells of oocytes are changed to columnar cell, folded and most penetrate into the oocytes (Fig. 16F).

Stage 7: The follicle cells begin to form a syncytium in the oocytes. It can be seen in the vitellogenesis and formation of the chorion, while yolk presses the follicular syncytium to the periphery of the oocyte (Fig. 16G).

Stage 8: Similar to stage 7 but the chorion appears rather distinct (Fig. 16H).

Stage 9: The follicular syncytium begins to degenerate (Fig. 16I).

Stage10: The follicular syncytium already degenerates and mature eggs are ready for the ovulation (Fig. 16J).
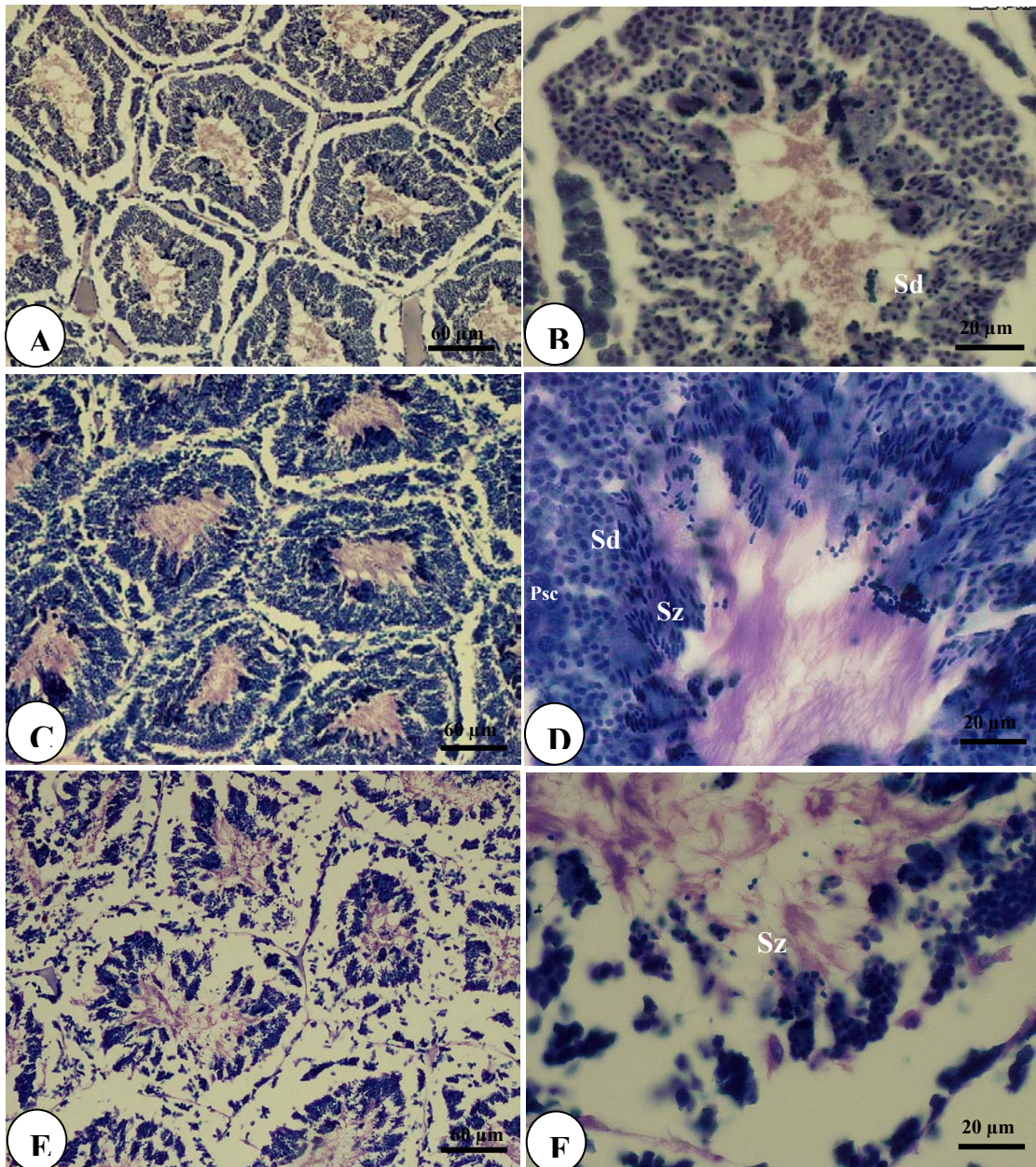
Figure 11. Transverse sections of *I. pygmaeus* testis (H&E stain). **A-B:** maturing stage. **C-D:** mature stage. **E-F:** spawning stage. Psc= primary spermatocyte, Sd= spermatid, Sz= spermatozoa.

In this study, the histological examination of *I. pygmaeus* testis found 3 gonadal stages as maturing, mature and spawning stages (Figs. 11- 12; detail in Table 4). Mature male sperms of *I. pygmaeus* (Fig. 13) were packaged into spermatophores (Fig. 14) and stored in the spermatophoric sac. The slender cylindrical body of the spermatophore of *I. pygmaeus* consisted of an outer tunic, middle tunic, sperm mass, cement body, an ejaculatory apparatus and fluid substances. Thick sections of

spermatophore structure showing the outer tunic is intensively stained with toludine blue, a pale blue stain in the middle tunic. The part of sperm mass appears to be preserved inside the spermatophore structure (Fig. 14).
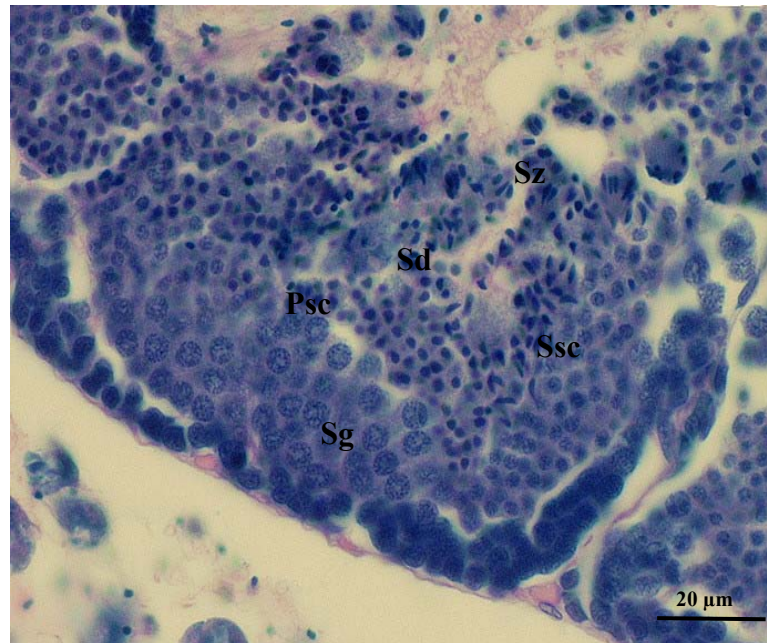
Figure 12.   Transverse section of *I. pygmaeus* testis (H&E stain). Psc= primary spermatocyte, Sd= spermatid, Sg= spermatogonia, Ssc= secondary spermatocyte, Sz= spermatozoa.
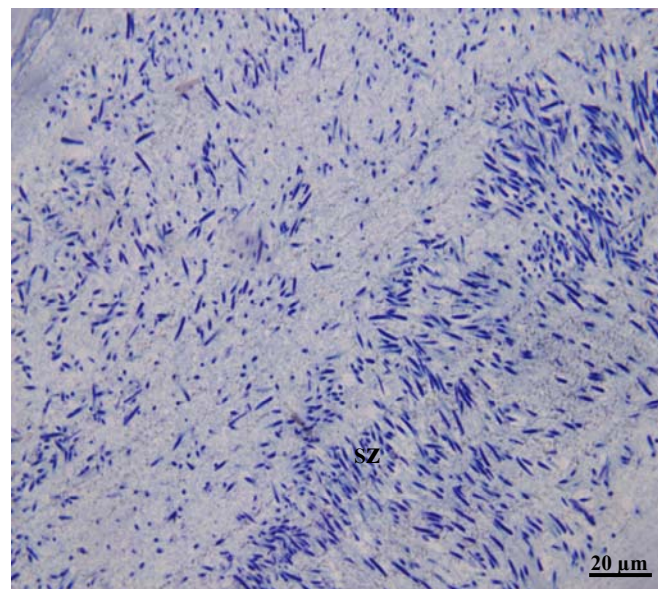
Figure 13.   Thick section of mature sperm of *I. pygmaeus* in the spermatophore (Toluidine blue stain). Sz= spermatozoa.
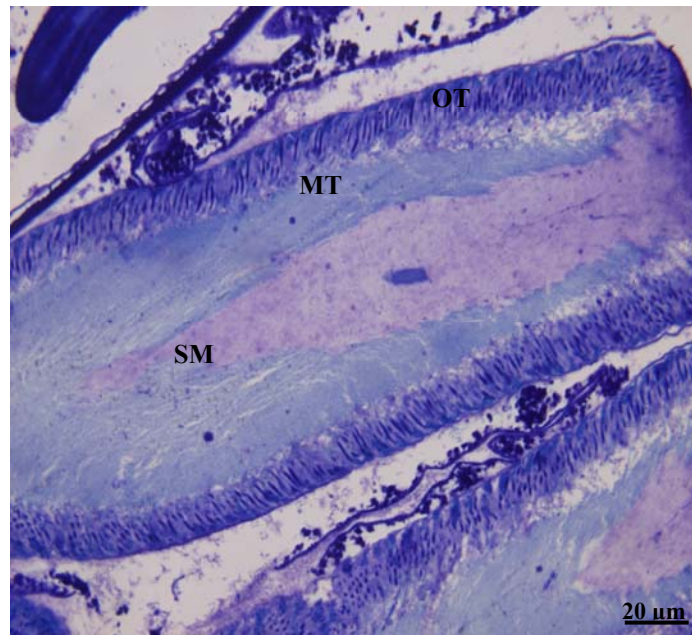
Figure 14. Thick section of spermatophore structures of *I. pygmaeus* (Toludine blue stain). MT= middle tunic, OT= outer tunic, SM= sperm mass.

Detailed histological examination of ovaries of *I. pygmaeus* can be divided into four gonadal stages: immature stage (oocyte stages 1-4), maturing stage (oocyte stages 1-6), pre-spawning stage (oocyte stages 1-10) and spawning stage (oocyte stages 8-10 and a few of stages 1-3) as the followings:

Stage I – Immature

Onset the first gonadal stage, oocytes of young female *I. pygmaeus* compactly filled the ovaries. Several of growing oocytes showed spherical nucleus with developing of a layer follicle cells. Oocytes were partially or entirely surrounded by a single layer of follicle cell with changing of the follicle from squamous into cuboidal cells. In this stage appeared the oocytes of stages 1 - 4 (Fig. 15A).

Stage II – Maturing

At this stage, the oocytes began to develop, showing the continuous growing layer of follicular cells with appear in stages 5-6. The shape of follicle cells

changed from cuboidal into columnar cells and the follicle cell of oocytes are folded and most penetrate into the oocytes (Fig. 15B).

Stage III – Pre-spawning

In the pre-spawning stage, showing the oocytes (stages 1-10) with a predominance of stages 7-8 and the follicle cells gradually invaded the oocytes to form the syncytium. Next, yolk pressed the follicular syncytium to the periphery of the oocyte. As the vitellogenesis and formation of the chorion can be seen in the oocytes. In stage 8, the chorion rather appeared distinctness (Fig. 15C).

Stage IV – Spawning

In the final stage, the predominance of follicular syncytium still appear and begin to degenerate later. The presence of the oocytes stages 8-10 and a few of stages 1-3 suggests the maturation occurs continuously. In stage 10**,** follicular syncytium degenerated completely and mature eggs are ready for the ovulation (Fig. 15D).
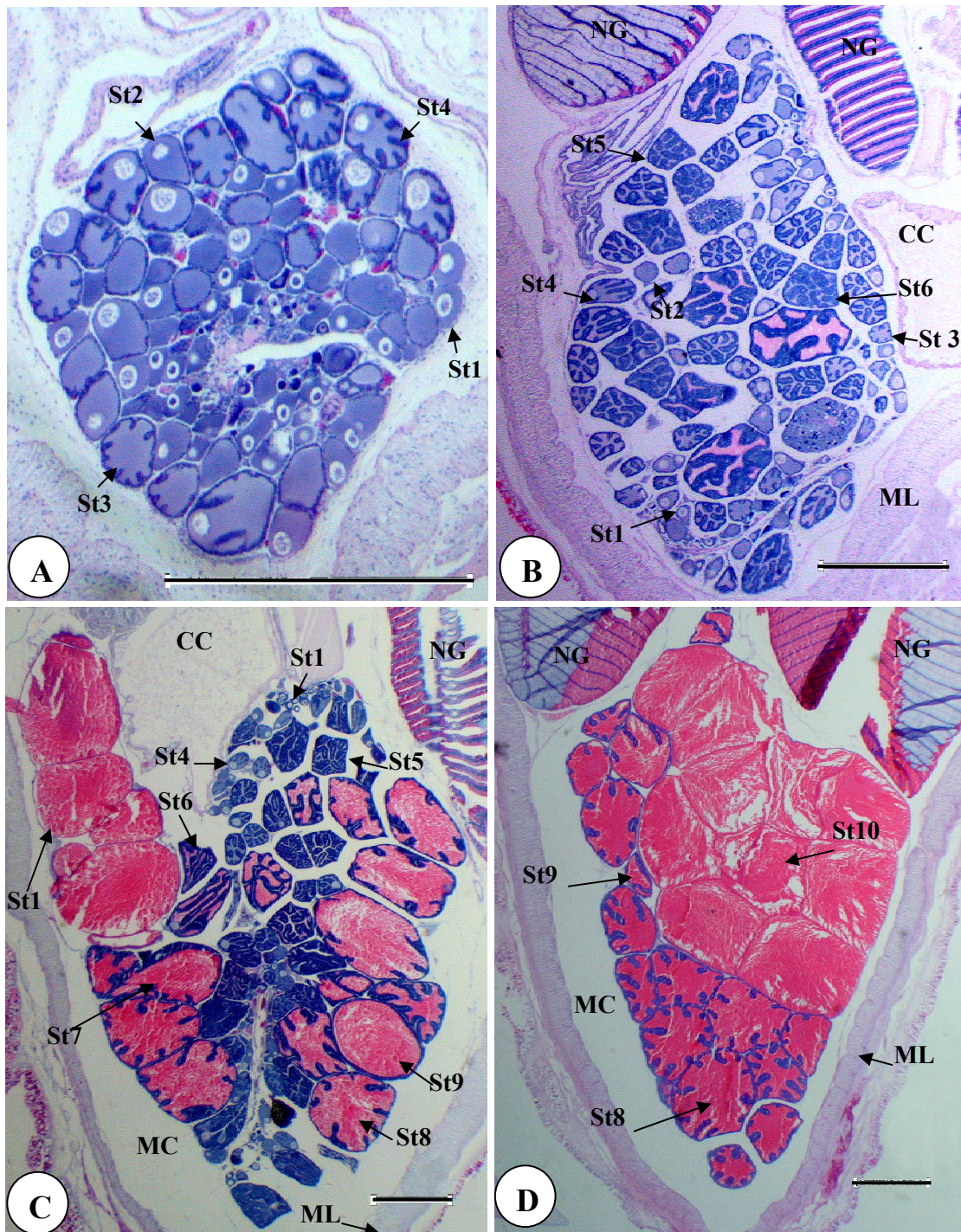
Figure 15. Longitudinal sections of *I. pygmaeus* ovaries (H&E stain). **A:** immature stage (oocyte stages 1-4). **B:** maturing stage (oocyte stages 1-6). **C:** pre-spawning stage (oocyte stages 1-10). **D:** spawning stage (oocyte stages 8-10). CC= caecum, MC= mantle cavity, ML= muscle layer, NG= nidamental gland, St= stage. Scale bars= 400 μm.
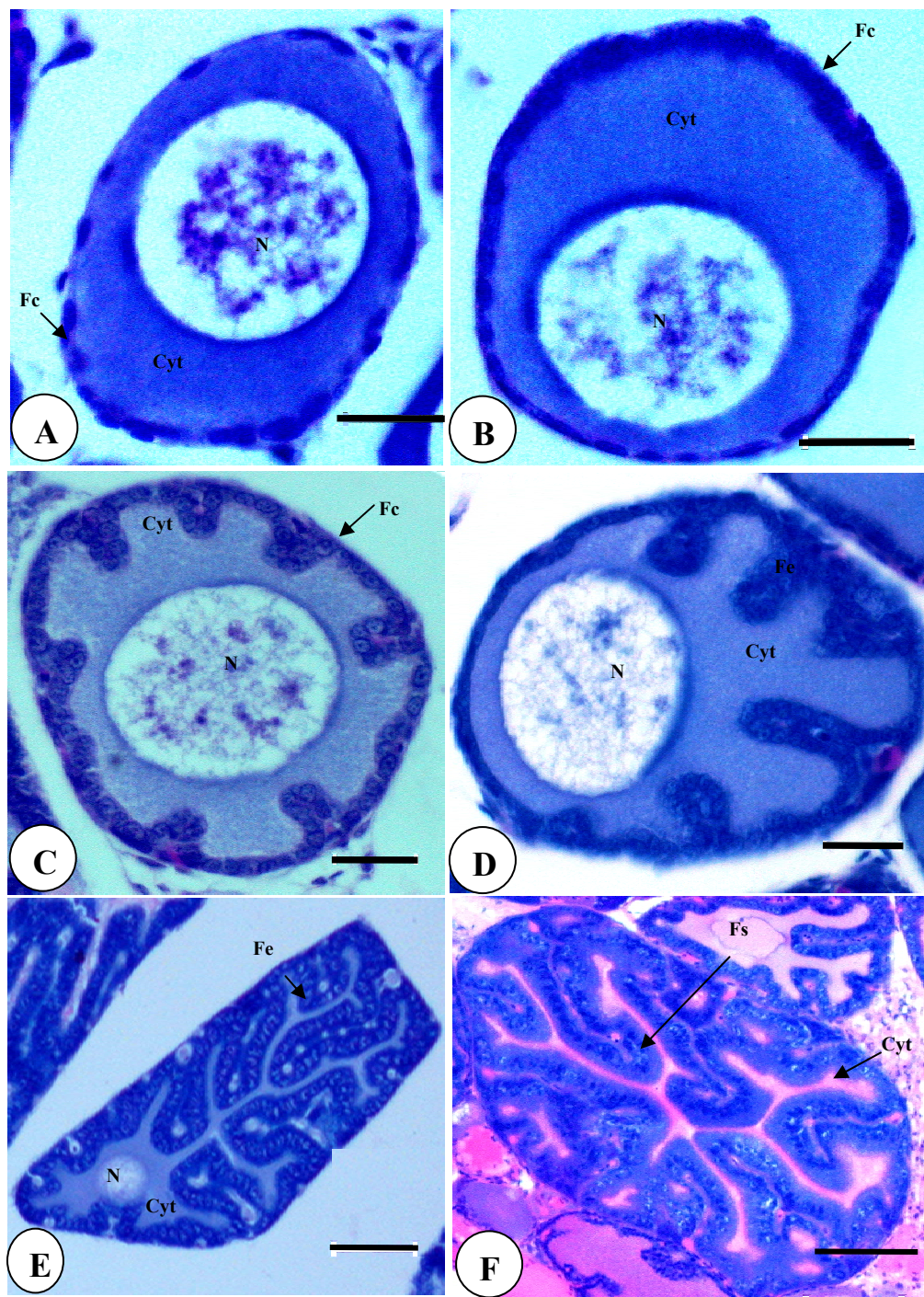
Figure 16. Longitudinal sections of *I. pygmaeus* oocytes in stages 1-10 (H&E stain). **A:** oocyte stage 1. **B:** oocyte stage 2. **C:** oocyte stage 3. **D:** oocyte stage 4. **E:** oocyte stage 5. **F**: oocyte stage 6. **G:** oocyte stage 7. **H:** oocyte stage 8. **I:** oocyte stage 9. **J:** oocyte stage 10. Cyt= cytoplasm, Fc= follicle cell, Fe= follicular epithelium, Fs= follicular syncytium, N= nucleus. Scale bars= 20 µm (A-D), 60 µm (E - F), 120 µm (G - H) and 200 µm (I - J).
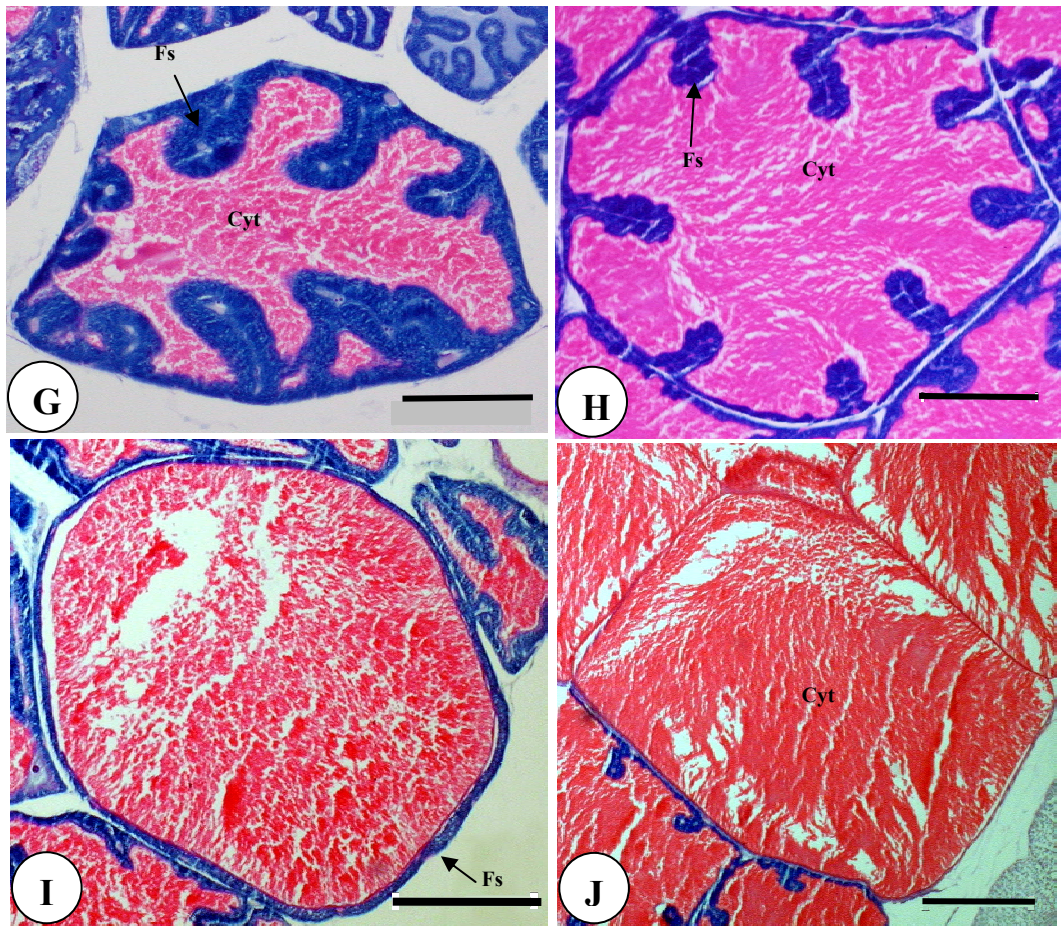
Figure 16. (Continued).

Monthly variation in the percentage of male and female *I. pygmaeus* at four gonadal stages from Andaman Sea, Phuket province is shown in Fig. 17; Table 5. As for male *I. pygmaeus*, maturing stage was observed in almost all months except August, with highest percentage (100%) in February, while lowest percentage (44.4%) in October and December. Male *I. pygmaeus* in immature stage was not found, while those at spawning stage was 11.1% in October. The present study found male *I. pygmaeus* at mature stage throughout the year, except February. They were predominant (100%) in August (Fig. 17A).

As for female *I. pygmaeus*, the immature stage was found in February, April, July, October, November and December with highest presence (100%) in December, while the maturing stage was found in January to July and again in September and October. The high percentage (60%) of maturing stage appeared in January and October. The lowest percentage (25%) of maturing stage was recorded in July. The highest and lowest percentages of pre- spawning stage were found in January (100%) and March (12.5%), respectively. The occurrence of spawning stage was observed in March, July, September, October and November with the high percentage in March (43.75%), July (50%) and September (60%). This data implies that the spawning period in female *I. pygmaeus* is more than once in its life time (Fig. 17B).
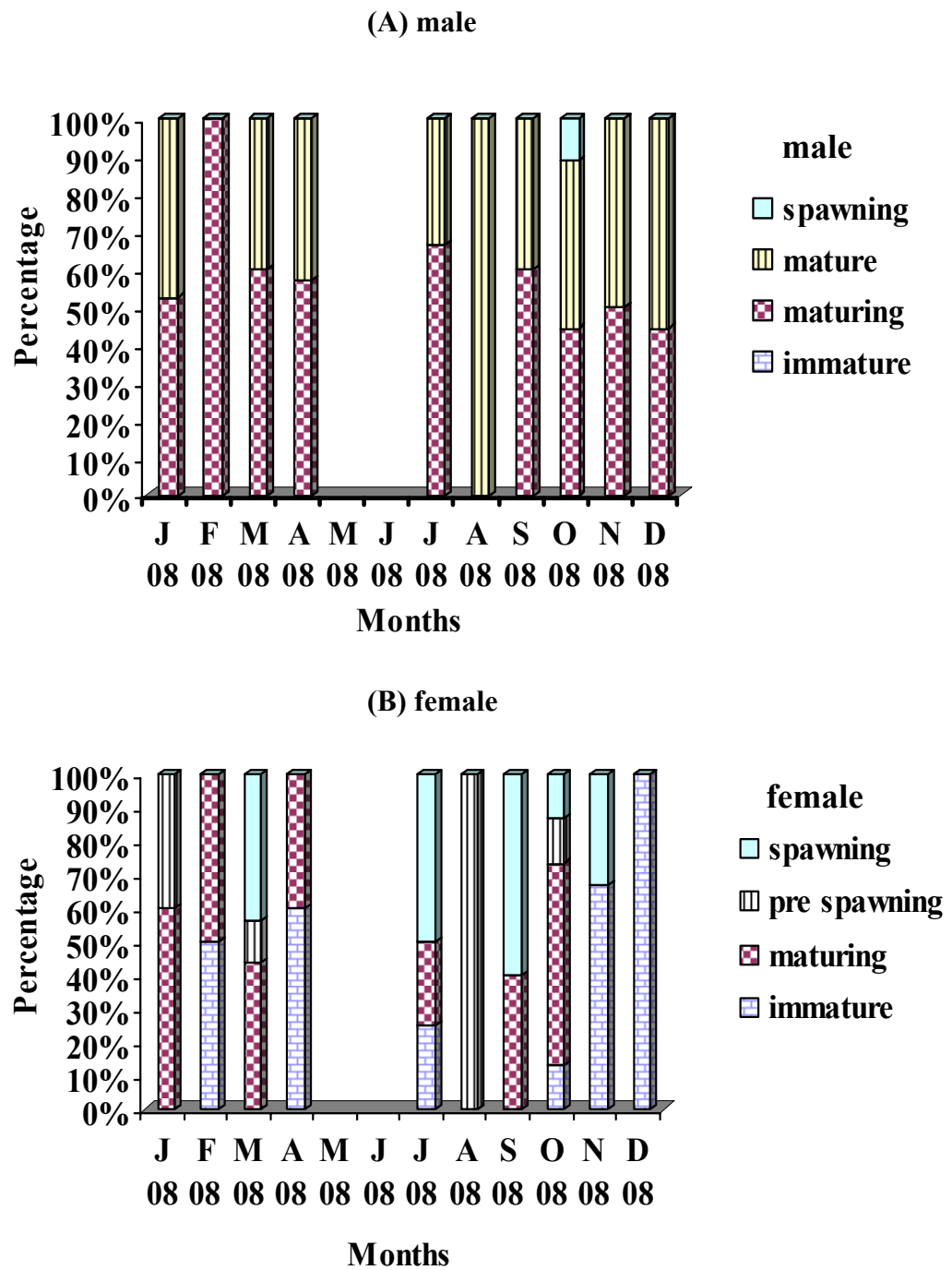
(A) male

(B) female

Figure 17. Monthly percentage change in the gonadal stages of *I. pygmaeus* during January 2008 and December 2008 at the study site. **A:** male. **B:** female.

Table 5. Percentage composition in the gonadal stages of *I. pygmaeus* during January 2008 and December 2008.

Month	Number examined	Male%				Female%			
		I	II	III	IV	I	II	III	IV
Jan	43	0.00	52.63	47.37	0.00	0.00	60.00	40.00	0.00
Feb	11	0.00	100.00	0.00	0.00	50.00	50.00	0.00	0.00
Mar	41	0.00	60.00	40.00	0.00	0.00	43.75	12.50	43.75
Apr	26	0.00	57.14	42.86	0.00	60.00	40.00	0.00	0.00
May	NA	NA	NA	NA	NA	NA	NA	NA	NA
Jun	NA	NA	NA	NA	NA	NA	NA	NA	NA
Jul	7	0.00	66.67	33.33	0.00	25.00	25.00	0.00	50.00
Aug	94	0.00	0.00	100.00	0.00	0.00	0.00	100.00	0.00
Sep	10	0.00	60.00	40.00	0.00	0.00	40.00	0.00	60.00
Oct	24	0.00	44.44	44.44	11.12	13.33	60.00	13.33	13.34
Nov	9	0.00	50.00	50.00	0.00	66.67	0.00	0.00	33.33
Dec	10	0.00	44.44	55.56	0.00	100.00	0.00	0.00	0.00

NA= Non - available

2.1 Gonadal index (GI)

The monthly GI values of females and males *I. pygmaeus* are presented in Fig. 18. These index values were correlated with the pattern of monthly variation in various gonadal stages of *I. pygmaeus*. The GI values ranged from 1.4 (April and September) to 3 (August) for females and from 2 (February) to 3 (August) for male. In female *I. pygmaeus*, the beginning of the GI values increase in January (2.4) and gradually tended to decrease continuously in February (1.5), March (1.69), April (1.4) and July (1.25). Afterward, the GI values increased again with a peak in August (3) and then, backed down again in September (1.4). In October the GI values increased very little (1.87) and steadily declined in November - December (1). This coincidence with the high percentage values of the specimens in spawning stage is shown in Fig. 17. The GI values of male *I. pygmaeus* throughout the year trended higher than those of female. This suggests that males can release mature sperm all year round. Both sexes have the gonadal index curves was a high values synchronously in January, August and October.
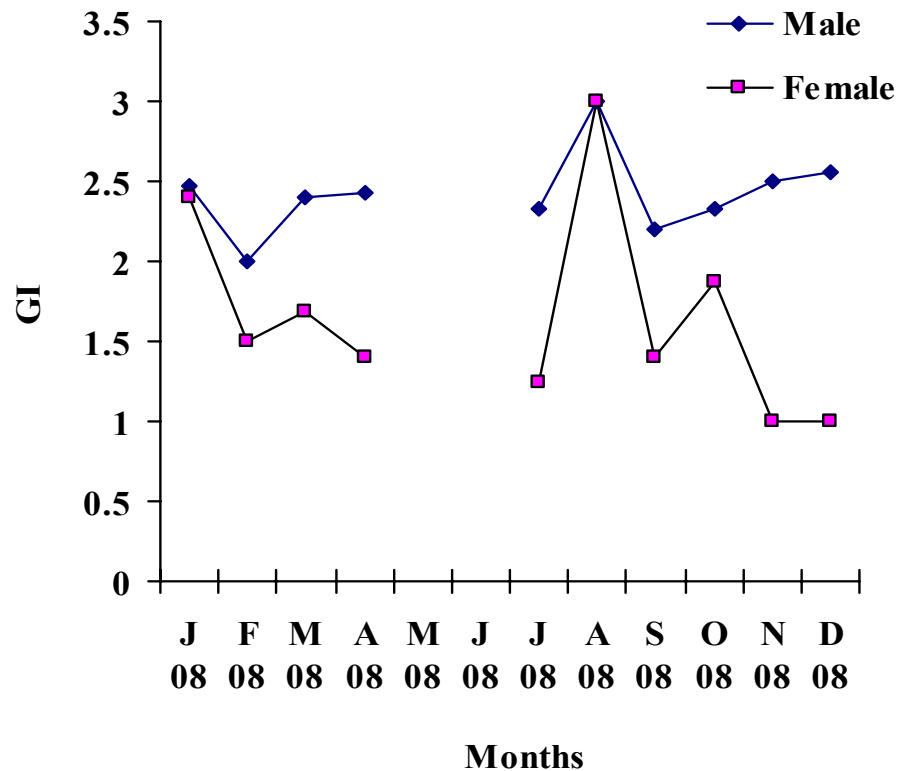
Figure 18. Monthly variation in gonadal index (GI) of both female and male *I. pygmaeus* during January 2008 and December 2008 (Data not available in May, June and December).

3. Ultrastructure of spermatogenesis in *I. pygmaeus*

3.1 Morphological characteristics, the pattern of chromatin condensation and nuclear shape in each stage

The region of testis in mature male *I. pygmaeus* was located near spermatophoric organ and prostate gland that were tightly packed together on the left side. Examining the ultrastructure of *I. pygmaeus* testis showed various stages of germ cells including spermatogonia, spermatocytes, and spermatids as described below.

Spermatogonia: Normally, spermatogonia were regularly found in the testicular tissue as attached to the epithelium of the seminiferous tubules of the testis. They had spherical and oval shape. Each spermatogonium contained a large oblong nucleus which was composed of one nucleolus. The nucleus contained mostly euchromatin which was partially or fully uncoiled, whereas small blocks of

heterochromatin were genetically inactive chromatin and tightly coiled. In the cytoplasm, golgi body and a few mitochondria can be found (Fig. 19).
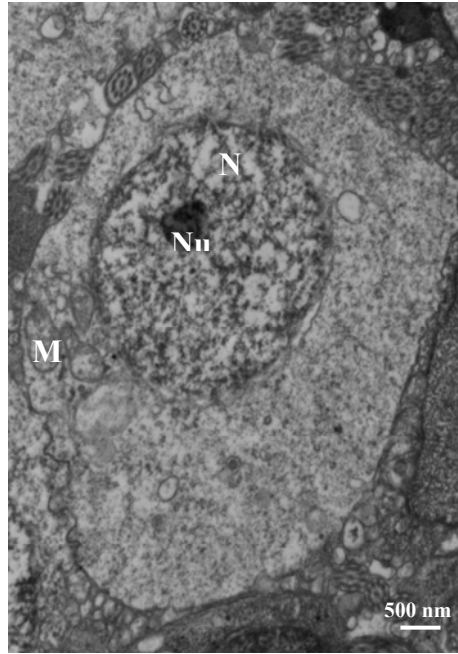
Figure 19.   TEM of early spermatogonium of *I. pygmaeus*.
M= mitochondria, N= nucleus, Nu= nucleolus.

Spermatocytes: The primary spermatocytes of *I. pygmaeus* consisted of six stages: leptotene, zygotene, pachytene, diplotene, metaphase and diakinetic.

Stage 1 Leptotene spermatocytes

The oblong-shaped cell of leptotene spermatocytes (LSc) was larger than spermatogonia. The size of the nucleus was approximately 4.62 μm wide and 7.1 μm long. Changes in chromosome structure were observed by appearing small blocks of heterochromatin which they were scattered throughout the nucleoplasm. The nucleolus was still present; however, its prominence was not the same as is found in the spermatogonium. The cytoplasm contained few mitochondria (Fig. 20A).

Stage 2 Zygotene spermatocytes

The zygotene spermatocytes (Zsc) had oval - shape. In this stage, the size of the cell was approximately 5.75 μm wide and 7.75 μm long. The nucleus was rather oblong-shaped and the nucleolus cannot be found. This stage

showed an increase in thickness of the heterochromatin blocks. The cytoplasm contained few mitochondria and rough endoplasmic reticulum (RER) (Fig. 20B).

Stage 3 Pachytene spermatocytes

The pachytene spermatocytes (PSc) were rather round. The nucleus of this stage contained mostly heterochromatin which appeared as long thick fibers. These thick fibres were twisted into the bouquet pattern, and obviously scattered in the nucleoplasm. The nucleolus cannot be seen in this stage. The cytoplasm contained few mitochondria (Fig. 20C).

Stage 4 Diplotene spermatocytes

The shape of diplotene spermatocytes (DSc) was not regular. The oval shape of nucleus was rather irregular. The chromatin strands as heterochromatin increasingly began to condense into dark blocks and were more visible in nucleoplasm than in earlier stages. The cytoplasm contained few mitochondria and a Golgi body (Fig. 20D).

Stages 5-6: Metaphase spermatocytes and diakinetic spermatocytes (No Pictures)
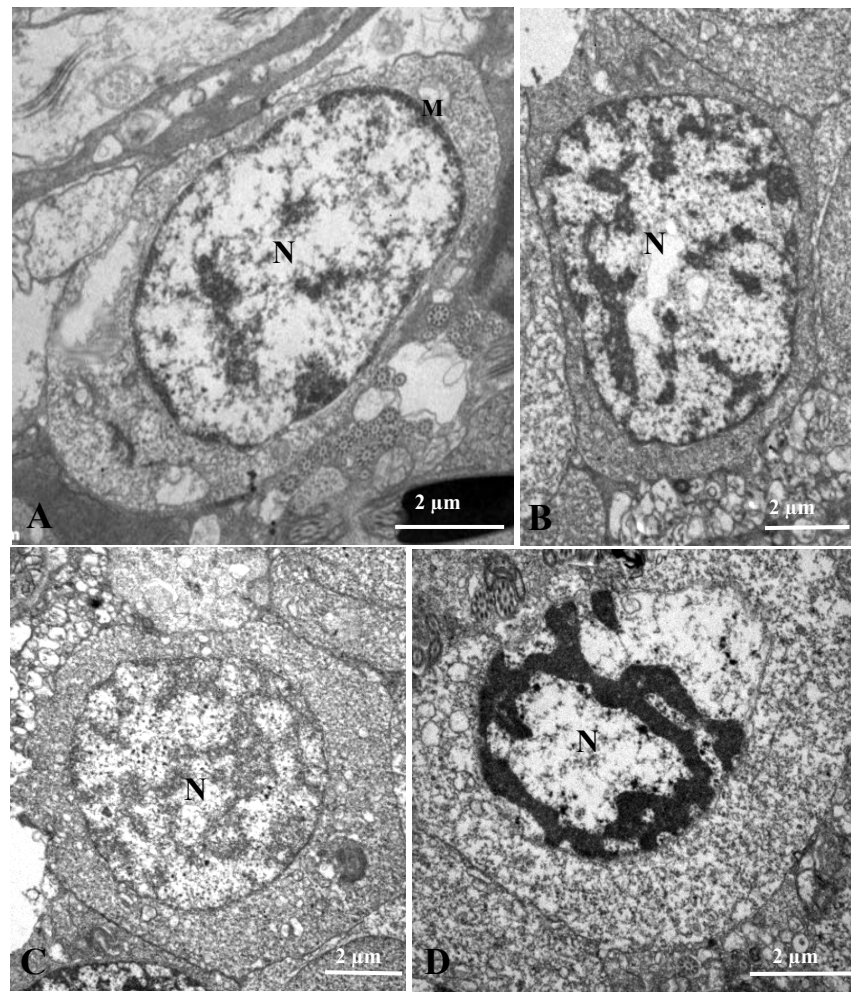
Figure 20.　TEMs of primary spermatocytes stages 1-4 of *I. pygmaeus*.
A: Leptotene spermatocyte. **B:** Zygotene spermatocyte.
C: Pachytene spermatocyte. **D:** Diplotene spermatocyte
M= mitochondria, N= nucleus.

In the primary spermatocytes, the pachytene stage showed the prominent synaptinemal complexes were well - developed obviously (Fig. 21).
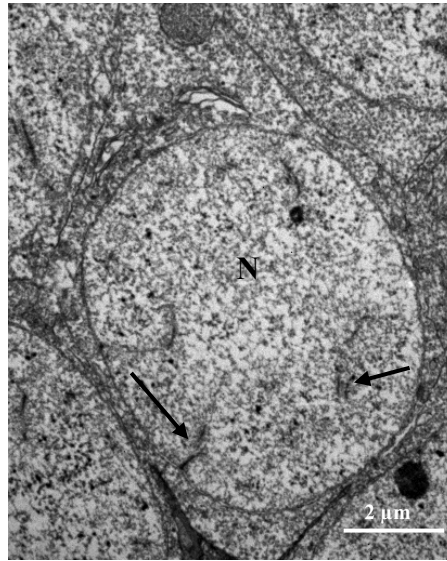
Figure 21. Synaptinemal complexes appeared in the pachytene spermatocyte (arrows) of *I. pygmaeus*. N= nucleus.

Secondary spermatocytes: The secondary spermatocyte derived from a primary spermatocyte by the first meiotic division showed that the number of chromosome was split into halves. Normally, the size of secondary spermatocyte was smaller than that of the primary spermatocytes (Fig. 22).
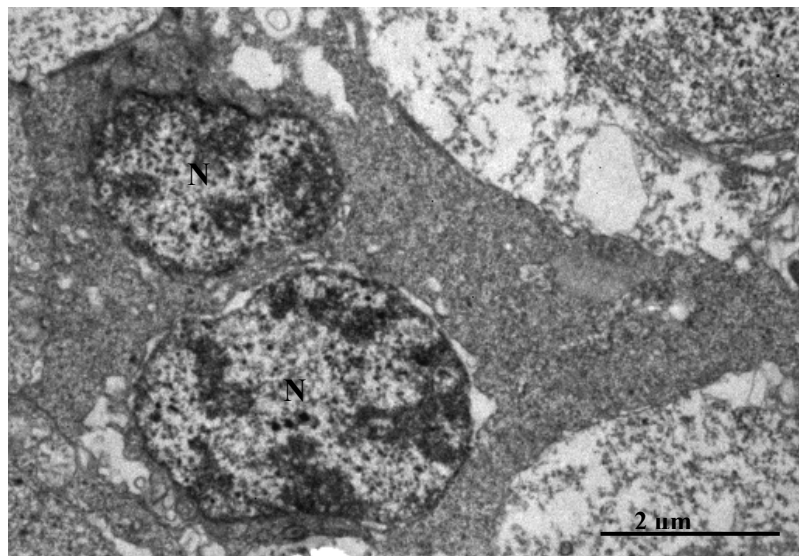
Figure 22. TEM of spermatocyte with two nuclei of *I. pygmaeus* during a change of the primary spermatocyte to secondary spermatocyte. N= nucleus.

Spermatids: In spermatid of *I. pygmaeus*, there were a change in pattern of chromatin condensation, nuclear shape, acrosome formation development of midpiece and flagellum as illustrated in Figs. 23-26.

Early spermatid: The earlier spermatid nucleus had chromatin structure like granule which was homogeneously packed and the nuclear shape was rather irregular. The acrosome formation was gradually developed as proacrosome (Fig. 23A). It was formed by Golgi body in earlier stage of spermiogenesis and after that it changed into acrosome (Fig. 23D). In the next stage, the granular chromatin began to transform into lightly homogenous fibers − shape. The nucleus was also changed into an oval shape (Figs. 23B-D). Microtubules can be seen near the nuclear membrane (Fig. 23).
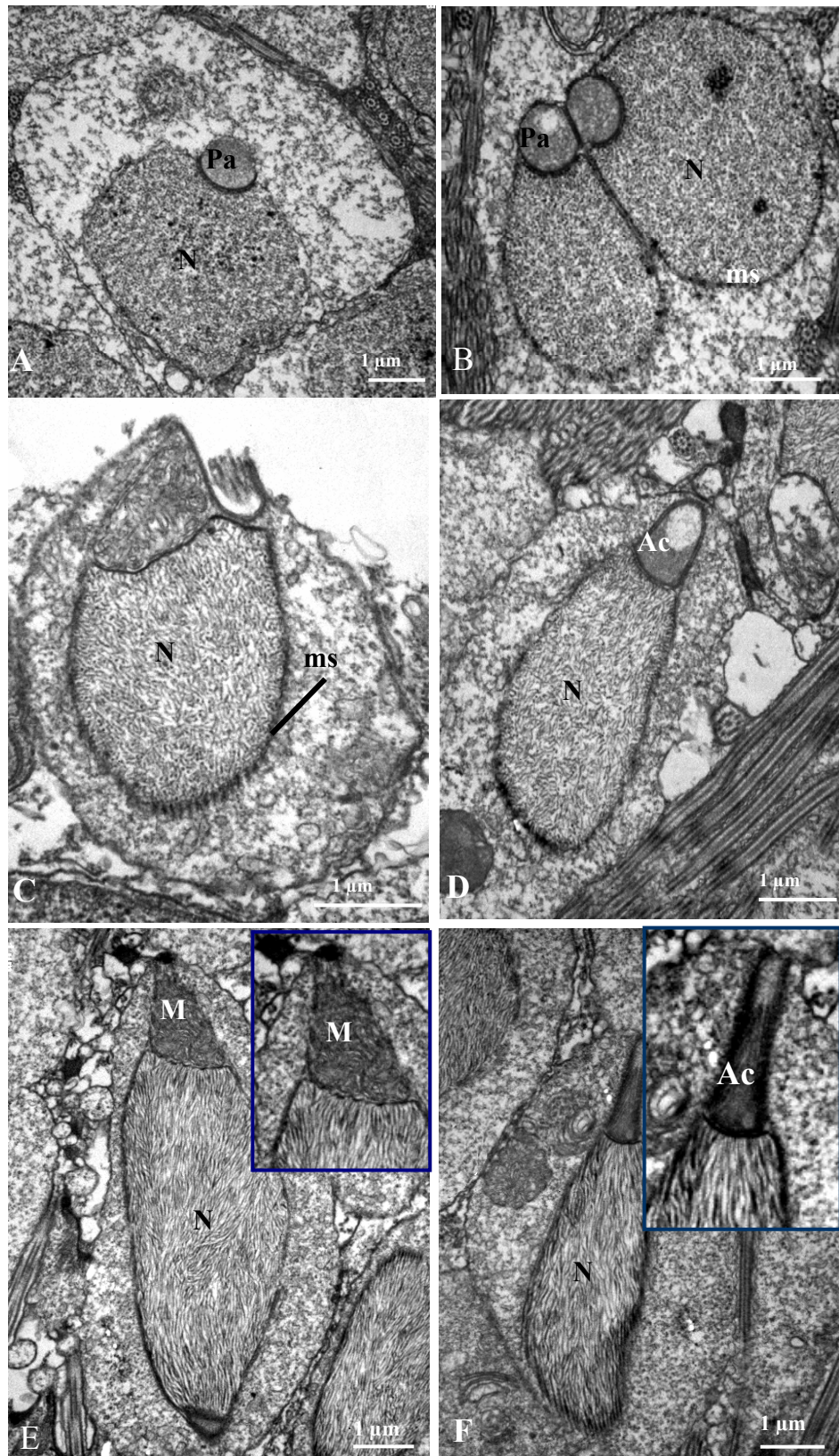
Figure 23. TEMs of early spermatid of *I. pygmaeus*. **A:** Proacrosome

(Continued). attached to the nucleus. **B-C:** Oval nuclei appeared homogenous fibers of chromatin. **D:** Acrosome formation is well-developed than Figs. 23A-C. **E:** Longitudinal section (LS) through acrosome, chromatin (lamellar pattern) and tail formation. **F:** LS through elongated acrosome. Ac= acrosome, M= mitochondria, ms= microtubular sheath, N= nucleus, Pa=proacrosome.

Afterwards, the chromatin pattern was changed into lamellar shape and the nucleus was gradually elongated as can be seen in Figs. 23B-F.

Mid spermatid: Afterwards, in the dorsal region of the nucleus of *I. pygmaeus* appeared the recruitment process of chromatin fiber (Fig. 24). In this stage showed with rather clearly in the morphology of acrosome which embedded in the apex of nucleus during the change of the pattern of chromatin (Fig. 24C). The morphology of nucleus became elongated and the centrioles were visible outside the basal invagination of nucleus. Microtubules originated from centriole, and formed to a sheath around the condensing nucleus called perinuclear microtubules and then the mitochondria migrated to base of nucleus. Finally, the mitochondria were begun with parallel to the proximal length of flagellum and then fused to form a mitochondria sleeve (Figs. 24E-F, 25). This characteristic showed clear in mature sperm of *I. pygmaeus*.
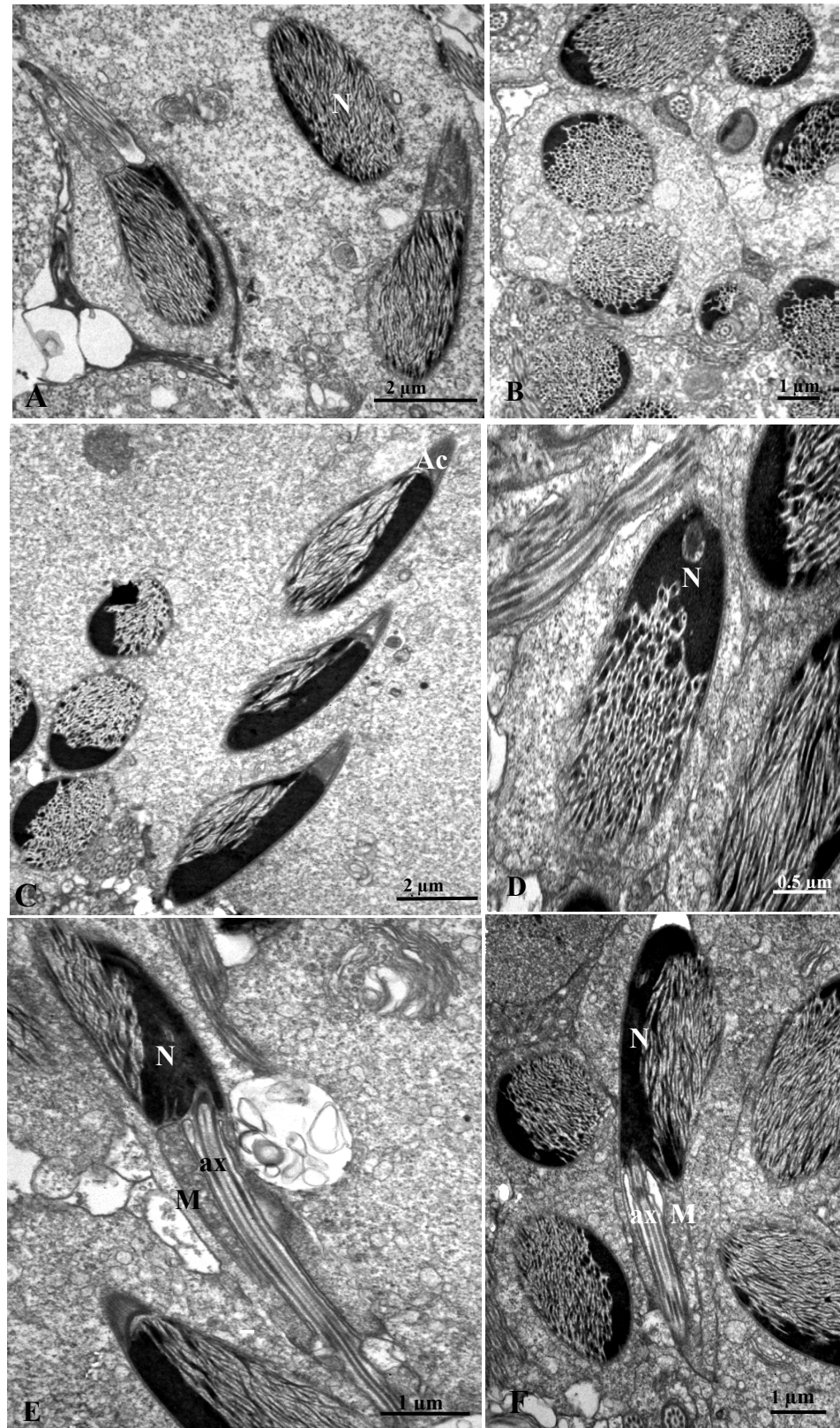
Figure 24. TEMs of mid spermatid of *I. pygmaeus*. **A:** Chromatin accumulated toward the dorsal region of nuclei. **B:** Transverse section (TS) through nuclei (showing the chromatin recruitment in the dorsal region). **C:** TS and quasi-longitudinal sections through nuclei.

(Continued). D: Chromatin recruitment directed to the dorsal region of nucleus. **E-F:** Recruitment of chromatin, reduction of nuclear volume and formation of tail. Ac= acrosome, ax= axoneme, M= mitochondria, N= nucleus.
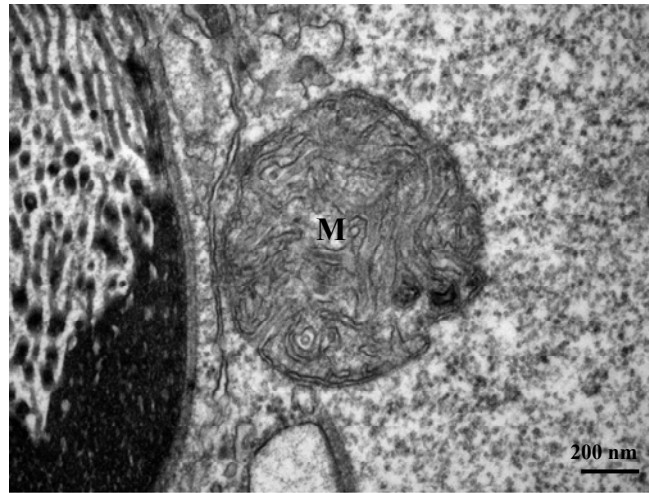
200 nm

Figure 25. Transverse section of a mitochondrion (M) at mid spermatid stage of *I. pygmaeus*. Scale bar= 200 nm.

Late spermatid: The final stage of spermatid in which the nucleus became condensed with the arrangement of chromatin structure called "homogenous e⁻dense" and also showed the development of mitochondria and flagellum (Fig. 26). The mitochondria located close to the base of the nucleus after they organized to surround the centriole as pericentriole. In late spermatid, the microtubule formation occurred with the microtubules array surrounded the nucleus and acrosome.
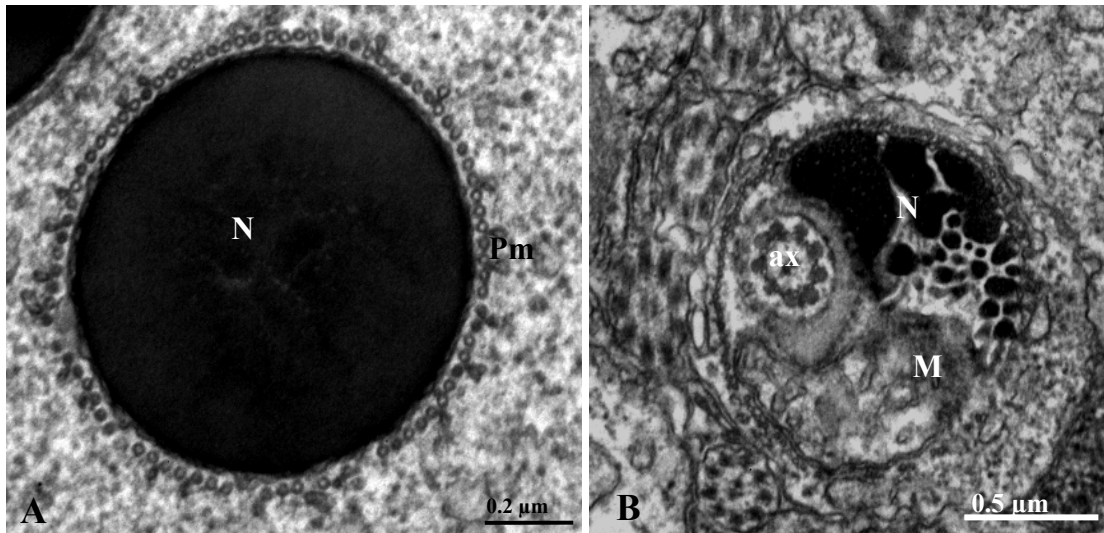
Figure 26. TEMs of late spermatid of *I. pygmaeus*. **A:** Transverse section (TS) through nucleus (showing condensed nucleus and perinuclear microtubules). **B:** TS through nucleus, axoneme and mitochondrion (showing the microtubules surround the nucleus). ax= axoneme, M= mitochondria, N= nucleus, Pm= perinuclear microtubule

Premature spermatozoa of *I. pygmaeus* composed of acrosomal complex, nucleus, flagellum and a mitochondrial sleeve which enclosed the proximal of flagellum was approximately 2.7 μm long. The external of acrosome of *I. pygmaeus* was surrounded by granular structure as microtubules (Fig. 27).
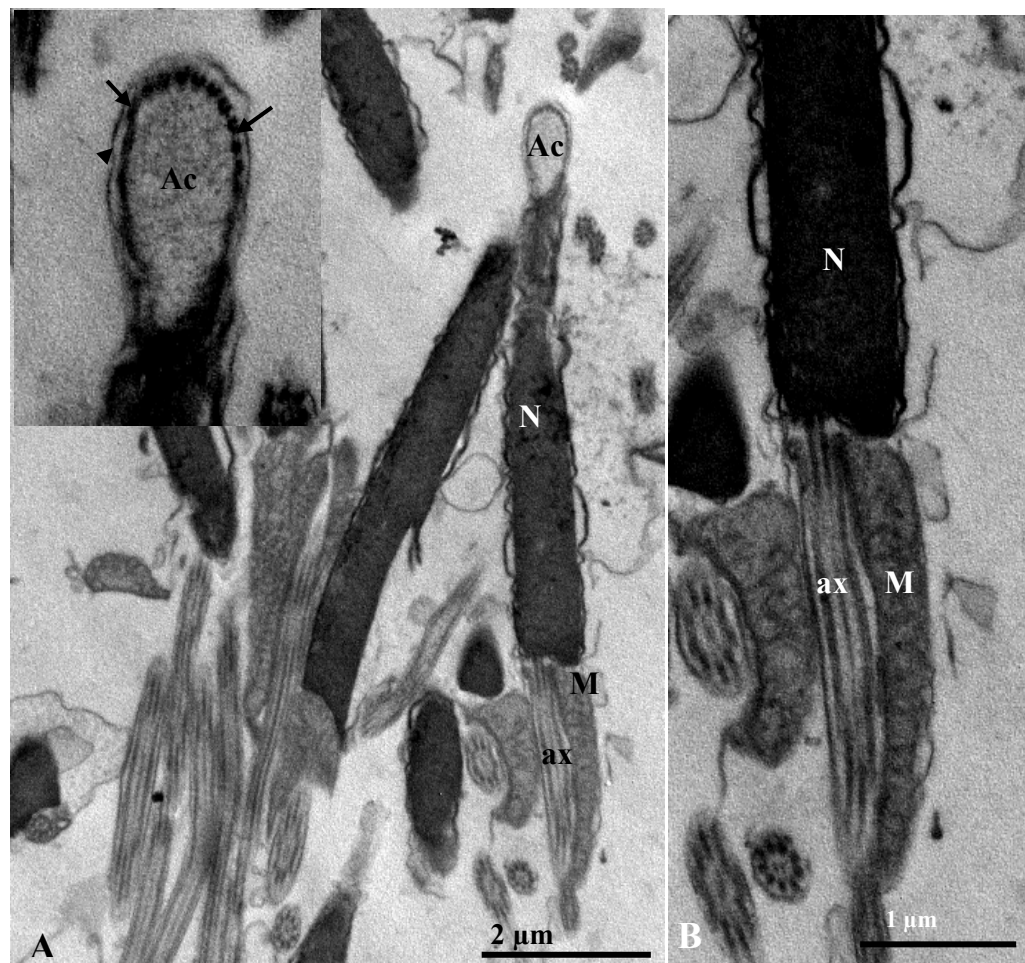
Figure 27. TEMs of premature sperm of *I. pygmaeus*. **A:** Longitudinal section (LS) through acrosomal complex, nucleus and proximal portion of mitochondrial sleeve. Note the membrane enclosed from acrosomal and nuclear regions. **B:** LS of nucleus, axoneme and mitochondrial sleeve. Ac= acrosome, ax= axoneme, M= mitochondria, N= nucleus.

Mature sperm: The mature sperm of *I. pygmaeus* was composed of three parts: the head, midpiece and the tail (flagellum with the typical 9+2 axoneme arrangement), with the fine structure as follows:

Head: The head of mature sperm of *I. pygmaeus* consisted of an elongated acrosomal complex and long straight nucleus. The length of *I. pygmaeus* head was approximately 6.9 μm (acrosome+nucleus) (Fig. 28A). The position of the acrosomal complex was located in the anterior portion of its mature sperm. Longitudinal section of the acrosome revealed that its length was approximately 1.75 μm long with a 0.2 μm deep basal invagination filled with packed granules (Fig. 28A). There was a space between the acrosomal complex and the nucleus called "the subacrosomal structure" (Fig. 28B). The microtubule as granular structure located

external the acrosome and its acrosome was enclosed entirely with a plasmalemma structure (Figs. 28A, 29A).

Nucleus: The nucleus of *I. pygmaeus* sperm was connected to acrosomal complex. It had a long cylindrical spindle – shape. Longitudinal and transverse sections of nucleus confirmed that a plasmalemma at the outside portion surrounded its nucleus. The chromatin of its nucleus was condensed with highly electron density as homogeneous electron dense (Figs. 28B, 29B). Its nucleus showed the central position of the basal invagination as the region of the centriole and flagellar, and then the centriole as a typical triplet substructure was filled in a centriolar pit that was located near the center of nucleus (Fig. 28C).

Mid-piece and tail: In this part, the mitochondria aggregated around the base of *I. pygmaeus* nucleus. Mitochondria of *I. pygmaeus* sperm tended to be straightly arranged along the flagellum which showed in one side only and was called a mitochondrial sleeve (Figs. 28C-D). Transverse sections through the mitochondria and axoneme in the midpiece region indicated the unique typical a 9+2 axoneme that modified to plasmalemma structure with granule attached to the external and the internal (Figs. 30A-C). The multiple layers of plasmalemma enclosed the axoneme loosely as seen in transverse section (Figs. 30D-E). Whereas, in the distal tip of the midpiece was not completely surrounded by plasmalemma sheath as thickness layer (Fig. 30F). The flagellum of *I. pygmaeus* originated from the posterior centriole and composed of a 9+2 axoneme was surrounded by nine coarse fibres. Transverse sections of mature flagellum in the distal tail region showed that the plasmalemma enclosed axoneme as a simple form, and then the flagellar axoneme degenerated into singlet microtubules (Fig. 30G). However, it still showed that the coarse fibres were reduced in size.
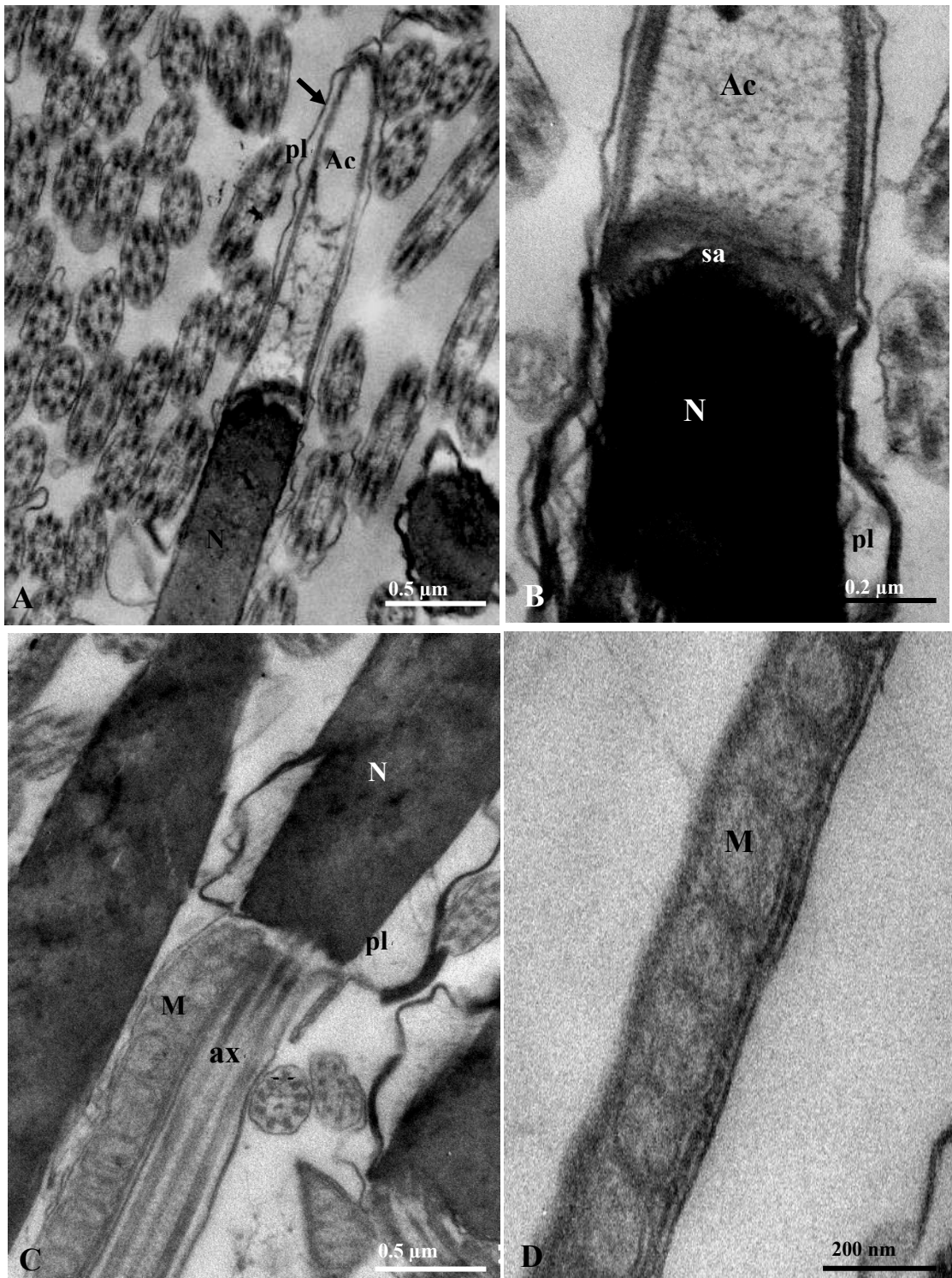
Figure 28. Longitudinal sections of mature sperm of *I. pygmaeus*. **A:** Acrosomal complex and the plasmalemma sheeth surrounded its structure (arrow). **B:** Acrosome and nucleus (showing the subacrosomal structure and plasmalemma enclosed continually in the part of acrosome into nucleus). **C:** Plasmalemma enclosed nucleus.

(Continued). D: Straight mitochondria of *I. pygmaeus* were parallel to axoneme. Ac= acrosome, ax= axoneme, M= mitochondria, N= nucleus, pl= plasmalemma, sa= subacrosome,
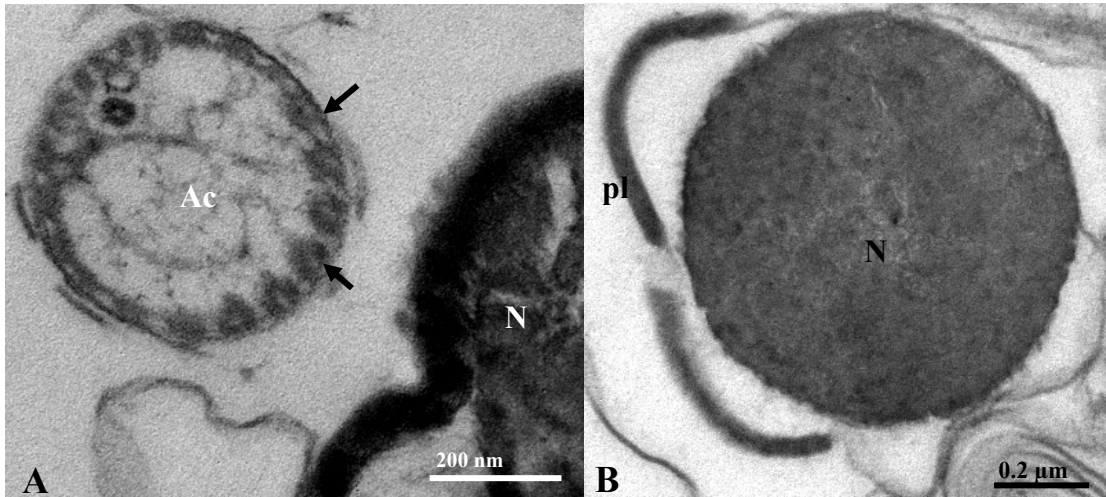
Figure 29. Transverse sections of mature sperm of *I. pygmaeus*. **A:** Section through acrosome (showing the microtubule as a granular structure (arrows) attached to external and enclosed with plasmalemma structure). **B:** Section through nucleus (showing the plasmalemma surrounding nucleus). Ac= acrosome, N= nucleus, pl= plasmalemma.
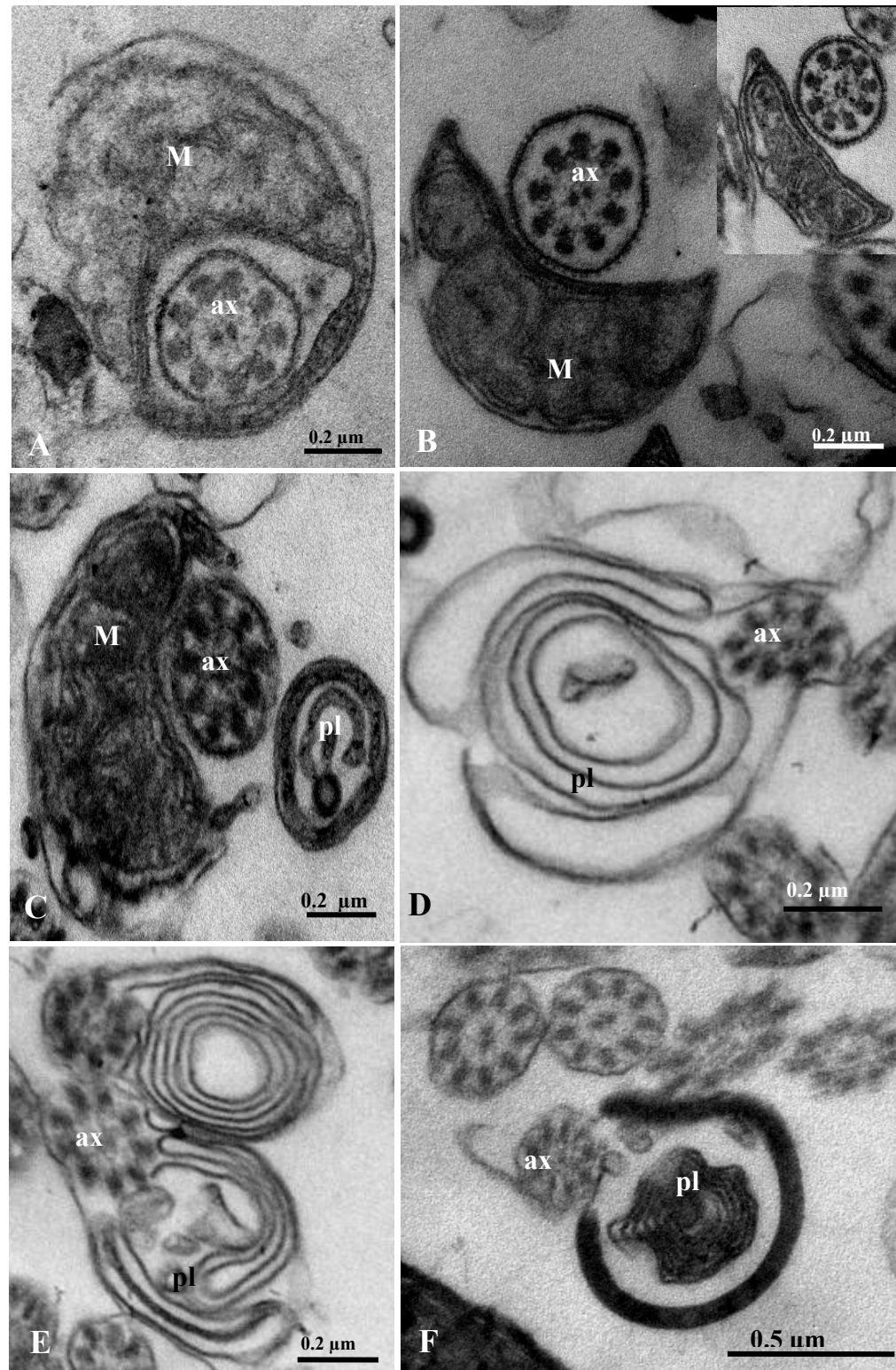
Figure 30. Transverse sections of axoneme of mature *I. pygmaeus* sperm. **A:** Mitochondria surrounding axoneme. **B:** Mitochondria attached to axoneme in midpiece. **C:** Flagellum was gradually enclosed by plamalemma. **D-E:** Plasmalemma as multiple layer loosely enclosed to flagellum. **F:** Section of distal tip of the midpiece. **G:** Sections through midpiece (arrows) and tail region (arrowheads). ax= axoneme, M= mitochondria, pl= plasmalemma.
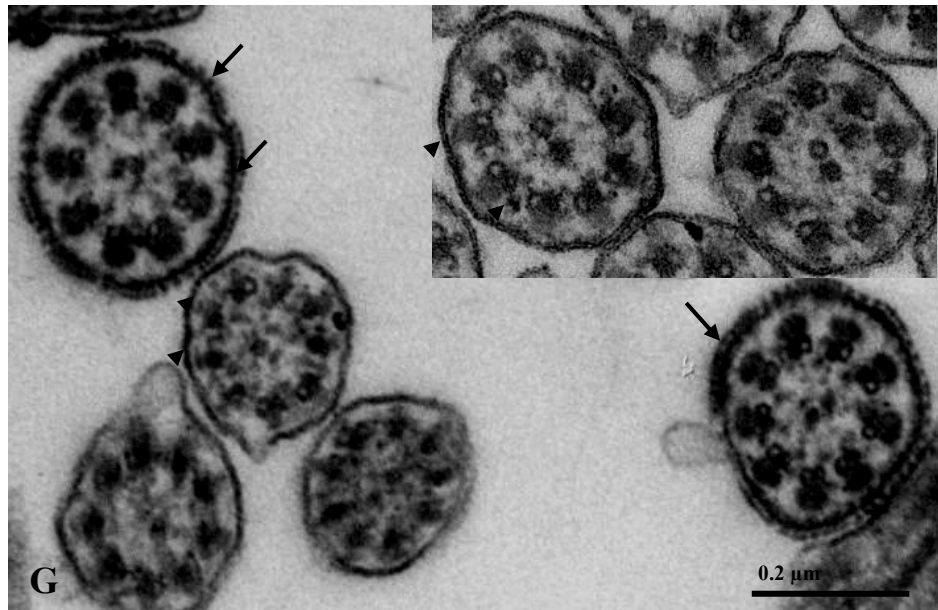
Figure 30.   **(Continued).**

4. Distributions of APGWamide in the brain and reproductive organs of adult *I. pygmaeus*

4.1 H&E histological sections of *I. pygmaeus* brain

The *I. pygmaeus* brain is divided into 4 distinct regions, consisting of the ventrally located subesophageal mass (SBM), the dorsally located supraesophageal mass (SPM) and a bilateral pair of optic lobes. The subesophageal mass is subdivided into the anterior (ASM), middle (MSM), and posterior (PSM) subesophageal masses (Fig. 31). H&E stained sections were used to show the position and morphological features of the brain and to outline the position of the palliovisceral lobe of the posterior subesophageal mass, the olfactory lobe and the optic tract region, vertical lobe and dorsal basal lobe of supraesophageal mass (Fig. 32). In the palliovisceral lobe of the posterior subesophageal mass, a square-shaped lobe was located under esophagus and nerve ring. The pale area of this lobe showed the neuropil, whereas the deep stained section showed the perikaryal layer consisting neuronal cell bodies and glial cells (Fig. 32A). The olfactory lobe, located in the optic tract near optic lobe showed the intensive neuron cell bodies and glial cells (Fig. 32B). In supraesophageal mass, the perikaryal areas of the vertical and dorsal basal lobes were stained deep blue (Figs. 32C-D). Particularly, in the vertical lobe, there was intensive H&E staining on the top edge of the lobe (Fig. 32C). When compared with the anti- APGWamide-staining (see below), there were immunopositive neurons in this area (see Figs. 33-35).
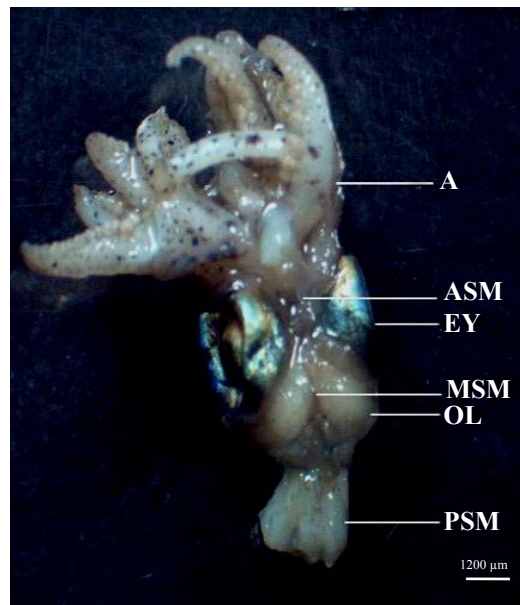
Figure 31. Ventral view of *I. pygmaeus* head. A= arm, ASM= anterior subesophageal mass, EY= eye, MSM= middle subesophageal mass, OL= optic lobe, PSM= posterior subesophageal mass. Scale bar= 1200 µm.
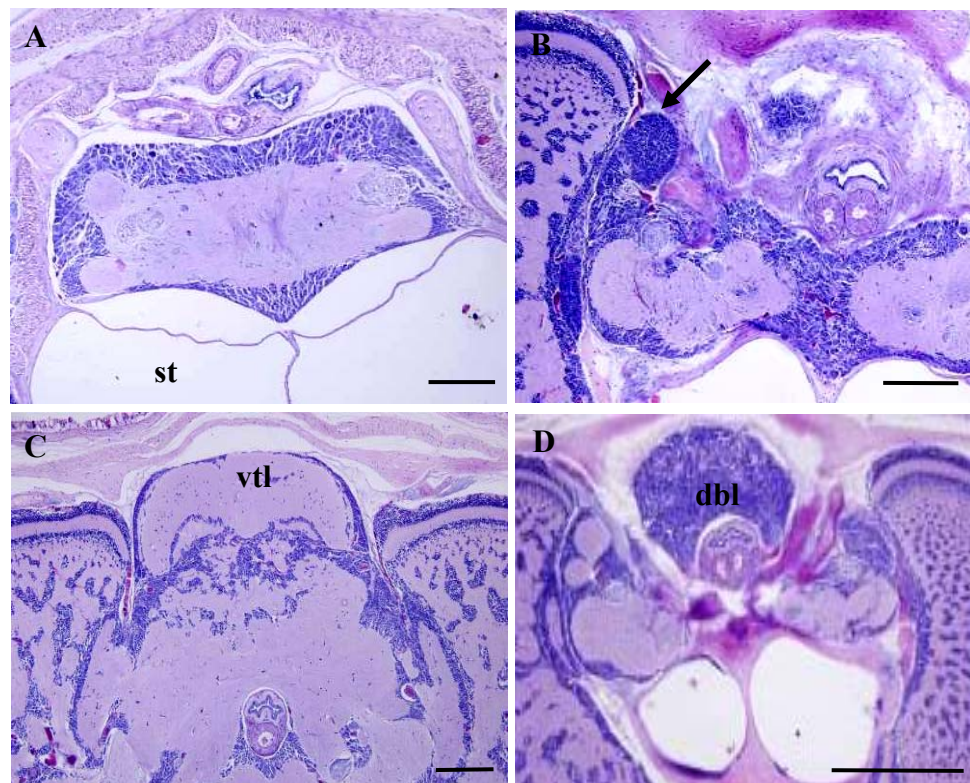
Figure 32. Transverse sections of *I. pygmaeus* brain (H&E stain). **A:** pallioviceral lobe of the posterior subesophageal mass. **B:** olfactory lobe in the optic tract region (arrow). **C-D:** vertical lobe and dorsal basal lobe of supraesophageal mass. dbl= dorsal basal lobe,

(Continued.) pvl= palliovisceral lobe, st= statocyst, vtl= vertical lobe. Scale bars= 200 μm (A - C) and 500 μm (D).
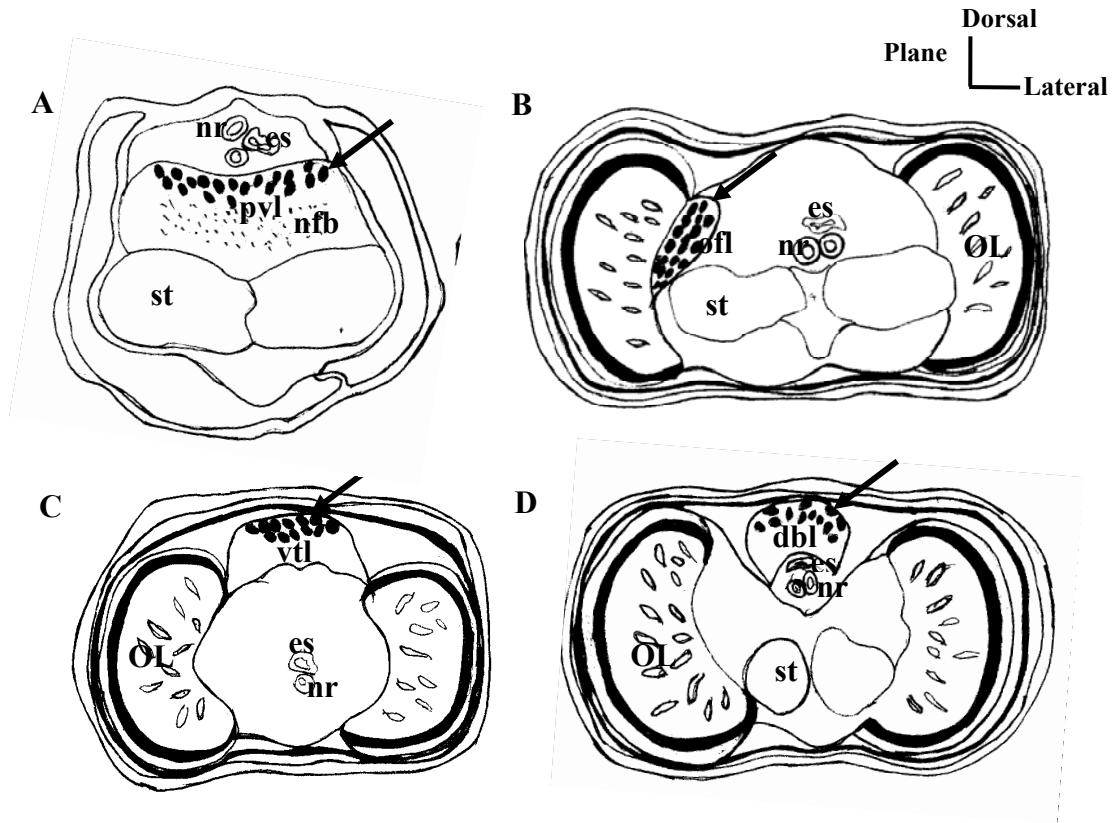
Figure 33. Diagram of the distribution of APGWamide within CNS of *I. pygmaeus* brain. **A:** palliovisceral lobe of the posterior subesophageal mass. **B:** olfactory lobe in the optic tract region (arrow). **C-D:** vertical lobe and dorsal basal lobe of supraesophageal mass. Arrows showing the location of identified neurons. dbl= dorsal basal lobe, es= esophagus, nfb= nerve fiber, nr = nerve ring, ofl= olfactory lobe, OL= optic lobe, pvl= palliovisceral lobe, st= statocyst, vtl= vertical lobe.

4.2 Immunocytochemistry on the localization of APGWamide in
I. pygmaeus brain

This work used immunocytochemistry to investigate the presence of APGWamide in *I. pygmaeus* brain. It showed that the localization of APGWamide immunoreactivity was found in both neurons and fibers in palliovisceral lobe of the posterior subesophageal mass (Figs. 34A and 35A), in the olfactory lobe in the optic tract region (Figs. 34B and 35B), the vertical lobe (Figs. 34C and 35C) and the dorsal basal lobe (Figs. 34D and 35D) of surpraesophageal mass. In supraesophageal mass, APGWamide immunoreactivity was detected only in neurons. Most immunoreactive neurons were found in the palliovisceral and olfactory lobe of both sexes (Figs. 34B and 35B, see also Figs.38-42).
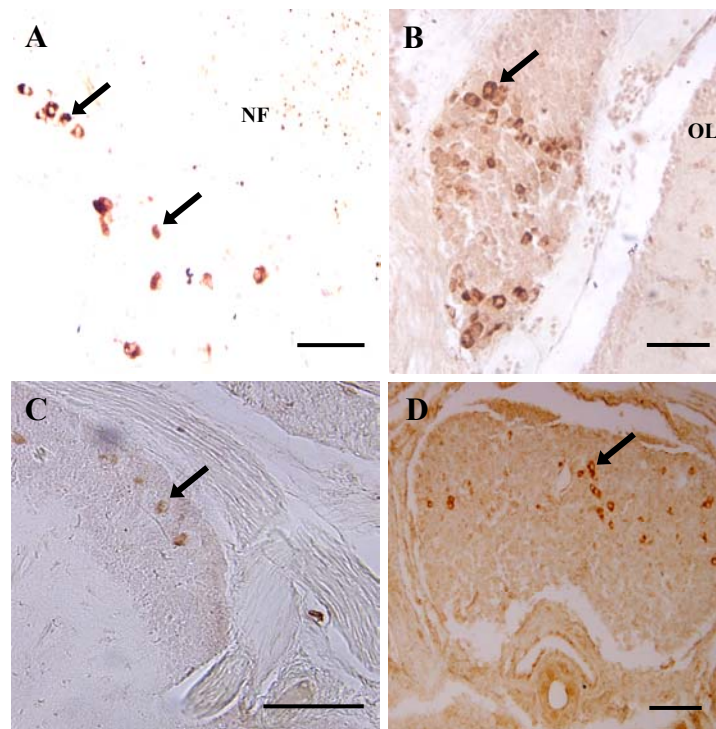
Figure 34.   Darkly stained APGWamide–immunopositive neurons in representative sections of the brain of a male *I. pygmaeus*. **A:** palliovisceral lobe of the posterior subesophageal mass. **B:** olfactory lobe in the optic tract region. **C-D:** vertical lobe and dorsal basal lobe of supraesophageal mass. Arrows point to a few examples of APGWamide – immunopositive neurons. NF= darkly stained immunoreactive nerve fibers, OL= optic lobe. Scale bars= 50 μm (A-B) and 100 μm (C-D).
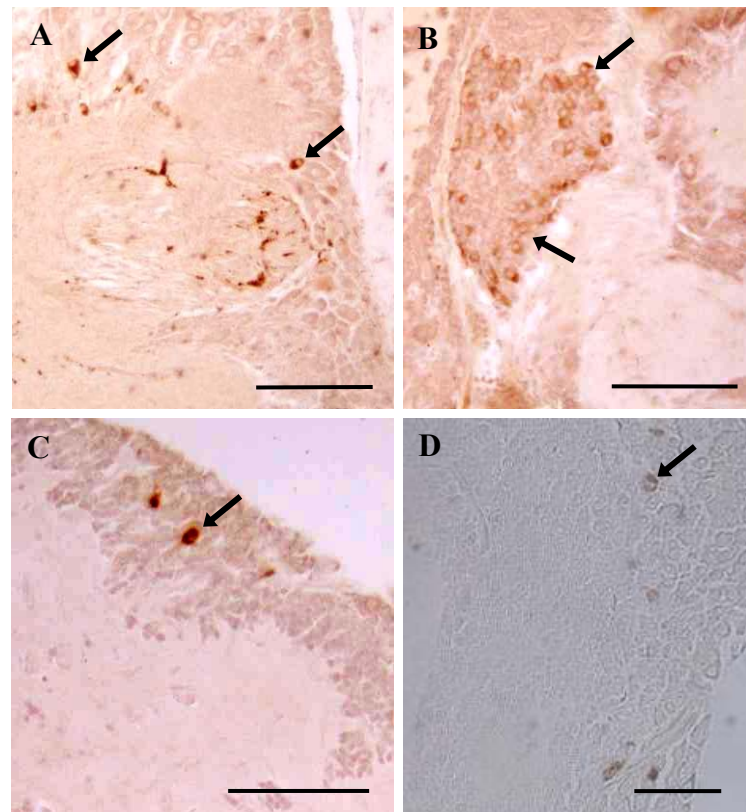
Figure 35. Darkly stained APGWamide–immunopositive neurons in representative sections of the brain of a female *I. pygmaeus*. **A:** palliovisceral lobe of the posterior subesophageal mass. **B:** olfactory lobe in the optic tract region. **C-D:** vertical lobe and dorsal basal lobe of supraesophageal mass. Arrows point to a few examples of APGWamide– immunopositive neurons. Scale bars= 100 μm (A - C) and 50 μm (D).

4.3 APGWamide in *I. pygmaeus* reproductive organ

The reproductive organs of male *I. pygmaeus* were composed of testis, vas deferens, proximal part of genital duct, seminal vesicle, prostate gland, distal part of genital duct and spermatophoric organ, which were tightly packed together and connected to a rather short penis. Female *I. pygmaeus* had a large ovary, which was located posteriorly and was connected through an oviduct with accessory glands namely the oviducal, nidamental and accessory nidamental glands. The oviduct extended from oviducal gland and opened via the female gonopore, which was located anteriorly to the left branchial heart, into the mantle cavity.

In male reproductive organs APGWamide-immunoreactive fibers were localized in the distal part of genital duct, Needham's sac (also called spermatophoric

sac), and the nervous plexus of the muscular layers of penis and mantle. The varicose appearance of these fibers suggests the presence of synapse-like structures contacting the smooth muscles cells (Figs. 36 - 37). No immunoreactivity was observed in female reproductive organs.
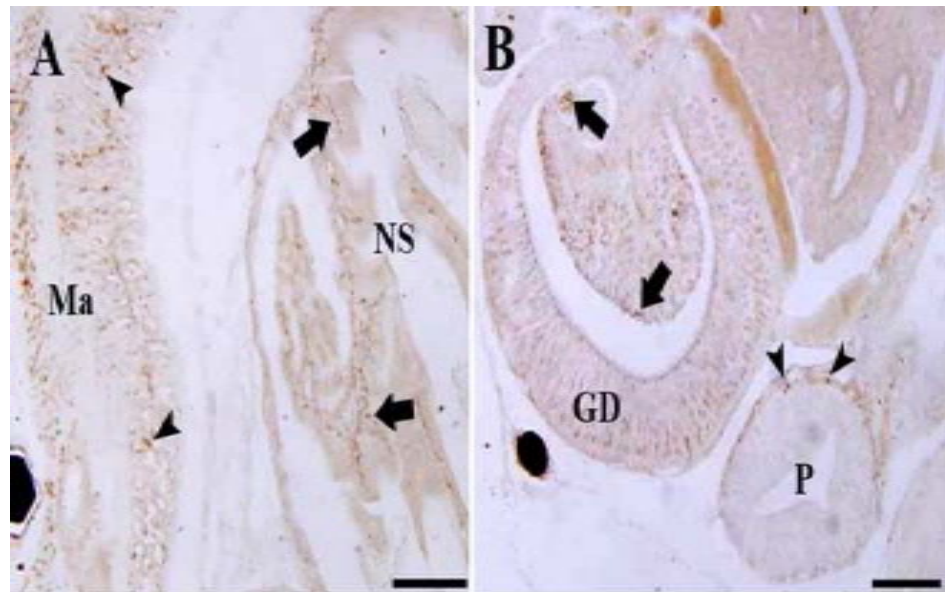
Figure 36.   APGWamide - immunoreactive fibers muscular layer of mantle of males and Needham's sac. **A–B:** the distal part of genital duct and muscular layer of penis. Arrowheads point to several darkly stained varicosities in the muscular layer of the mantle, arrows to varicosities in the Needhams's sac and outer layer of the penis. GD= distal part of genital duct, Ma= muscular layer of mantle, NS= Needham's sac, P= Penis. Scale bars= 100 μm (A-B).
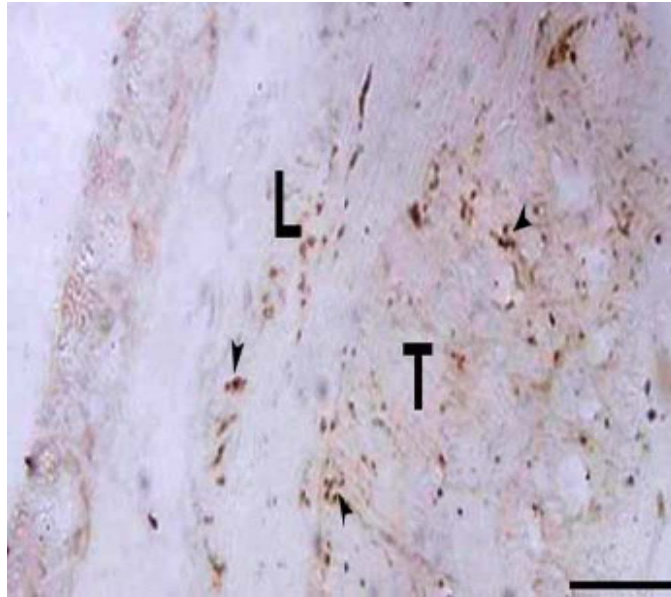
Figure 37. Detail of darkly stained APGWamide - immunoreactive fibers (arrowheads) in the muscular layer of the mantle from male *I. pygmaeus*, showing varicosities on both the longitudinal (L) and transverse (T) muscles. Scale bar= 50 µm.

4.4 Quantification of APGWamide-immunoreactive neurons related to the gonadal development

The total number of APGWa immunoreactive neurons in mature stage brains from male *I. pygmaeus* was significantly higher (P<0.001) than that in females. In males, these neurons were detected in the dorsal basal, vertical, pallioviseral and olfactory lobes, with the highest numbers in the latter two lobes. In females, APGWa immunoreactive neurons were present in the pallioviseral and olfactory lobes, and their numbers were significantly lower than in their male counterparts. No APGWa immunoreactive neurons were detected in the dorsal basal and vertical lobes of females. The quantitative data are summarized in Fig. 38.

The overall results showed the number of anti - APGWamide positive neurons of male *I. pygmaeus*, in PSM (pvl) and OTR (ofl) lobes was higher than SPM (dbl) and SPM (vtl) lobes, while the changes in the number of APGWamide-immunoreactive neurons in female *I. pygmaeus* was highest in OTR (ofl) lobe. Most neurons in males were found in the mature stage whereas in females *I. pygmaeus*, the

highest number were found in maturing and pre-spawning stages, especially as in OTR (ofl) lobe (Figs. 39 – 42).
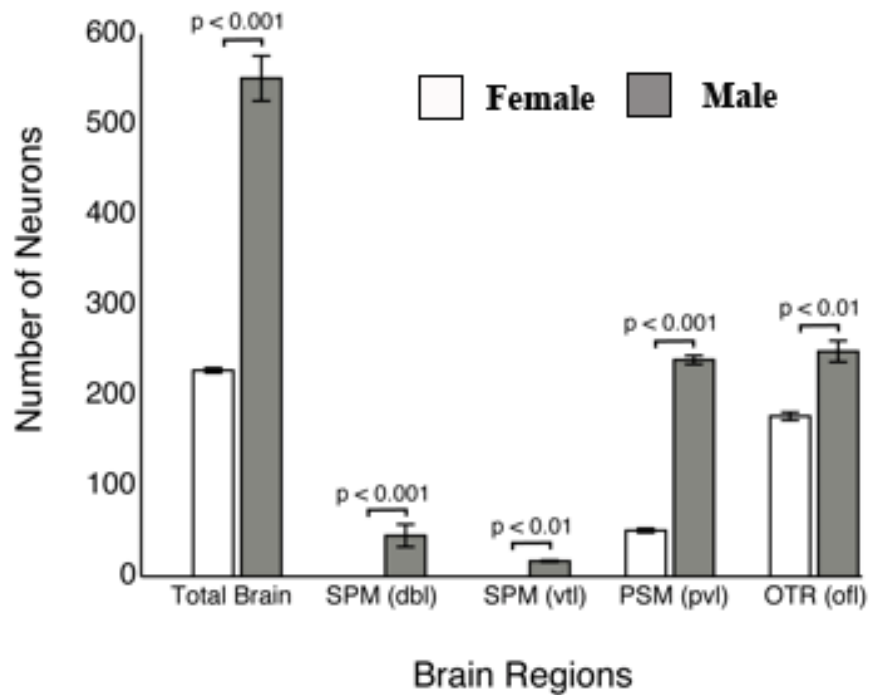
Figure 38. Quantification of anti-APGWamideimmunoreactive neurons ± standard deviation in the brain of adult male (gray columns) and female (white columns) animals. The data show that males (gray colums) contain significantly more APGWa-immunoreactive neurons in total brain, as well as in the individual brain lobes. P-values are displayed above the columns. SPM= supraesophageal mass, PSM= posterior subesophageal mass; OTR= optic tract region, dbl= dorsal basal lobe, vtl= vertical lobe, pvl= palliovisceral lobe, ofl= olfactory lobe.
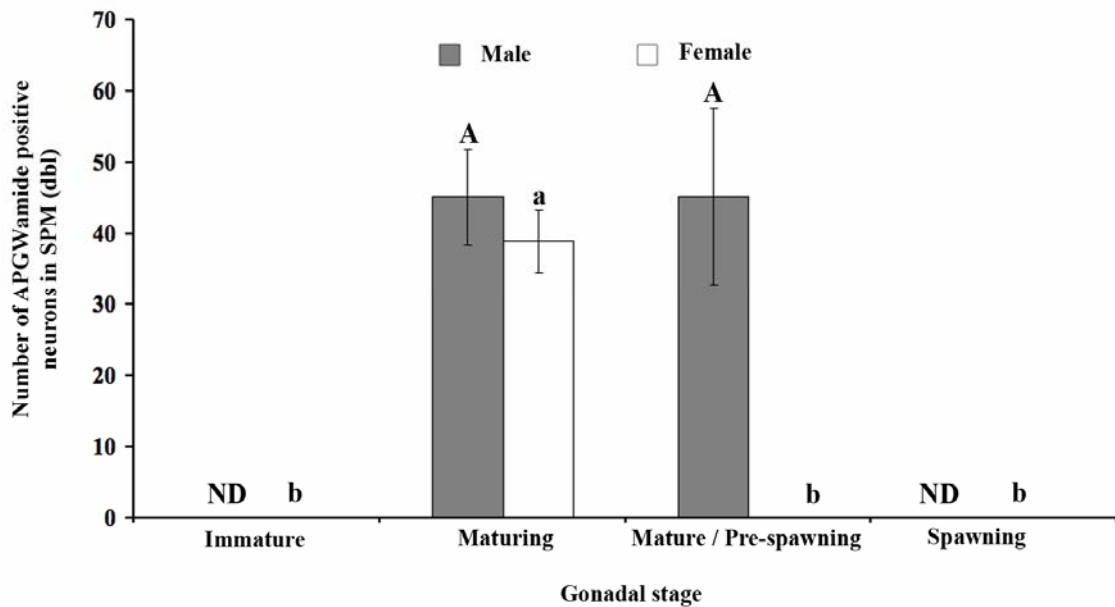
Figure 39. The expression of anti-APGWamide – positive neurons in supraesophageal mass (dorsal basal lobe) of male and female *I. pygmaeus* at different gonadal stages. *Different letters (Capital letter for male and small letter for female) above the bars indicate significant difference among at each sampling the gonadal stage by TKMCT (mean± SD, P< 0.05), ND= not determined.

In males, the number of anti - APGWamide positive neurons in posterior subesophageal masses (palliovisceral lobe) and optic tract region (olfactory lobe) was higher than those in supraesophageal mass (dorsal basal lobe) and supraesophageal mass (vertical lobe). In females, the number of APGWamide-immunoreactive neurons was highest in optic tract region (olfactory lobe). The number of APGWamide-immunoreactive neurons in males was highest in mature animals whereas in females, the highest in maturing and pre-spawning stages. As can be seen in Figs. 39 - 42, the expression of APGWamide- immunopositive neurons in male *I. pygmaeus* was rather dominant in optic tract region (olfactory lobe) and posterior subesophageal masses (palliovisceral lobe). Specimens of male *I. pygmaeus* in immature stage were not available in this work because no squids in this stage were able to capture from the study site.

In the supraesophageal mass (dorsal basal lobe) of males there was no significant difference between maturing and mature stages in the number of APGWa immunoreactive neurons (P> 0.05), whereas in female *I. pygmaeus*, the APGWamide immunoreactivity was only detected in the maturing stage (Fig. 39). In

supraesophageal mass (vertical lobe), APGWamide-positive neurons in males were detected in the mature stage only, whereas in females *I. pygmaeus* they were exclusively detected in and the immature stages (Fig. 40).
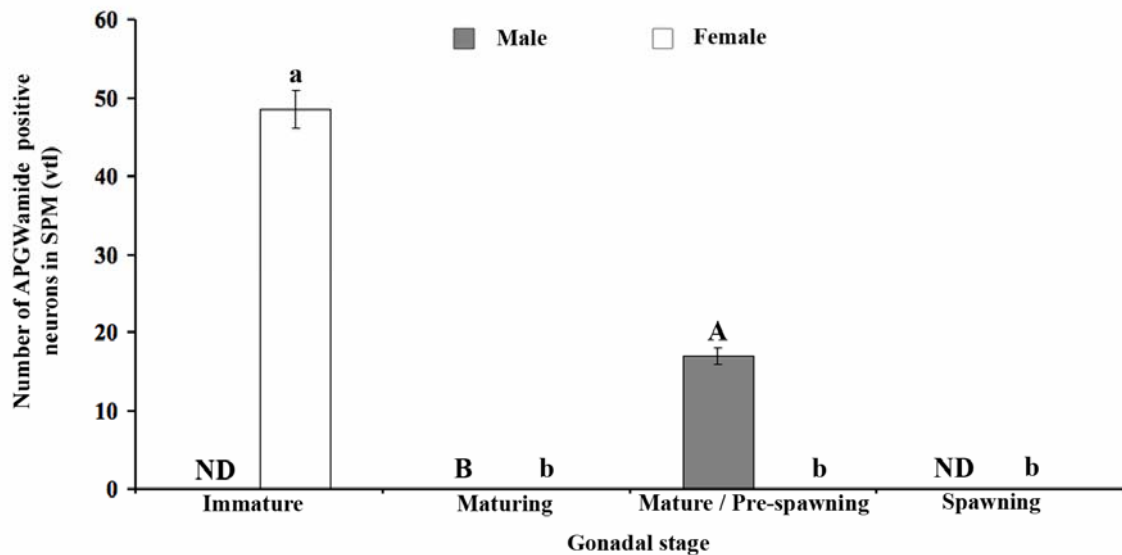
Figure 40. The expression of anti-APGWamide – positive neurons in supraesophageal mass (vertical lobe) of male and female *I. pygmaeus* at different gonadal stages. *Different letters (Capital letter for male and small letter for female) above the bars indicate significant difference among at each sampling the gonadal stage by TKMCT (mean± SD, P< 0.05), ND= not determined

In posterior subesophageal masses (pallioviscreal lobe), the number of anti- APGWamide- positive neurons in both sexes showed highly significant differences in the different gonadal stages (P < 0.05). In males there was a high increase in expression from the maturing to the mature stage, after which the number decreased sharpely in the spawning stage, whereas in females, the number of APGWa neurons showed a gradual increase from immature to spawning stages (Fig. 41).
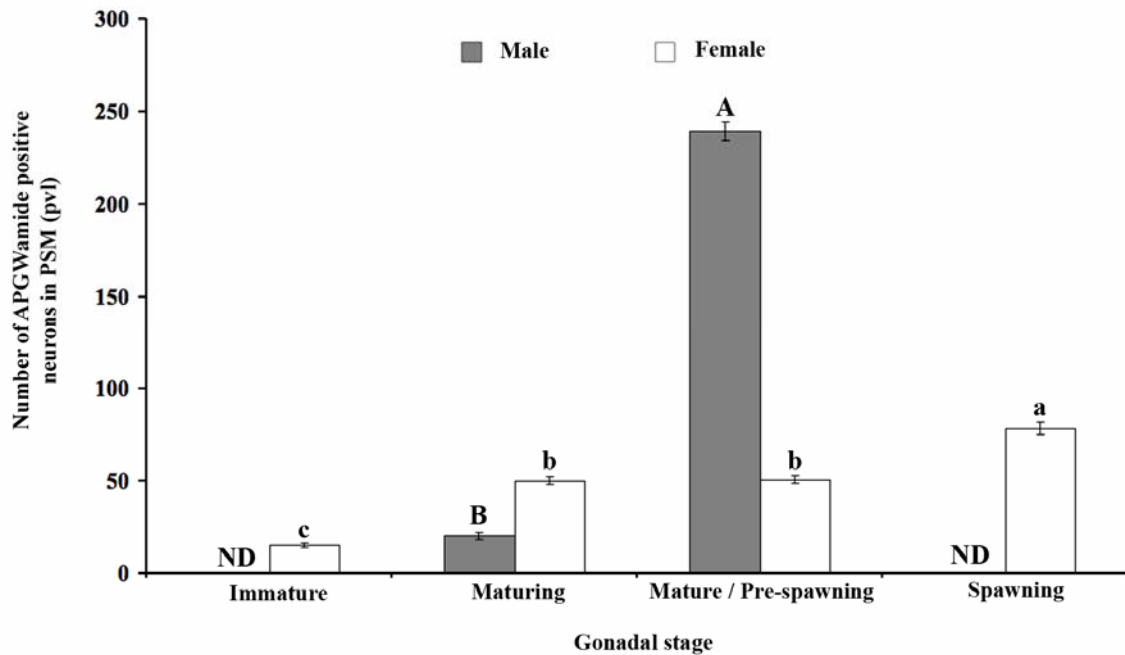
Figure 41. The expression of anti-APGWamide – positive neurons in posterior subesophageal mass (palliovisceral lobe) of male and female *I. pygmaeus* at different gonadal stages. *Different letters (Capital letter for male and small letter for female) above the bars indicate significant difference among at each sampling the gonadal stage by TKMCT (mean± SD, P< 0.05), ND= not determined.

In the OTR (ofl) lobes of both sexes, high numbers of APGWamide expressing neurons were found in all stages of gonadal maturation. In males no specimens of immature stage were captured, so we were unable to determine APGWa expression. The number increased strongly, reaching a peak in the mature stage after which the number decreased in the spawning stage. In female*s* there was high APGWa expression in the first three stages, whereas after that, the number decreased significantly in the spawning stage (Fig. 42).
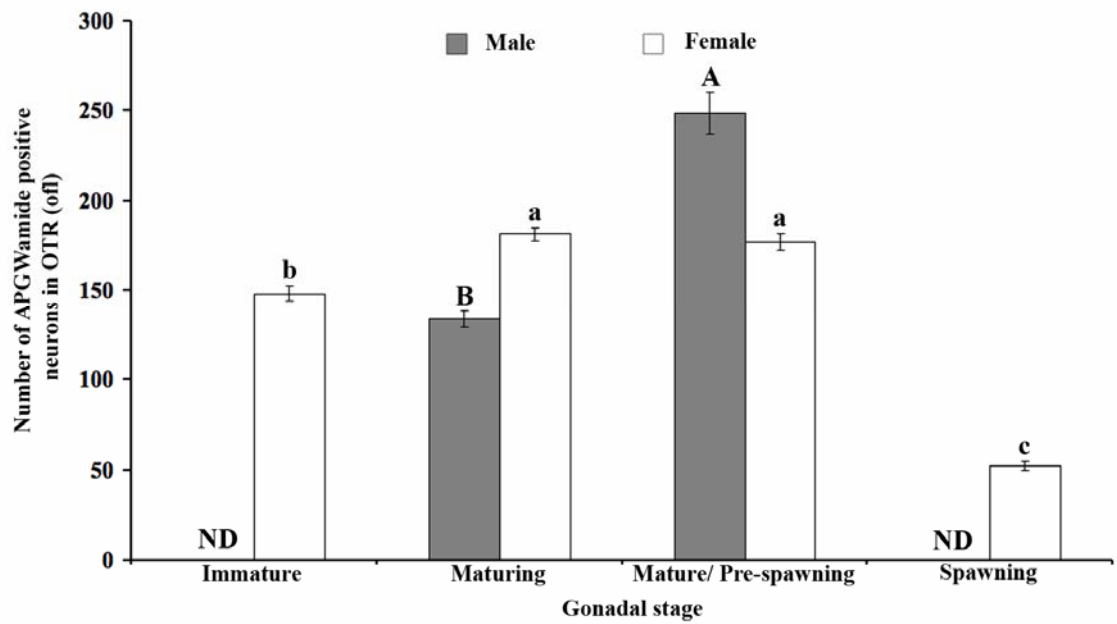
Figure 42. The expression of anti-APGWamide – positive neurons in optic tract region (olfactory lobe) of male and female *I. pygmaeus* at different gonadal stages. *Different letters (Capital letter for male and small letter for female) above the bars indicate significant difference among at each sampling the gonadal stage by TKMCT (mean± SD, $P < 0.05$), ND= not determined.

CHAPTER 4

DISCUSSION

Reproductive biology of *I. pygmaeus*

The specimens of this study which were collected from Andaman Sea water near Sarasin Bridge, Phuket province, revealed that the maximum dorsal mantle lengths of female and male *I. pygmaeus* were 18.17 mm and 15.17 mm, and their maximum body weights were 0.532 g and 0.274 g, respectively. They were larger than those collected from tropical waters off Townsville, North Queensland which were 18 mm and 10 mm and the maximum body weights as 0.655 g and 0.159 g, respectively (Jackson, 1989). By comparison, the recorded characteristics of female *I. pygmaeus* were similar to those reported by Jackson (1989), while for males the maximum values of dorsal mantle length and body weight were clearly higher than Jackson's. A comparison between sexes of the observed body sizes suggests that sexual maturity of male *I. pygmaeus* might occur at a smaller size than for females. The correlation between dorsal mantle length and body weight in both sexes of *I. pygmaeus* were significantly positive, similar to those of *I. paradoxus* as described by Kasuga and Segawa (2005) and other cephalopods such as *Sepioteuthis lessoniana* (Mhitu et al., 2001). The comparison of the dorsal mantle length and spermatophore length of male *I. pygmaeus* also showed a significant positive correlation, indicating that the larger mature *I. pygmaeus* could have larger spermatophore than smaller mature specimens. A similar observation has been reported in some other study of cephalopods such as *Loligo vulgaris* (Krstulovic Sifner and Vrgoc, 2004); *Vulcanoctopus hydrothermalis* (Gonzalez et al., 2002); and *Rossia macrosoma* (Salman and Onsoy, 2010). Moreover, the sex ratio of *I. pygmaeus* peaked to significantly (P<0.05) high values in January, April and December, suggesting that the predominance of males *I. pygmaeus* were more numerous than females. While an observation bias could be suspected, a biological explanation is offered by the observations of Lewis and Choat (1993) that female *I. pygmaeus* dies after finishing the spawning. The changes of dorsal mantle length in various gonadal stages of both male and female sexes of *I. pygmaeus* were assessed. They showed the highest dorsal

mantle length of 12.87 mm in a male in the mature stage (in July) and similarly 17.03 mm in a female in the pre-spawning stage (in October). It seems that both sexes in these stages experience intensive growth, whereas the lowest dorsal mantle lengths were represented in the first gonadal stage, especially observed in the female *I. pygmaeus*. These discoveries were different from those reported on some other related species, such as *I. paradoxus* collected from the Zostera Bed by the temperate coast of central Honshu, Japan, that showed the maximum dorsal mantle length for both sexes in April or May (Kasugai et al., 2003). Such difference may be caused by different environmental conditions. Regarding gametogenesis of *I. pygmaeus* collected from the current study site, it occurred throughout the year, with the spawning periods in female *I. pygmaeus* in March (43.75%), July (50 %), September (60%), October (13.34 %) and November (33.33 %) whereas the spawning period in male *I. pygmaeus*, was found only 11.12 % in October. These results may be also affected by the sampling time within each month. This study corroborates multiple spawning periods of female *I. pygmaeus*, in accordance with Jackson (1991) who reported that this species performs multiple spawning. As for the related species, *I. paradoxus* has its spawning period from June to October for the generation with a small body size and in November to May for those with a larger body size (Kasugai et al., 2003). The male *I. pygmaeus* was observed mostly in the maturing and mature stages, indicating that its spermatogenesis may occur rapidly. However, the spawning period of both sexes of *I. pygmaeus* was simultaneous in October. The gonadal index is an indicator of sexual maturity (Suwanjarat et al., 2009). The observations of the gonadal index of both sexes showed high values synchronously in January, August and October, and these are the times when the breeding seasons of *I. pygmaeus* begins. The gonadal index values of male *I. pygmaeus* were higher than those of females, with values above 2.0, indicating that male *I. pygmaeus* can release mature sperms all year. In this work, the lowest decline in gonadal index values of *I. pygmaeus* was observed between November and December in females, suggesting the beginning of a major spawning period. This study also revealed that no significant correlation exists between GI values in either sex of *I. pygmaeus* and such environmental parameters as transparency, temperature, alkaline, hardness, ammonia, nitrite, nitrate, phosphate, pH and salinity, except for nitrate that showed a significant

correlation with the GI values of both sexes of *I. pygmaeus* (r = 0.74, p = 0.04 for males; r= 0.91, p= 0.00 for females). A similar pattern was observed for the GI values of female *I. pygmaeus* and phosphate (r= 0.86; p= 0.01) see Appendix A, Table. 1. The environmental parameter data was accessed from Tipaporn Traithong Phangnga Coastal Fisheries Research and Development Center. It can be inferred that the environmental conditions for *I. pygmaeus* may not have direct impact on its reproductive cycle. Other species such as *I. paradoxus*, however, are known to be affected by the seawater temperature and photoperiod, with influences on their sexual maturation and gonadal development (Kasugai et al, 2003; Sato et al., 2009). Such effects may vary by observation sites, as well as by species.

Gonadal development of *I. pygmaeus*

The histological observations at the light microscopic level showed that the developmental pattern of oocytes and the number of oocyte stages in the smallest cuttlefish, Pygmy squid, *I. pygmaeus*, is similar to that described by Lewis and Choat (1993) in the same species collected from North Queensland, Australia. Other studies of *I. pygmaeus* reported that sizes of oocytes, the morphology of nucleus, and the relationship between oocytes and the follicle cells play a role in oocyte development – these have been used to define four stages of oocyte development (Arnold and Williams-Arnold, 1977; Lewis and Choat, 1993). In addition, other cephalopods have also been similarly investigated (Knipe and Beeman, 1978; Laptikhovsky and Arkhipkin, 2001). For example, in *Loligo gahi*, the degree of follicular cell development can be used to label eight stages of oocyte development (Laptikhovsky and Arkhipkin, 2001). However, the developmental pattern of oocytes and the number of stages in the different cephalopod groups also showed similar patterns. In an early stage the oocytes are surrounded by a simple layer of squamous follicle cells, then formation with the follicle cells of a syncytium, followed by vitellogenesis. Finally the follicular syncytium degenerates and the mature eggs are ready for the ovulation (Arnold and Williams-Arnold, 1977). These four stages therefore seem to have some generality, and allow fairly clear labeling with little uncertainties. In this study, the gonadal development of female *I. pygmaeus* was divided into four stages as stage I immature, stage II maturing, stage III pre-spawning

and stage IV spawning, defined by observations of the oocytes that appear in its ovary. For the male *I. pygmaeus*, light microscopic analysis showed that its spermatogenesis in the seminiferous tubules of testis as well as the spermatophoric organ are different from those other cephalopod group reported in literature, such as *L. opalescens* (Grieb and Beeman, 1978). This prior work reports that the primary spermatocytes disappear in the maturing and mature stage, in contrast to *I. pygmaeus* that clearly shows the primary spermatocytes in these stages. The labeling of the stages of gonadal development in male *I. pygmaeus* is adapted from Gabr et al. (1998) who also observed the gonadal development in the cuttlefish groups of *Sepia pharaonis* and *S. dollfusi*. Data from a histological analysis of the gonads would be needed for a more detailed study that also involves the ultrastructure level.

Spermatogenesis in *I. pygmaeus*

The present thesis provides the first reported study of the ultrastructure of sperm and spermatogenesis of the Pygmy squid, *I. pygmaeus*, describing the details of the morphological characteristics, the pattern of chromatin condensation and nuclear shape including the appearance of the perinuclear microtubules in the spermatogonia, spermatocytes, spermatids and spermatozoa stage. There has not been any report on details of spermatogenesis in the family Idiosepiidae. However, many studies on the spermatogenesis and spermiogenesis in other families of cephalopod groups are available, such as *Eledone cirrhosa* (Maxwell, 1974), *Eusepia officinalis, Loligo forbesi* and *Alloteuthis subulata* (Maxwell, 1975), *Vampyroteuthis infernalis* (Healy, 1990a), and *Spirula spirula* (Healy, 1990b).

The ultrastructural morphology of the spermatogonia, spermatocyte and spermatid of the tiniest cuttlefish, *I. pygmaeus*, is basically similar to that of some other cephalopods; especially in the cuttlefish, *Sepia officinalis*, which shows a pattern of changing chromatin condensation and nuclear shape during spermatogenesis in various stages of germ cells (Martinez-Soler et al., 2007). The changing patterns of chromatin condensation in spermatogenesis of *I. pygmaeus* occurred with the transformation of granular structure into homogenous e- dense. The four structures of chromatin of *I. pygmaeus* are granular, fibrous, lamellar, and

homogenous e- dense. The nuclear shapes of *I. pygmaeus* are similar to those of *Sepia officinalis*. They were round at first before transforming into a spindle. Reports on the fine structure of mature sperms in cephalopod groups are available for *Eusepia officinalis*, *Loligo forbesi*, *Alloteuthis subulata* (Maxwell, 1975), *Rossia pacifica* (Fields and Thompson, 1976), *Vampyroteuthis infernalis* (Healy, 1989; 1990a), *O. tankahkeei* (Jun-Quan et al., 2005) and *Octopus ocellatus* (Jianmin et al., 2010). In the present work, the morphological events during the spermatogenesis of *I. pygmaeus* appear to have several characters. The ultrastructural characteristics of *I. pygmaeus* sperm were compared with those of other cephalopod species. The acrosome of *I. pygmaeus* sperm is straightly elongated, similar to those of *Rossia pacifica* (Fields and Thompson, 1976) *Sepietta* sp. (Franzen, 1955) and *Spirula spirula* (Healy, 1990b); nevertheless, they are remarkably different from those of *Sepia* sp., *Eusepia officinalis*, *Loligo forbesi*, *Alloteuthis subulata* (Maxwell, 1975), and *Vampyroteuthis infernalis* (Healy, 1989; 1990a) in which their acrosomal vesicles are in a dome-shaped structure. The acrosome of *Octopus tankahkeei* appears spiral and cone shaped, with striations on the inner surface of acrosome (Jun-Quan et al., 2005). The subacrosomal space of *I. pygmaeus* is curved and narrow like that found in *Eusepia officinalis*, *Loligo forbesi*, *Alloteuthis subulata* (Maxwell, 1975). A straight nucleus contains condensed chromatin of *I. pygmaeus* with central shallow basal invagination filled by a dense plug. It is also found in *Spirula spirula* (Healy, 1990b). In the midpiece, only one side of the mitochondrial sleeve of *I. pygmaeus* flagellum is present and this is different from some cephalopods that show two sides of mitochondria sleeve, *Spirula spirula* being an example (Healy, 1990b). Other reports revealed the arrangement of mitochondria called "mitochondria spur" manifest in *Eusepia officinalis*, *Loligo forbesi* and *Alloteuthis subulata* (Maxwell, 1975), and *Rossia pacifica* (Fields and Thompson, 1976). The appearance of mitochondria in *I. pygmaeus* has not been observed in other cephalopod groups. Similar to *Spirula spirula*, *I. pygmaeus* had a flagellum that had a typical 9+2 microtubular structure.

APGWamide in the brain and reproductive organs of adult *I. pygmaeus*

Examining the role of APGWamide in the brain and reproductive organs of adult *I. pygmaeus* through immunocytochemical analysis showed that APGWamide – immunopositive neurons and fibers were present in four of the brain lobes of male and female *I. pygmaeus* in all stages*,* namely in the supraesophageal mass (dorsal basal lobe), supraesophageal mass (vertical lobe), posterior subesophageal mass (palliovisceral lobe) and optic tract region (olfactory lobe). However, focusing on the mature stage of male *I. pygmaeus*, APGWamide-immunopositive neurons and fibers are present in all four of the brain lobes. The presence of APGWamide in the central nervous system and nerve fibers of *I. pygmaeus* was similar to that in other molluscs such as in *Haliothis asinine*, in which the results of detecting APGWamide using the immunoperoxidase technique showed APGWamide immunoreactivity located in the cerebral ganglia and nerve fibers (Chansela et al., 2010). In contrast, in the giant freshwater prawn, *Macrobrachium rosenbergii*, APGWamide immunoreactivity was only detected within the sinus gland (SG) of the eyestalk whereas it was not detected in the regions of brain and the peripheral nerves (Palasoon et al, 2011). The *I. pygmaeus* brain shows a large degree of homology to a previously described closely related species, *I. paradoxus* (Shigeno and Yamamoto, 2002*)*. The morphology of the reproductive organs of *I. pygmaeus* is very similar to that of *I. biserialis* (Hylleberg and Nateewathana, 1991a, b). In the pre-spawning stage of female *I. pygmaeus*, anti-APGWa-positive neurons were found only in the palliovisceral and olfactory lobes. In other cephalopods, in particular *O. vulgaris*, APGWamide immunoreactivity was confined to two lobes, the posterior olfactory lobule and inferior frontal lobe (Di Cristo et al., 2005). These observations are consistent with those described in *I. paradoxus* (Shigeno and Yamamoto, 2002), where the authors suggested that APGWa immunoreactive neurons have important functions in olfactory processing, with indirect effects on reproduction. Furthermore, the results demonstrate that males have more APGWa expressing neurons than females. In addition, the fact that only male reproductive organs and mantles are innervated by APGWa containing fibers suggests a role specific to the control of male reproduction. APGWamide-

immunopositive fibers showing many varicosities were found on the muscle fibers surrounding the distal part of genital duct, Needham's sac, and the muscular layers of penis and mantle. This morphology suggests that muscle cells are innervated by APGWa containing synapse-like structures and that sperm transport and ejaculation might be (in part) regulated by these synapses. A similar conclusion was drawn from studies on *L. stagnalis,* where it was shown that APGWamide-immunopositive fibers innervated the retractor muscles of the penis and inner surface of the vas deferens and penis sheath (Croll and Van Minnen, 1992). Furthermore, physiological experiments showed that APGWa is involved in the control of peristalsis of the vas deferens (Van Golen et al., 1995). This situation differs from that observed in *O. vulgaris* (Di Cristo et al., 2005), where APGWamide-immunoreactivity was found in the reproductive organs of both sexes, suggesting a role in controlling both male and female reproductive functions. However, this result was similar to those in a study of sexually mature *Haliothis asinine*, in which APGWamide immunoreactivity was found only in the reproductive organs of the male (appearing in a region of testis) but it was not found in the ovary (Chansela et al., 2008). Physiological experiments will be necessary to pinpoint the exact role of APGWa in controlling reproduction and sexual behavior of *I. pygmaeus*.

The present work emphasized the comparison of the pre-spawning stage (for female) and mature stage (for male) because in the reproductive organs of these stages are fully matured, and because there was only one specimen of male in the spawning stage. The pre-spawning females and mature males had neurons in their brain, but only the males had the axons that innervate their reproductive tracts. The research found the APGWa immunoreactivity in the brain of both sexes of *I. pygmaeus* and the reproductive organ of males as well.

CHAPTER 5
CONCLUSION

The findings of this study are as follows:

1. An inspection of *I. pygmaeus* sizes and proportions revealed significant statistics that

- Female *I. pygmaeus* has on average a higher body weight than males.

- The dorsal mantle lengths of *I. pygmaeus* differ between the sexes, with its dorsal mantle length varied through the gonadal stages of both sexes.

- On average, male *I. pygmaeus* has a higher number than female.

2. A classification scheme was created, based on histological analyses, to structure the gonadal development into four stages. These stages are descriptively labeled as "immature", "maturing", "pre-spawning" or "mature" (for female and male, respectively), and "spawning". The histological analysis was based on determining the localization and distribution of APGWamide, which is a neuropeptide that prior knowledge associates with gonadal development. The initiating periods of breeding seasons were discovered from these data, as gonadal index curves for both male and female *I. pygmaeus* showed high values synchronously in January, August and October, with the mean GI values of males *I. pygmaeus* throughout the year higher than those of females. This indicated that males could release mature sperms all year round.

3. An aquisition of detailed records of gametogenesis of *I. pygmaeus*, particularly spermatogenesis through the use of TEM imaging.

4. The immunocytochemical analyses revealed higher concentration of APGWamide in males' brain than in females'. It also showed that this neuropeptide was present in male reproductive organ only. The distribution of this neurohormone in brain lobes also differed in males and females, with the highest numbers of

APGWamide- immonoreactive neurons in the palliovisceral and olfactory lobes of the males.

Author's comments and suggestions:

This research raises some interesting points that should be given attention in future as follows:

1. The specimen collection for the current study was undertaken monthly, but a higher collection frequency may improve or sharpen the results because of the short lifespan of this species. The three-month lifespan (Boletzky, 2003) suggests that various development stages can be much shorter than one month, and can be missed with small infrequent samples.

2. The discovery of APGWamide immunoreactivity in the mantles of male *I. pygmaeus* suggests that it may play a role in regulating some muscles for reproduction purposes. Therefore, there should be studies of this or other neuropeptides in other speices or genera.

REFERENCES

Amano, M., Oka, Y., Nagai, Y., Amiya, N. and Yamamori, K. 2008. Immunohistochemical localization of a GnRH-like peptide in the brain of the cephalopod spear-squid, *Loligo bleekeri*. General and Comparative Endocrinology. 156: 277-284.

Arnold, J.M. and Williams-Arnold, L.D. 1977. Cephalopoda: Decapoda. In: A. C. Giese and J. S. Pearse (Ed.) Reproduction in marine invertebrates. Academic Press, New York., Vol. 4, pp 243-290.

Bancroft, J.D. and Gamble, M. 2002. Theory and Practice of Histological Techniques. Churchill Livingstone: London.

Boletzky, S.V. 2003. A lower limit to adult size in coleoid cephalopods: elements of a discussion. Berliner Palaobiologie Abhandlung. 3: 19-28.

Bottke, W. 1974. The fine structure of the ovarian follicle of *Alloteuthis subulata* Lam. (Mollusca, Cephalopoda). Cell and Tissue Research.150: 463-479.

Boyle, P. and Rodhouse, P. 2005. Cephalopods: ecology and fisheries. Blackwell Science Ltd.

Chansela, P., Saitongdee, P., Stewart, P., Soonklang, N., Stewart, M., Suphamungmee, W., Poomtong, T. and Sobhon, P. 2008. Existence of APGWamide in the testis and its induction of spermiation in *Haliotis asinine* Linneaus. Aquaculture. 279: 142-149.

Chansela, P., Saitongdee, P., Stewart, P., Soonklang, N., Hanna, P.J., Nuurai, P., Poomtong, T. and Sobhon, P. 2010. The Tetrapeptide Apgw-Amide Induces Somatic Growth in *Haliotis asinina* Linnaeus. Journal of Shellfish Research 29(3):753-756.

Chen, M. L. and Walker, R. J. 1992. Actions of APGW-amide and GW-amide on identified central neurons of the snail, *Helix aspersa*. Comparative Biochemistry and Physiology. 102(3): 509-516.

Chin, G.J., Payza, K., Price, D.A., Greenberg, M.J. and Doble, K.E. 1994. Characterization and solubilization of the FMRFamide receptor of squid. Biology Bulletin.187(2): 185-199.

Croll, R.P. and Van Minnen, J. 1992. Distribution of the peptide Ala-Pro-Gly-Trp-NH$_2$ (APGWamide) in the nervous system and periphery of the snail *Lymnaea stagnalis* as revealed by immunocytochemistry and in situ hybridization. Journal of Comparative Neurology. 324(4): 567-574.

De Boer, P.A., Ter Maat, A., Pieneman, A.W., Croll, R.P., Kurokawa, M. and Jansen RF. 1997. Functional role of peptidergic anterior lobe neurons in male sexual behavior of the snail *Lymnaea stagnalis*. Journal of Neurophysiology. 8(6):2823-2833.

De Lang, R.P. and Van Minnen, J. 1998. Localization of the neuropeptide APGWamide in gastropod mollusks by in situ hybridization and immunocytochemistry. General and Comparative Endocrinology. 109(2): 166-174.

Di Cosmo, A. and Di Cristo, C. 1998. Neuropeptidergic control of the optic gland of *Octopus vulgaris*: FMRFamide and GnRH immunoreactivity. Journal of Comparative Neurology. 398(1): 1-12.

Di Cristo, C., Bovi, P.D. and Di Cosmo, A. 2003. Role of FMRFamide in the reproduction of *Octopus vulgaris*: molecular analysis and effect on visual input. Peptides. 24: 1525-1532.

Di Cristo, C., De Lisa, E. and Di Cosmo, A. 2009. GnRH in the brain and ovary of *Sepia officinalis*. Peptides. 30(3): 531-537.

Di Cristo, C. and Di Cosmo, A. 2007. Neuropeptidergic control of *Octopus* oviducal gland. Peptides. 28(1): 163-168.

Di Cristo, C., Paolucci, M., Iglesias, J., Sanchez, J. and Di Cosmo, A. 2002. Presence of two neuropeptides in the fusiform ganglion and reproductive ducts of *Octopus vulgaris*: FMRFamide and Gonadotropin-Releasing Hormone (GnRH). Journal of Experimental Zoology. 292(3): 267-276.

Di Cristo, C., Van Minnen, J. and Di Cosmo, A. 2005. The presence of APGWamide in *Octopus vulgaris*: a possible role in the reproductive behavior. Peptides. 26: 53-62.

Fan, X., Croll, R.P., Wu, B., Fang, L., Shen, Q., Painter, S.D. and Nagle, G.T. 1997. Molecular cloning of a cDNA encoding the neuropeptides APGWamide and cerebral peptide 1: localization of APGWamide-like immunoreactivity in the

central nervous system and male reproductive organs of *Aplysia*. The Journal of Comparative Neurology. 387(1): 53-62.

Favrel, P. and Mathieu, M. 1996. Molecular cloning of a cDNA encoding the precursor of Ala-Pro-Gly-Trp amide-related neuropeptides from the bivalve mollusc *Mytilus edulis*. Neuroscience Letters. 205: 210-214.

Fields, W.G. and Thompson, K.A. 1976. Ultrastructure and functional morphology of spermatozoa *Rossia pacifica* (Cephalopoda, Decapoda). Canadian Journal of Zoology. 54: 908-932.

Fox, R. 2001. Invertebrate Anatomy OnLine *Lolliguncula brevis*, Brief Squid. http://webs.lander.edu/rsfox/invertebrates/lolliguncula.html.(accessed 1/02/11).

Franzea, A. 1955. Comparative morphological investigations into the spermiogenesis amomg Mollusca. Zoologiska Bidragen fran Uppsala. 30: 399-456.

Gabr, H.R., Hanlon, R.T., Hanafy, M.H. and El-Etreby, S.G. 1998. Maturation, fecundity and seasonality of reproduction of two commercially valuable cuttlefish, *Sepia pharaonis* and *S. dollfusi*, in the Suez Canal. Fisheries Research. 36: 99-115.

Gonzalez, A.F.and Guerra, Á. 2002. Morpholoical variation in males of *Vulcanoctopus hydrothermalis* (Mollusca, Cephalopod) Bulletin of Marine Science. 71(1): 289–298.

Grieb, T.M. and Beeman, R.D. 1978. A study of spermatogenesis in the spawning population of the squid *Loligo opalescens*. Fisheries Bulletin California. 169: 11-21.

Griffond, B., Van Minnen, J. and Colard, C. 1992. Distribution of APGWa-immunoreactive substances in the central nervous system and reproductive apparatus of *Helix aspersa*. Zoological Science. 9(3): 533-539.

Healy, J.M. 1989. Spermatozoa of the deep-sea cephalopod *Vampyroteuthis infernalis* Chun: ultrastructure and possible phylogenetic significance. Philosophical Transactions of the Royal Society. 323: 589-600.

Healy, J.M. 1990a. Ultrastructure of spermiogenesis in *Vampyroteuthis infernalis* Chun—a relict cephalopod mollusk. Helgolander Meeresunters. 44: 95-107.

Healy, J.M. 1990b. Ultrastructure of spermatozoa and spermiogenesis in *Spirula spirula* (L.): systematic importance and comparison with other cephalopods. Helgolander Meeresunters. 44: 109-123.

Healy, J.M. 1993. Sperm and spermiogenesis in *Opisthoteuthis Persephone* (Octopoda: Cirrata): ultrastructure, comparison with other cephalopods and evolutionary significance. Journal of Molluscan Studies. 59: 105-115.

Henry, J., Favrel, P. and Boucaud-Camou, E. 1997. Isolation and identification of a novel Ala-Pro-Gly-Trp amide - related peptides inhibiting the motility of the mature oviduct in the cuttlefish, *Sepia officinalis*. Peptides. 18(10): 1469-1474.

Henry, J. and Zatylny, C. 2002. Identification and tissue mapping of APGWamide-related peptides in *Sepia officinalis* using LC-ESI-MS/MS. Peptides. 23: 1031-1037.

Hernandez-Garcia, V., Hernandez-Lopez, J.L. and Castro-Hdez, J.J. 2002. On the reproduction of *Octopus vulgaris* off the coast of the Canary Islands. Fisheries Research. 57: 197-203.

Hylleberg, J. and Nateewathana, A. 1991a. Morphology, internal anatomy, and biomatrics of the cephalopod *Idiosepius biserialis* Voss, 1962, a new record for the Andaman Sea. Phuket Marine Biological Center Research Bulletin. 56: 1-9.

Hylleberg, J. and Nateewathana, A. 1991b. Redescription of *Idiosepius pygmaeus* Steenstrup, 1881. (Cephalopoda: Idiosepiidae) with mention of additional morphological characters. Phuket Marine Biological Center Research Bulletin. 55: 33-42.

Iwakoshi, E., Takuwa-Kuroda, K., Fujisawa, Y., Hisada, M., Ukena, K., Tsutsui, K. and Minakata, H. 2002. Isolation and characterization of a GnRH-like peptide from *Octopus vulgaris*. Biochemical and Biophysical Research Communications. 291(5): 1187-1193.

Iwakoshi-Ukena, E., Ukena, K., Takuwa-Kuroda, K., Kanda, A., Tsutsui, K. and Minakata, H. 2004. Expression and distribution of octopus gonadotropin-

releasing hormone in the central nervous system and peripheral organs of the octopus (*Octopus vulgaris*) by in situ hybridization and immunohistochemistry. Journal of Comparative Neurology. 477(3): 310-323.

Jackson, G.D., 1989. The use of statolith microstructures to analyze life-history events in the small tropical cephalopod *Idiosepius pygmaeus*. Fishery Bulletin. 87: 265-272.

Jackson, G.D., 1991. Age, growth and population dynamics of tropical squid and sepioid populations in waters off Townsville, North Queensland, Australia. Ph.D. thesis, James Cook University of North Queensland, Australia.

Jackson, G.D. 1992. Seasonal abundance of the small tropical sepioid *Idiosepius pygmaeus* (Cephalopoda:Idiosepiidae) at two localities off Townsville, North Queensland, Australia. Veliger. 35: 396-397.

Jianmin, V., Weijun, W., Xiaodong, Z., Quanli, Z., Yu, Z., Guohua, S and Xiangquan, L. 2010. The ultrastructure of the spermatozoon of *Octopus ocellatus* Gray, 1849 (Cephalopoda: Octopoda). Chinese Journal of Oceanology and Limnology. 29(1): 199-205.

Jun-Quan, Z., Wan-Xi, Y., Zhong-Jie, Y and Hai-Fong, H. 2005. The ultrastructure of the spermatozoon of *Octpous tankahkeei*. Journal of Shellfish Research. 24(4): 1203-1207.

Kasugai, T., Inoue, M. and Koya, Y. 2003. Reproductive cycle based on histological observations of Japanese pygmy squid, *Idiosepius paradoxus*, in the Zostera red on the coast of central Japan. Zoological Science. 20(12):1617.

Kasugai, T and Segawa, S. 2005. Life cycle of the Japanese pygmy squid *Idiosepius paradoxus* (Cephalopoda: Idiosepiidae) in the Zostera .beds of the temperate coast of central Honshu, Japan**.** Phuket Marine Biological Center Research Bulletin. 66: 249-258.

Knipe, J.H. and Beeman, R.D. 1978. Histological observations on oogenesis in *Loligo opalescens*. California. Fish and Game, Fisheries Bulletin. 169: 23-33.

Krstulovic Sifner, S. and Vrgoc, N. 2004. Population structure, maturation and reproduction of the European squid, *Loligo vulgaris*, in the Central Adriatic Sea. Fisheries Research. 69: 239-249.

Kuroki, Y., Kanda, T., Kubota, I., Fujisawa, Y., Ikeda, T., Miura, A., Minamitake, Y. and Muneoka, Y. 1990. A molluscan neuropeptide related to the crustacean hormone, RPCH. Biochemical and Biophysical Research Communications. 167(1): 273-279.

Laptikhovsky, V.V. and Arkhipkin, J. H. 2001. Oogenesis and gonad development in the cold water loliginid squid *Loligo gahi* (Cephalopoda: Myopsida) on the Falkland shelf). Journal of Molluscan Studies. 67: 475-482.

Laptikhovsky, V.V., Arkhipkin, A.I. and Hoving, H.J.T. 2007. Reproductive biology in two species of deep-sea squids. Marine Biology. 152: 981-990.

Laptikhovsky, V.V, Nigmatullin, Ch.M., Hoving, H.J.T., Onsoy, B., Salman, A., Zumholz, K. and Shevtsov, G.A. 2008. Reproductive strategies in female polar and deep-sea bobtail squid genera *Rossia* and *Neorossia* (Cephalopoda: Sepiolidae). Polar Biology. 31(12): 1499-1507.

Le Gall, S., Féral, C, Van Minnen, J. and Marchand, C.R. 1988. Evidence for peptidergic innervation of the endocrine optic gland in *Sepia* by neurons showing FMRFamide-like immunoreactivity. Brain Research. 462: 83-88.

Lewis, A.R. and Choat, J.H. 1993. Spawning mode and reproductive output of the tropical cephalopod *Idiosepius pygmaeus*. Canadian Journal of Fisheries and Aquatic Sciences. 50: 20-28.

Lu, C.C. and Dunning, M.C. 1998. Subclass Coleoidea. In: P. L. Beesley, G.J.B. Ross, A., Wells (eds.). Mollusca: The southern synthesis, fauna of Australia, Part A xvi. CSIRO Publishing Melbourne., Vol. 5, pp. 499-563.

Martinez-Soler, F., Kurtz, K. and Chiva, M. 2007. Sperm nucleomorphogenesis in the cephalopod *Sepia officinalis*. Tissue Cell. 39(2): 99-108.

Maxwell, W.L. 1974. Spermiogenesis of *Eledone cirrhosa* Lamarck (Cephalopoda. Octopoda). Proceedings of the Royal Society of London. 186:181-190.

Maxwell, W.L. 1975. Spermiogenesis of *Eusepia officinalis* (L.), *Loligo forbesi* (Steenstrup) and *Alloteuthis subulata* (L.) (Cephalopoda, Decapoda). Proceedings of the Royal Society of London (B). 191: 527-535.

McCrohan, C.R. and Croll, R.P. 1997. Characterization of an identified cerebrobuccal neuron containing the neuropeptide APGWamide (Ala-Pro-Gly-Trp-NH2) in the snail *Lymnaea stagnalis*. Invertebrate Neuroscience. 2(4):273-282.

Meneghetti, F., Moschino, V. and Ros, L.D. 2004. Gametogenic cycle and variations in oocyte size of *Tapes phillippinarum* from the Lagoon of Venice. Aquatic Culture. 240: 473-488.

Mhitu, H.A., Mgaya,Y.D. and Ngoile, M.A.K. 2001. Western Indian Ocean Marine Science Association, Zanzibar (Tanzania) and Institute of Marine Sciences, Zanzibar (Tanzania) University of Dar es Salaam. In: Richmond, M.D. and J. Francis (Eds.). Growth and Reproduction of the Big Fin Squid, *Sepioteuthis lessoniana* in the Coastal Waters of Zanzibar, IMS/WIOMSA, Zanzibar, Tanzania.

Nabhitabhata, J. 1994a. Rearing of Thai Pygmy Cuttlefish, *Idiosepius thailandicus* Chot., Okut. and Chai., I: Some Biological Aspects. Technical Paper No. 23/1994, Rayong Coastal Aquaculture Station. 19 pp. (In Thai, with English Abstract).

Nabhitabhata, J. 1994b. Rearing of Thai Pygmy Cuttlefish, *Idiosepius thailandicus* Chot., Okut. and Chai.,II: Mating and spawning Behavior. Technical Paper No. 25/1994, Rayong Coastal Aquaculture Station. 19 pp. (In Thai, with English Abstract).

Nabhitabhata, J. 1998. Distinctive of Thai pygmy squid, *Idiosepius thailandicus* Chotiyaputta, Okutani and Chaitiamvong, 1991. Phuket Marine Biological Center Special Publication. 18: 25-40.

Oberdorster, E., Romano, J. and McClellan-Green, P. 2005. The neuropeptide APGWamide as a Penis Morphogenic Factor (PMF) in Gastropod Mollusks. Integrative and Comparative Biology. 45: 28-32.

Onsoy, B. and Salman, A. 2005. Reproductive biology of the Common Cuttlefish *Sepia officinalis* L. (Sepooda: Cephalopoda) in the Aegean Sea. Turkish Journal of Veterinary and Animal Sciences. 29: 613-619.

Otero, J., Gonźalez, A.F., Pilar Sieiro, M., and Guerra, A. 2007. Reproductive cycle and energy allocation of *Octopus vulgaris* in Galician waters, NE Atlantic. Fisheries Research. 85(1-2). 122-129.

Palasoon, R., Panasophonkul, S., Sretarugsa, P., Hanna, P., Sobhon, P. and Chavadej, J. 2011. The distribution of APGWamide and RFamides in the central

nervous system and ovary of the giant freshwater prawn, *Macrobrachium rosenbergii*. Invertebrate Neuroscience. 11(1):29-42.

Rodriguez-Rua, A., Pozuelo, I., Prado, M.A., Gomez, M.J. and Bruzon, M.A. 2005. The gametogenic cycle of. *Octopus vulgaris*. (Mollusca: Cephalopoda) as observed on the atlantic coast of Andalusia (south of Spain). Marine Biology. 147: 927-933.

Rottmann, R.W., Shireman, J.V. and Chapman, F.A. 1991. Hormonal control of reproduction in fish for induced spawning. Southern Regional Aquaculture Center Publication. 424: 1-4.

Ruppert, E.E., Fox, R.S. and Barnes, R.D. 2004. Invertebrate Zoology: a functional evolutionary approach. 7 [th] Ed. Thomson: Australia.

Salman, A. 1998. Reproductive biology of *Sepietta oweniana* (Pfeffer, 1908) (Sepiolidae: Cephalopoda) in the Aegean Sea. Journal of Marine Science. 62(4): 379-383.

Salman, A. and Onsoy, B. 2010. Reproductive Biology of the Bobtail Squid *Rossia macrosoma* (Cephalopoda: Sepiolidea) from the Eastern Mediterranean. Turkish Journal of Fisheries and Aquatic Sciences. 10: 81-86.

Sato, N., Awata, S., and Munehara, H. 2009. Seasonal occurrence and sexual maturation of Japanese pygmy squid (*Idiosepius paradoxus*) at the northern limits of their distribution. Journal of Marine Science. 66(5): 811-815.

Selmi, M.G. 1996. Spermatozoa of two *Eledone* species (Cephalopoda, Octopoda). Tissue Cell. 28: 613-620.

Semmens, J.M., Moltschaniwskyj, N.A. and Alexander, C.G. 1995. Effect of feeding on the structure of the digestive gland of the the tropical sepioid *Idiosepius pygmaeus*. Journal of the Marine Biological Association of the United Kingdom. 75: 885-897.

Shigeno, S. and Yamamoto, M. 2002. Organization of the nervous system in the pygmy cuttlefish, *Idiosepius paradoxus* Ortmann (Idiosepiidae, Cephalopoda). Journal of Morphology. 254: 65-80.

Smith A.B., Jiménez, C.R., Dirks, R.W., Croll, R.P. and Geraerts, W.P. 1992. Characterization of a cDNA clone encoding multiple copies of the

neuropeptide APGWamide in the mollusk *Lymnaea stagnalis.* Journal of Neuroscience. 12(5): 1709-1715.

Smith, S.A., Nason, J. and Croll, R.P. 1997. Detection of APGWamide-like immunoreactivity in the sea scallop, *Placopecten magellanicus.* Neuropeptides. 31(2): 155-165.

Suwanjarat, J. Pituksalee, C. and Thongchai, S. 2009. Reproductive cycle of *Anadara granosa* at Pattani Bay and its relationship with metal concentrations in the sediments. Songklanakarin Journal of Science and Technology. 31(5): 471-479.

Van Golen, F.A., Li, K.W., De Lange, R.P., Van Kesteren, R.E., Van Der Schors, R.C. and Geraerts, W.P. 1995. Co-localized neuropeptides conopressin and ALAPRO-GLY-TRP-NH2 have antagonistic effects on the vas deferens of *Lymnaea*. Neuroscience. 69: 1275-1287.

Wells, M. and Wells, J. 1959. Hormonal control of sexual maturity in *Octopus.* Journal of Experimental Biology. 36: 1-33.

Wollesen, T., Loesel, R. and Wanninger, A. 2008. FMRFamide-like immunoreactivity in the central nervous system of the cephalopod mollusc, *Idiosepius notoides*. Acta Biologica Hungarica. 59: 111-116.

Yamamoto, M., Shimazaki, Y and Shigeno, S. 2003. Atlas of the embryonic brain in the pygmy squid, *Idiosepius paradoxus*. Zoological Science. 20: 163–179.

Young, R.E., Vecchione, M. and Mangold, K.M. 1999. Cephalopoda Glossary. Tree of Life Web Project.

Zhu, J.Q., Yang, W.X., Zhong, J. and Jiao, H.F. 2005. The Ultrastructure of the spermatozoon of *Octopus tankahkeei*. Journal of Shellfish Research. 24(4): 1203-1207.

Appendix A

1. Environmental parameter at the study site

In the study site, the average values of temperature in seawater ranged between 27.5°C and 32 °C. Maximum temperature was observed for the seawater at 32°C in April, while the minimum temperature was observed at 27.5°C in October. Transparency range was 1.77 m (April) up to the peak values at 3.48 in March, with the average of transparency for all the years was 2.40 m (Fig. 1).
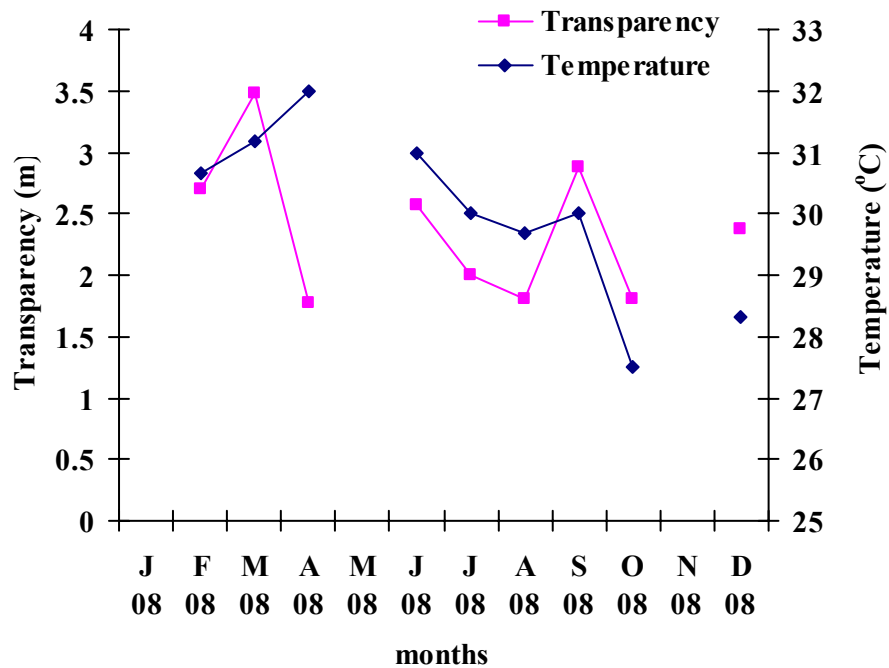
Figure 1.   Monthly average values of transparency and temperature of seawater during January 2008 and December 2008 at the study site (source: Tipaporn Traithong Phangnga Coastal Fisheries Research and Development center).
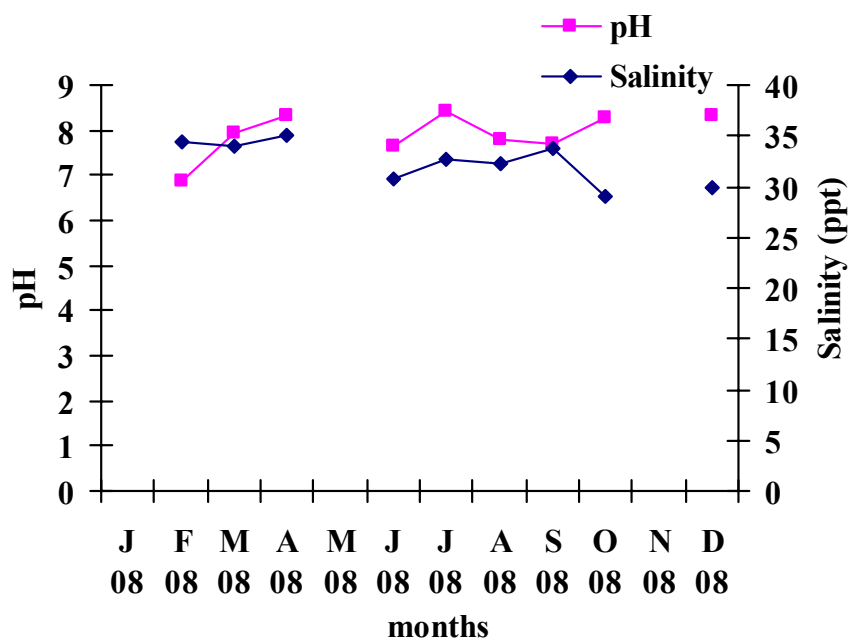
Figure 2. Monthly average values of pH and salinity of seawater during January 2008 and December 2008 at the study site (source: Tipaporn Traithong, Phangnga Coastal Fisheries Research and Development center).

The average values of pH were found between 6.9 and 8.4 as the highest and lowest value of pH were observed in July at pH 8.4 and in February at pH 6.9, respectively. The highest salinity value of 35 ppt in April and the lowest value of 29 ppt in October were recorded (Fig. 2).
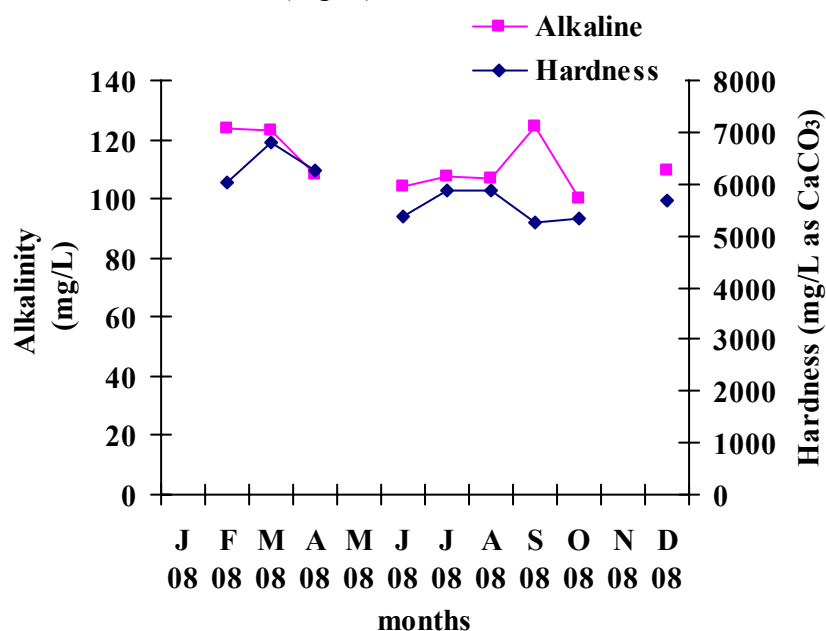
Figure 3. Monthly average values of alkaline and hardness of seawater during January 2008 and December 2008 at the study site

(Continued). (source: Tipaporn Traithong, Phangnga Coastal Fisheries
Research and Development center).

Average values of alkalinity ranged from 100 mg/L (October) to 125
mg/L (September), while the hardness values was observed to be averaged 5274 mg/L
as $CaCO_3$ to 6817 mg/L as $CaCO_3$ in September and March, respectively as shown in
Figure 3.
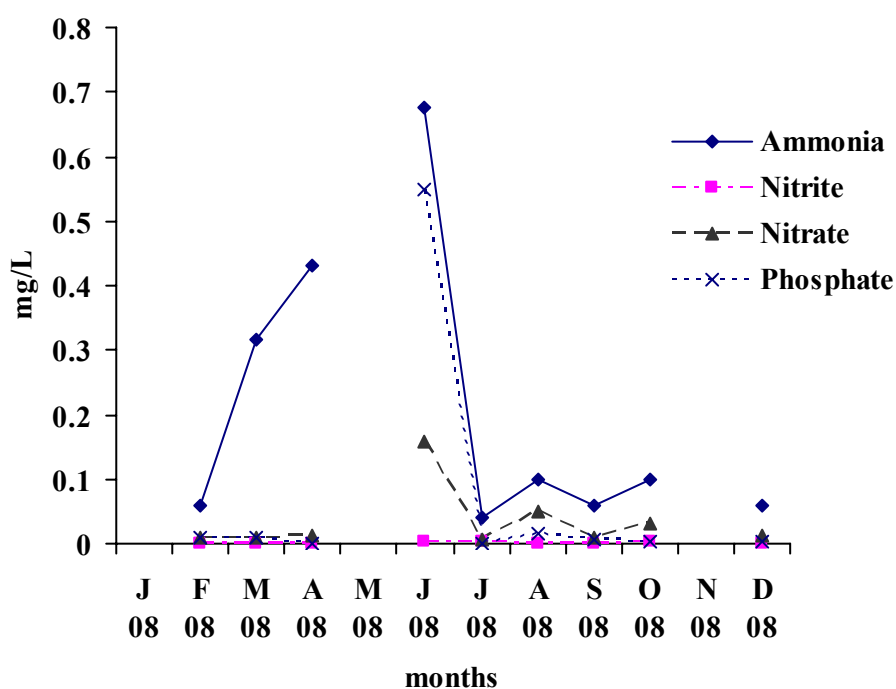
Figure 4.   Monthly average values of ammonia, nitrite, nitrate, phosphate
of seawater during January 2008 and December 2008 at the
study site (source: Tipaporn Traithong Phangnga Coastal
Fisheries Research and Development center) (Mean values
from surface, 3 m depth and bottom).

The average values of ammonia ranged from 0.041 mg/L in July and
0.675 mg/L in June. Similar to the highest values of nitrate and phosphate were in
July as 0.158 and 0.550 mg/L, respectively. While, the lowest values were in June as
0.007 and 0 mg/L, respectively. However, there was no appearance of nitrite in the
study site (Fig. 4).

Table 1. Correlation co-efficient (r) and significance of correlation between GI males and GI females, GI and environmental parameters for *I. pygmaeus* from Andaman Sea, Phuket province.

Variables	Mean ± SD.	GI male			GI female		
		r	P	SC	r	P	SC
GI male	2.42 ±0.25	1	-	-	0.55	0.10	ns
GI female	1.65±0.63	0.35	0.10	ns	1	-	-
Transparency	2.40±0.56	-0.41	0.31	ns	-0.27	0.51	ns
Temperature	30.16±1.39	-0.17	0.69	ns	-0.08	0.90	ns
Alkaline	112.60±9.03	-0.51	0.2	ns	-0.24	0.57	ns
Hardness	5891±497.87	0.08	0.84	ns	0.04	0.92	ns
Ammonia	0.21±0.21	0.1	0.82	ns	-0.01	0.99	ns
Nitrite	0.00±0.00	0.03	0.95	ns	0.03	0.95	ns
Nitrate	0.03±0.05	0.74	0.04	∗	0.91	0.00	∗
Phosphate	0.06±0.17	0.56	0.15	ns	0.86	0.01	∗
pH	7.92±0.49	0.40	0.33	ns	-0.2	0.64	ns
Salinity	32.41±2.09	-0.27	0.52	ns	-0.06	0.89	ns

GI= gonadal index, SD= standard deviation, r= correlation coefficient, P= probability, SC= significance of correlation (* *P <0.05*, ** *P<0.01*, ns= not significant).

Appendix B

Tissue processing for paraffin sections (Bancroft and Gamble, 2002)

1. **Formulae for fixative solution**

   Bouin's fluid

Saturated aqueous picric acid solution	75 ml
40% formaldehyde	25 ml
Glacial acetic acid	5 ml

2. **Tissue processing**

   Fixation

Bouin's fluid	18-24 hours

   (Transfer to 70% alcohol for washing out picric acid)

   Dehydration

70% ethanol	2 hours-overnight
95% ethanol	2 hours
Absolute ethanol	2 hours
Absolute ethanol	overnight

   Clearing

Xylene	1 hour

   Infiltration

Xylene: Wax_1	1 hour
Wax_1	1 hour
Wax_2	1 hour

   Embedding   Tissue is embedded in paraffin

   Sectioning   Cut at 5-6 μm using microtome

Appendix C

Staining methods for paraffin sections (Bancroft and Gamble, 2002)

    1. Preparation of solution

        Hariss's hematoxyline (Harris, 1900 cited by Bancroft and Gamble, 2002)

Hematoxyline	2.5 g
Absolute alcohol	25.0 g
Potassium alum	50.0 g
Distilled water	500 ml
Mercuric oxide	1.25 g
Glacial acetic acid	20 ml

The hematoxyline is dissolved in the absolute alcohol, and is then added to the alum, which has previously been dissolved in the warm distilled water in a 2-litre flask. The mixture is rapidly brought to the boil and the mercuric oxide is then slowly and carefully added. Plunging the flask into cold water or into a sink containing chopped ice rapidly cools the stain. When solution is cold, the acetic acid is added, and the stain is ready for immediate use.

        Eosin

            Stock solution (1% Alcoholic eosin)

Eosin Y	10.0 g
Distilled water	50.0 ml
95% alcohol	940.0 ml

            Working solution (1% Alcoholic eosin)

Stock (1% Alcoholic eosin)	1 part
95% alcohol	1 part

    2. Staining processing

        Deparafinization section

Xylene	2 minutes (2 times)

        Hydration

Absolute ethanol	2 minutes (2 times)

95% alcohol	2 minutes (2 times)
Running tap water	5 minutes
Staining	
Hematoxylin	6 minutes
1% acid alcohol (Differentiate)	5 seconds
Tap water	2 minutes
Saturated lithium carbonate (Blueing or neutralize)	30 seconds
Distilled water	1-2 minutes
Eosin	30 seconds-1 minute
95% ethanol	5-10 dips (2 times)
Dehydration	
Absolute alcohol	2 minutes (2 times)
Clearing	
Xylene	2 minutes (2-3 times)
Mounting with permount	

Appendix D

Tissue processing for transmission electron microscope (TEM) (Bancroft and Gamble, 2002)

   1. **Preparation of solution**

       1.1 *Phosphate buffer* (0.1 mol/l, pH 7.4)

             Stock reagents

                Solution A

Disodium hydrogen orthophosphate	14.2 g
(Na_2HPO_4 anhydrous)	
Distilled water	1.0 l

                Solution B

Sodium dihydrogen phosphate	15.6 g
($NaH_2PO_42H_2O$)	
Distilled water	1.0 l

Mix 40.5 ml of solution A with 9.5 ml of solution B. The pH should be checked and adjust if necessary, using 0.1 mol/l hydrochloric acid or 0.1 mol/l sodium hydroxide.

       1.2 *2.5% glutaraldehyde*

0.2 mol/L phosphate buffer, pH 7.4	50 ml
25% aqueous glutaraldehyde	12 ml
Distilled/deionized water	to 100 ml

Mix aqueous glutaraldehyde with buffer. Check the pH of the mixure and adjust if necessary to pH 7.4 and then add distilled water to make 100 ml.

   2. **Tissue processing**

      Fixation

2.5% glutaraldehyde	24 hours
Wash in 0.1 M phosphate buffer, pH 7.4	10 minutes (three times)
Post-fix in 1% OsO4 in phosphate buffer	2 h

Wash in 0.1 M phosphate buffer, pH 7.4	10 minutes (three times)

Dyhydration

30% ethanol	30 minutes
50% ethanol	15 minutes
70% ethanol	15 minutes
75% ethanol	15 minutes
80% ethanol	15 minutes
85% ethanol	15 minutes
90% ethanol	15 minutes
50% ethanol	15 minutes
100% ethanol	15 minutes

Propylene oxide	30 minutes (2 times)

Infiltration

Propylene oxide: resin (2:1)	overnight
Propylene oxide: resin (1:2)	7 hours
Pure resin	overnight

Embedding

Polymerize at 60 ºC for 24 hours

3. **Contrasting the ultra-thin section**

Uranyl acetate:

3.1 Put a parafilm sheet on the bench, fix parafilm by pressing the edges to the bench's surface.

3.2 Place one small droplet of uranyle acetate solution (2%, light sensitive, radioactive) per grid onto parafilm.

3.3 Place grids onto drops (dull surface towards drop). Cover with petri dish and shade (cardboard box). Leave for 30 minutes.

3.4 Prepare three plastic beakers with distilled water. Wash grids subsequently in the three beakers.

3.5 Dry grids on filter paper.

Lead citrate:

3.6 Put a parafilm sheet on the bench, fix parafilm by pressing the edges to the bench's surface.

3.7 Place one small droplet of lead citrate solution (0.5%, CO_2 sensitive, toxic) per grid onto parafilm. Maximum five nets at one time.

3.8 Place two NaOH pellets on the edge of parafilm sheet to prevent carbonate precipitation.

3.9 Place grids onto drops (dull surface towards drop). Cover with petri dish and shade (cardboard box). Leave for 7-8 minutes.

3.10 Prepare three plastic beakers with distilled. Wash grids subsequently inthe three beakers.

3.11 Dry grids on filter paper.

3.12 Let grids air dry for at least 15 minutes.

3.13 Grids are ready for TEM.

Appendix E

Tissue processing for immunocytochemistry (after fixation and tissue processing for paraffin sections)

1. **Preparation of solutions**

   1.1 *DAB solution*

   - added 1 drop of buffer stock solution into 2.5 ml of tab water, mixed
   - added 2 drops of DAB, mixed
   - added 1 drop of hydrogen peroxide, mixed
   - added 1 drop of nickel, mixed

To prepare incubation medium (IM):

IM	for 2 ml	for 1 ml
10% serum	200 μl	100 μl
1% Triton x 100	20 μl	10 μl
In 1x PBS	1,796 μl	895 μl

2. **Preparation of sections**

   2.1 Deparaffinized in xylene.

Xylene I	10 minutes
Xylene II	10 minutes

   2.2 Rehydrated in descending concentration of ethanol.

Absolute alcohol I	10 minutes
Absolute alcohol II	10 minutes
95% alcohol	5 minutes
80% alcohol	5 minutes
70% alcohol	5 minutes

   2.3 Rinsed 5 minutes in tab water.

3. Immunocytochemistry

3.1 Washed sections in PBS (Phosphate Buffered Saline) 2 x 5 minutes.

3.2 Pre-incubated in incubation medium (IM) (200 μl/slide) for 10 minutes.

3.3 Incubated in the primary antiserum: rabbit polyclonal anti-APGWamide (final serum dilution 1:500 diluted in IM) (200 μl/slide) for 1 hour at room temperature (RT) or over night at 4 ^{0} C (put a piece of parafilm over the slide to prevent it from drying out).

3.4 Washed 2 x 10 minutes in PBS.

3.5 Incubated in the secondary antibody: peroxidase-conjugated swine antirabbit (rabbit & HRP) (1:100 diluted in IM) (200 μl/slide) for 1 h at room temperature or overnight at 4 ^{0} C in the dark.

3.6 Washed 2 x 10 minutes in PBS.

3.7 Visualized with DAB for 10 minutes.

3.8 Stopped reaction with tap water.

3.9 Dehydrated in the increasing concentration of ethanol

95% alcohol	2 minutes
80% alcohol	2 minutes
70% alcohol	2 minutes
Absolute alcohol	2 minutes

3.10 Cleared in xylene:

Xylene I	5 minutes
Xylene II	5 minutes

3.11 Mounted the slides with Entellan.

VITAE

Name   Mrs. Pattanasuda Sirinupong

Student ID   4910230023

Educational Attainment

Degree	Name of Institution	Year of Graduation
Bachelor of Science (Biology)	Kasetsart university	2000
Master of Science (Zoology)	Kasetsart university	2004

Scholarship Awards during Enrollment

December/2006 - November /2009   Royal Golden Jubilee (RGJ) PhD program.
From Thailand Research Found (TRF),
(Grant no. PHD/0247/2548)

Lists of Publications and Proceedings

Sirinupong, P. and Suwanjarat, J. 2009. Histology of Brain and Eye in the Pygmy Squid, *Idiosepius pygmaeus*. Proceeding of the 26th MST Annual Conference. Maeung, Chiangmai, January 28-30, 2009. pp. 59-60.

Sirinupong, P. and Suwanjarat, J. 2010. Localizations and Levels of APGWamide in Relation to Gonadal stage of Pygmy Squid, *Idiosepius pygmaeus*. Proceeding of the RGJ – Ph.D. Congress XI. Jomtien Palm Beach Resort Pattaya, Chonburi, April 1-3, 2010. pp. 325.

Sirinupong, P., Suwanjarat, J. and van Minnen, J. 2011. Distribution of APGWamide-immunoreactivity in the brain and reproductive organs of adult Pygmy squid, *Idiosepius pygmaeus*. Invertebrate Neuroscience. 11(2):97-102.